MASS, SALT, AND HEAT TRANSPORT ACROSS 40°N LATITUDE IN THE ATLANTIC OCEAN BASED ON IGY DATA AND DYNAMIC HEIGHT CALCULATIONS

Tommy Darell Greeson

DUDLEY KNOX LIBRARY
NAVAL POSTGRADUATE SCHOOL
MONTEREY, CALIFORNIA 93940

NAVAL POSTGRADUATE SCHOOL
Monterey, California

THESIS

MASS, SALT, AND HEAT TRANSPORT ACROSS 40°N LATITUDE IN THE ATLANTIC OCEAN BASED ON IGY DATA AND DYNAMIC HEIGHT CALCULATIONS

by

Tommy Darell Greeson

September 1974

Thesis Advisor: G.H. Jung

Approved for public release; distribution unlimited.

T 163895

UNCLASSIFIED

SECURITY CLASSIFICATION OF THIS PAGE (When Date Entered)

REPORT DOCUMENTATION PAGE

READ INSTRUCTIONS BEFORE COMPLETING FORM

1. REPORT NUMBER

2. GOVT ACCESSION NO.

3. RECIPIENT'S CATALOG NUMBER

4. TITLE (and Subtitle)
Mass, Salt, and Heat Transport Across 40°N Latitude in the Atlantic Ocean Based on IGY Data and Dynamic Height Calculations

5. TYPE OF REPORT & PERIOD COVERED
Master's Thesis; September 1974

6. PERFORMING ORG. REPORT NUMBER

7. AUTHOR(s)
Tommy Darell Greeson

8. CONTRACT OR GRANT NUMBER(s)

9. PERFORMING ORGANIZATION NAME AND ADDRESS
Naval Postgraduate School
Monterey, CA 93940

10. PROGRAM ELEMENT, PROJECT, TASK AREA & WORK UNIT NUMBERS

11. CONTROLLING OFFICE NAME AND ADDRESS
Naval Postgraduate School
Monterey, CA 93940

12. REPORT DATE
September 1974

13. NUMBER OF PAGES
137

14. MONITORING AGENCY NAME & ADDRESS(if different from Controlling Office)
Naval Postgraduate School
Monterey, CA 93940

15. SECURITY CLASS. (of this report)
Unclassified

15a. DECLASSIFICATION/DOWNGRADING SCHEDULE

16. DISTRIBUTION STATEMENT (of this Report)
Approved for public release; distribution unlimited.

17. DISTRIBUTION STATEMENT (of the abstract entered in Block 20, if different from Report)

18. SUPPLEMENTARY NOTES

19. KEY WORDS (Continue on reverse side if necessary and identify by block number)
Heat Transport
40°N Atlantic Ocean

20. ABSTRACT (Continue on reverse side if necessary and identify by block number)
This study discusses the development of a computer program capable of performing the necessary dynamic computations to obtain estimates of the transports of mass, salt, and heat across the vertical cross section at 40°N within the North Atlantic Ocean. Previous studies have used either different approaches to the problem or, if the same approach was used, then the data were averaged to eliminate seasonal effects.

DD FORM 1 JAN 73 1473 EDITION OF 1 NOV 65 IS OBSOLETE
S/N 0102-014-6601 |
(Page 1)

UNCLASSIFIED
SECURITY CLASSIFICATION OF THIS PAGE (When Date Entered)

(20. ABSTRACT Continued)

Temperature and salinity data from Crawford Cruise 16, 2 to 22 October 1957 of the International Geophysical Year, are used for the entire cross section of ocean. These observations provide data that are both homogeneous and consistent.

General interpolation methods are evaluated for determining the temperature and salinity observations at standard depths. A combination of linear and mean parabolic interpolation methods is found to be the most accurate method of estimating the continuous vertical temperature and salinity profiles at each station.

The velocity estimates are obtained for the cross section by the classical dynamic method. A level of no motion is established where there is a balance of the net transports of mass and salt.

Based on this level of no motion, a heat transport figure is obtained that compares favorably with those of earlier studies by Sverdrup, Jung, and Budyko.

Mass, Salt, and Heat Transport Across 40°N Latitude in the Atlantic Ocean Based on IGY Data and Dynamic Height Calculations

by

Tommy Darell Greeson
Lieutenant Commander, United States Navy
B.S., Clemson University, 1962

Submitted in partial fulfillment of the
requirements for the degree of

MASTER OF SCIENCE IN OCEANOGRAPHY

from the

NAVAL POSTGRADUATE SCHOOL
September 1974

Thesis
c.1

DUDLEY KNOX LIBRARY
NAVAL POSTGRADUATE SCHOOL
MONTEREY, CALIFORNIA 93940

ABSTRACT

This study discusses the development of a computer program capable of performing the necessary dynamic computations to obtain estimates of the transports of mass, salt, and heat across the vertical cross section at 40°N within the North Atlantic Ocean. Previous studies have used either different approaches to the problem or, if the same approach was used, then the data were averaged to eliminate seasonal effects.

Temperature and salinity data from Crawford Cruise 16, 2 to 22 October 1957 of the International Geophysical Year, are used for the entire cross section of ocean. These observations provide data that are both homogeneous and consistent.

General interpolation methods are evaluated for determining the temperature and salinity observations at standard depths. A combination of linear and mean parabolic interpolation methods is found to be the most accurate method of estimating the continuous vertical temperature and salinity profiles at each station.

The velocity estimates are obtained for the cross section by the classical dynamic method. A level of no motion is established where there is a balance of the net transports of mass and salt.

Based on this level of no motion, a heat transport figure is obtained that compares favorably with those of earlier studies by Sverdrup, Jung, and Budyko.

TABLE OF CONTENTS

I. INTRODUCTION ---------- 11

II. BACKGROUND ---------- 13

A. HEAT TRANSPORT ---------- 13

B. DETERMINATION OF THE LEVEL OF NO MOTION --- 14

III. STATEMENT OF THE PROBLEM ---------- 20

IV. PROCEDURE ---------- 24

A. DATA SOURCES ---------- 24

B. DEVELOPMENT OF THE COMPUTER PROGRAM ------- 29

C. SELECTION OF THE INTERPOLATION METHOD ----- 29

D. COMPUTATIONS OF VELOCITIES AND THE TRANSPORTS OF MASS, SALT CONTENT, AND HEAT ---------- 30

V. DISCUSSION OF RESULTS ---------- 44

A. COMPARISON OF VARIOUS INTERPOLATION METHODS ---------- 44

B. LEVEL OF NO MOTION ---------- 52

C. VELOCITIES ---------- 61

D. TRANSPORTS OF MASS, SALT, AND HEAT -------- 70

E. WATER MASSES AND THEIR RELATIVE LOCATION TO THE LEVEL OF NO MOTION ---------- 76

VI. CONCLUSIONS AND RECOMMENDATIONS ---------- 81

APPENDIX A: COMPUTER PROGRAM ---------- 83

APPENDIX B: T-S DIAGRAMS FOR CRAWFORD STATIONS 218-255 ---------- 93

APPENDIX C: LATITUDE AND LONGITUDE FOR CRAWFORD STATIONS 218-255 ----------132

BIBLIOGRAPHY ---------- 134

INITIAL DISTRIBUTION LIST ---------- 136

LIST OF FIGURES

Figure 1 — Crawford's transit of the North Atlantic Ocean at 40°N, 2-22 October 1957 ---------- 25

Figure 2 — Vertical cross section of the North Atlantic Ocean at 40°N showing the vertical and horizontal extent of temperature and salinity observations ---- 26

Figure 3 — Illustration of the averaging process in order to make values of velocity, density, temperature, and salinity compatible within a sample rectangular area ---------- 34

Figure 4 — Illustration of the summation process performed in the computer program for a sample cross section of ocean ---------- 37

Figure 5 — Vertical cross section through the North Atlantic Ocean at 40°N showing the deepest level common to a pair of stations for which the transports of mass, salt, and heat are computed -------- 40

Figure 6 — Vertical cross section through the North Atlantic Ocean at 40°N showing the areas for which the estimates of the transports of mass, salt, and heat are made from extrapolated temperature and salinity values ---------- 41

Figure 7 — Computer plot of the linear interpolation method for the vertical temperature profile at Crawford Station 221 ----- 47

Figure 8 — Computer plot of the mean linear-parabolic interpolation method for the vertical temperature profile at Crawford Station 221 ---------- 48

Figure 9 — Computer plot of the piecewise-cubic polynomial interpolation method for the vertical temperature profile at Crawford Station 221 ---------- 49

Figure 10 Computer plot of the combination linear and mean parabolic interpolation method for the vertical temperature profile at Crawford Station 221 ---------- 50

Figure 11 Comparison of the level of no motion determined solely from Crawford data with the level of no motion determined after the inclusion of all areas in the vertical cross section not covered with Crawford data ---------- 57

Figure 12 Surface geostrophic velocities at 40°N within the North Atlantic Ocean ---------- 63

Figure 13 Geostrophic velocities at 1000m within the North Atlantic Ocean at 40°N --------- 64

Figure 14 Geostrophic velocities at 2000m within the North Atlantic Ocean at 40°N --------- 65

Figure 15 Geostrophic velocities at 3000m within the North Atlantic Ocean at 40°N --------- 66

Figure 16 Geostrophic velocities at 4000m within the North Atlantic Ocean at 40°N --------- 67

Figure 17 Surface current observations "Gulf Stream '60" (Fuglister, 1964) ---------- 68

Figure 18 Integrated transport of mass for Crawford Stations 218-255 ---------- 71

Figure 19 Integrated transport of salt for Crawford Stations 218-255 ---------- 72

Figure 20 Integrated transport of heat for Crawford Stations 218-255 ---------- 73

Figure 21 Relative position of the level of no motion to the various water masses within the North Atlantic Ocean at 40°N -- 79

LIST OF TABLES

TABLE I	Comparison of the effect of various interpolation methods on the transports of mass, salt content, and heat at 40°N within the North Atlantic Ocean ----------	51
TABLE II	Level of no motion for each pair of Crawford Stations at 40°N within the North Atlantic Ocean ----------	53
TABLE III	Integrated transports of mass, salt, and heat ----------	55
TABLE IV	Transports of mass, salt, and heat including all areas not covered by Crawford data ----------	58
TABLE V	Comparison of the net transports of mass, salt, and heat for the vertical cross section at 40°N within the North Atlantic Ocean when the level of no motion is varied 50m above and below the level of no motion obtained from actual Crawford data ----------	60
TABLE VI	Comparison of heat transport values ------	75

ACKNOWLEDGMENTS

The writer wishes to thank Dr. Glenn H. Jung for his assistance and guidance in the preparation of this thesis and Dr. J.J. von Schwind for his constructive review of the text.

I. INTRODUCTION

It has long been recognized that the earth and its atmosphere receive a surplus of heat at the equator and lose more heat at the poles than is received from the sun. Since the poles of this system are not becoming progressively colder, nor the equatorial regions progressively warmer, there must be a transfer mechanism within the system that transports heat from the equatorial regions to the poleward regions of the earth. The excess heat lost at the earth's poles is balanced by a meridional transfer of heat from low latitudes in both the atmosphere and the oceans. How this heat transfer is partitioned between the atmosphere and the oceans still remains a question although a number of studies have considered this problem in recent years (Sverdrup, 1957; Budyko, 1956; Jung, 1955; Bryan, 1962).

Jung (1952) was one of the first to point out that the ocean currents might be of greater significance in transferring heat energy than had been previously assumed. He made an extensive study (1955) in an attempt to clarify how heat is transported by deep ocean currents in the North Atlantic Ocean. This investigation was one of the first attempts to compute heat transport based on geostrophic calculations from hydrographic data.

As stated by Bryan (1962) only the derivative of the geostrophic velocity with respect to depth can be computed

directly from hydrographic data. To determine the velocity itself an integration must be carried out, which in turn presents the problem of choosing the correct constant of integration. The selection of a level of no motion at which the geostrophic velocity is set equal to zero is usually identified with this constant.

The identification of this level of least water movement in the oceans still remains a problem today. Different scientists have devised various methods for determining this level, none of which work in all cases. A discussion of these various techniques is included in the next section.

The magnitudes of the transports of mass, salt, and heat when based on geostrophic calculations are indirectly related to the choice of the level of no motion through the conversion of the derivative of geostrophic velocity to the velocity itself. Since the object of this study is to compute the transports of mass, salt, and heat across a particular latitude section within the North Atlantic Ocean, considerable effort has been devoted to the establishment of the criteria for determining a satisfactory level of no motion.

II. BACKGROUND

A. HEAT TRANSPORT

The important mechanisms are the transport of sensible and latent heat by the atmosphere and the transport of sensible heat by the ocean. Scientific opinions have fluctuated over the years as to whether the ocean or the atmosphere is the principle contributor to heat transport.

According to Neumann et al. (1966) such noted scientists as Maury (1856) and Ferrel (1890) expressed views that the ocean has the predominant role in transporting excess heat from the equatorial regions to the polar regions of the earth. Angström, in 1925, estimated that the ocean transported an amount of heat equal to that transported by the atmosphere. Others, including Bjerknes et al. (1933) and Sverdrup et al. (1942) expressed agreement that the atmosphere predominated in the poleward transport of heat and that the ocean was relatively insignificant. Sverdrup, however, suggested that in certain areas heat transport by ocean currents could be of importance.

Neumann et al. (1966) wrote: "The atmosphere appears to be doing the lion's share of the heat transport. However, an appreciable part of the transport is latent heat, and the latent heat transport increases from a value near zero at about 20°N to 4×10^{14} cal/sec at 40°N. This latent heat was taken from the oceans by the air, thus decreasing

the store of heat in the ocean and increasing the total heat of the air. The ocean should be credited with carrying this heat to points where it is available to the atmosphere for a further transport poleward. If the latent heat at 40°N is credited to the ocean, this, plus the sensible heat transported by the ocean, accounts for half of the total required by radiation theory.

"The oceans are thus important in bringing about this required balance through both the evaporation-precipitation mechanism and the actual transport of sensible heat."

The present investigation is interested only in the magnitude of transport of sensible heat by ocean currents across the vertical cross section of the North Atlantic Ocean at 40°N.

B. DETERMINATION OF THE LEVEL OF NO MOTION

The importance of determining an accurate level of no motion for the computation of the transports of mass, salt, and heat by the dynamic method has been stated previously. Until the present no universal method has been devised that works in all cases. Most of the methods developed in the last 60 years for determining the level of no motion are indirect approaches which try to find a characteristic that relates to minimum motion in some water layer.

Sverdrup et al. (1942) recommended that the "zero" surface in the ocean be determined by comparing water discharges

computed by the dynamic method from a horizontal reference surface that is successively placed at different depths. The no motion level is selected so that the net mass transported across an ocean section is zero. This, of course, would require that the oceanographic stations span an entire vertical cross section of the ocean which extends from shore to shore. Preferably the stations should be taken within a reasonable time interval to ensure the data are synoptic.

Jacobson (1916) advanced the idea that the oxygen minimum in sea water corresponds to the layer with minimum horizontal water motion. Wüst (1935) and Dietrich (1936) developed the idea and applied it in practice; it is known as Dietrich's method. These two scientists believed that oxygen is lost from sea water as a result of oxidation of organic matter except in a thin surface layer. It was reasoned that if this oxidation process takes place at all levels, due to biological processes, then the minimum oxygen content is found where the replenishment of oxygen by horizontal flow is at a minimum because of weak motion.

When Dietrich applied his method to compute the water transport in the Gulf Stream from the sea surface to the oxygen minimum layer, his computations showed that the water transport for the counter current below the Gulf Stream was twice the amount transferred by the layer above the oxygen minimum. This result is unrealistic and suggests that there are serious difficulties with determining the level of no motion in this manner.

The difficulty is underscored by Seiwell (1937) who examined the causes for minimum oxygen concentrations at intermediate depths in the northwestern part of the Atlantic Ocean and found that the minimum is a result of the ratio between oxygen supply and consumption. In his studies, he examined a hypothetical example and showed that the oxygen minimum does not necessarily occur at a level of minimal horizontal motion.

Parr (1938) tried to relate the vertical current velocity distribution to the disturbance of the density field. The method is based on the assumption of motion along isopycnal surfaces in that the thickness of the layer bounded by two isopycnal surfaces cannot remain constant in the region of a current. In other words, the distance between the two isopycnal surfaces varies in a direction perpendicular to the direction of the current. If the distortion of the layer between two isopycnal surfaces is minimal, or no distortion is evident, then there must be either minimal water movement there or complete lack of water motion. Fomin (1964) pointed out that an undistorted isopycnal layer is a necessary but insufficient condition for the existence of a layer of no motion in the sea. He states, "If there is a layer with a strong vertical pressure gradient at intermediate depth, then the isopycnal layers will be least distorted as compared with the overlying and underlying layers in the presence of a strong gradient current in this layer."

In areas where there is no intermediate vertical gradient maximum, selection of an undistorted isopycnal layer is a difficult if not impossible task.

Another method for determining the level of no motion is described by Stommel (1956) in which the vertical component of velocity, by mass conservation, must equal that induced at the bottom of the frictional layer by the winds. He determined formally the specific reference level at which this matching occurs. When this method was applied to Atlantis Stations 5203 (32° 00'N 63° 03'W) and 5210 (32° 00'N 50° 41'W), the depth of no meridional motion was found to be about 1500m. As stated by Stommel, in that location this was very nearly the depth of the high-salinity anomaly water from the Mediterranean.

Hidaka (1940) used the fact that there is mutual adjustment between the current velocity field and the fields of the physical-chemical properties of sea water to develop his method for determining the layer of no motion. The method was based on continuity considerations for the stationary distribution of certain properties of oceanic water masses. If a triangle of three oceanic stations is considered, at the corners of the triangle there are three vertical and two horizontal planes forming the boundaries of a prism extending throughout the water column. As assumption is made that no gain or loss occurs through the stationary surface boundary and that the sum of volume transports through the remaining

four boundaries must equal zero. If an oceanic property such as salinity is considered, then the sum of the products of salinity and volume transports through each boundary must also equal zero.

Hidaka applied his method to the four triangles formed by four oceanographic stations in an attempt to find a reference level for the conversion of relative into absolute dynamic height topography. Hidaka's simplification of the condition of continuity, and the fact that his system of equations cannot be solved with the existing accuracy of measurements at sea, raised objections by other noted oceanographers.

To the present, the most practical and probably the most widely used method is that developed by Defant (1941). While examining the differences in the dynamic depths of isobaric surfaces at a great number of pairs of neighboring stations, Defant discovered a layer of relatively great thickness in which these differences changed very little along the vertical. The thickness of this layer in the Atlantic Ocean ranges from 300 to 800m; its depth varies rather uniformly in the horizontal direction, and the change in differences in the dynamic depths of isobaric surfaces only amounts to several dynamic millimeters. Defant assumes that this water layer is almost motionless and considers it to be the layer directly adjoining the "zero" surface.

In a strict sense, Defant's method may be expressed as

$$\Delta D_A = \Delta D_B \qquad (1)$$

where ΔD_A and ΔD_B are the increments in dynamic depths between the isobaric surfaces p_n and p_{n+1} at stations A and B. This states that the differences in the dynamic depths of isobaric surfaces at some depth interval are equal at two neighboring stations A and B.

As pointed out by Fomin (1964), it is doubtful whether the layer with similar differences can be identified with the layer of no motion when the current computed by the dynamic method has the same direction above and below the "zero" layer.

Jung (1955) emphasized that the level of no motion is still an open problem although the Sverdrup approach appeared the most reasonable solution. He recommended that the problem be investigated further when sufficient data were available.

III. STATEMENT OF THE PROBLEM

This study consists of four parts: (1) the development of a program for the IBM 360/67 computer that performs the calculations necessary to arrive at values for mass, salt, and heat transport across a section of the ocean; (2) the evaluation and selection, from various interpolation schemes, of the one which performs the interpolation to standard depths with the best accuracy; (3) the establishment of a reference level for which the mass and salt transports equal zero and, based on this reference level, (4) the computation of the transport of sensible heat by the ocean currents across the selected vertical section.

The transfer of energy through a vertical cross section of the ocean is accomplished by processes such as large-scale advection, smaller-scale eddy diffusion, and molecular diffusion. Large-scale advection is the principal contributor in determining the transfer of energy while eddy and molecular diffusion contributions are several orders of magnitude smaller. Eddies smaller than approximately two degrees of longitude have been neglected. Molecular diffusion has been neglected entirely.

Jung (1952) showed that the transfer of all forms of energy in the ocean is very accurately approximated by the transfer of thermal energy alone. To show this he used Starr's (1951) general equation for the advective energy

flux, F, across any section of fluid,

$$F = \int_A (P + \rho c_v T - \rho g Z + \rho \frac{C^2}{2}) V_n \, dA \qquad (2)$$

where dA represents an element of area of the cross section which extends along a latitude circle across the ocean and from the surface to the ocean bottom, P is pressure, T is absolute temperature, Z is vertical distance downward from the ocean surface, ρ is the density, c_v is the specific heat at constant volume of ocean water, g is the acceleration of gravity, C is the ocean current speed, and V_n is the poleward component of velocity. Assuming hydrostatic equilibrium in the vertical, the pressure term, P, nearly cancels the potential energy term, ρgZ. This cancellation would be exact for the case of uniform density. Further, the advection of kinetic energy has been shown to be several orders of magnitude smaller than the transport of internal energy; thus, upon assuming reasonable values of C, the kinetic energy term involving $C^2/2$, can be neglected. With these simplifications, (2) can be written

$$F = \int_A \rho c_v T V_n \, dA \qquad (3)$$

where $\rho c_v T V_n \, dA$ closely approximates internal energy (heat transport) and determines the total energy flux across a vertical cross section of area dA within the ocean.

The specific heat of sea water, c_v, is assumed to have a value of unity with the introduction of an error of less than 1% for depths less than 6000m (see Sverdrup et al., 1942, p. 62).

Procedures outlined by Sverdrup et al. (1942, pp. 408-411 and pp. 447-448) are used to determine the velocity estimates in this study. In using this procedure, one must assume geostrophic balance within the ocean. Since the cross section of the ocean under consideration is outside the equatorial region and only large-scale motion is considered, this assumption seems to be valid (Jung, 1955).

Dynamic heights are determined by standard procedures and then used to compute the velocity difference between depths 1 and 2 in a region between pairs of stations from

$$V_1 - V_2 = \frac{10}{fL}(D_A - D_B) \qquad (4)$$

where f is the Coriolis parameter, $2\Omega\sin\phi$ (Ω being the angular velocity of the earth, ϕ the latitude of the station), L is the distance between stations A and B, and D_A and D_B the dynamic heights (depths) at the two stations.

As stated previously, it is necessary to establish a level of no motion when using this computational procedure. In this study the two criteria which must be satisfied for the determination of this depth are

$$\int_A \rho V_n \, dA = 0 \tag{5}$$

and

$$\int_A \rho S V_n \, dA = 0 \tag{6}$$

where S is the salinity. These equations assert that the net transports of total mass and salt must equal zero when computed across an entire latitude section of the ocean of area A.

Having used these criteria to establish the level of no motion, a value is obtained for the heat transported across the vertical cross section by ocean currents.

IV. PROCEDURE

A. DATA SOURCES

To perform the calculations described in the preceding sections one needs the distribution of temperature and salinity over the vertical cross section of ocean under investigation. The oceanographic data collected during the International Geophysical Year provides the numerous observations of temperature and salinity required for the computation of the transports of mass, salt, and heat across the vertical cross section within the North Atlantic Ocean at 40°N.

The oceanographic ship, Crawford, transited the North Atlantic Ocean along 40°N from 2 to 22 October 1957, occupying a total of 38 oceanographic stations with observations of temperature and salinity being collected at each station. This particular transit was designated Crawford 16, stations 218 to 255, and hereafter, will be referred to only by these station numbers.

These 38 stations extend along 40°N from a point off the New Jersey coast to a point off the coast of Spain (see Figure 1). The maximum distance between any pair of stations is 170.93 km or approximately two degrees of longitude. The horizontal and vertical extent of the data coverage of the cross section is shown in Figure 2. Due to the relatively short period of time in which the data were collected, it

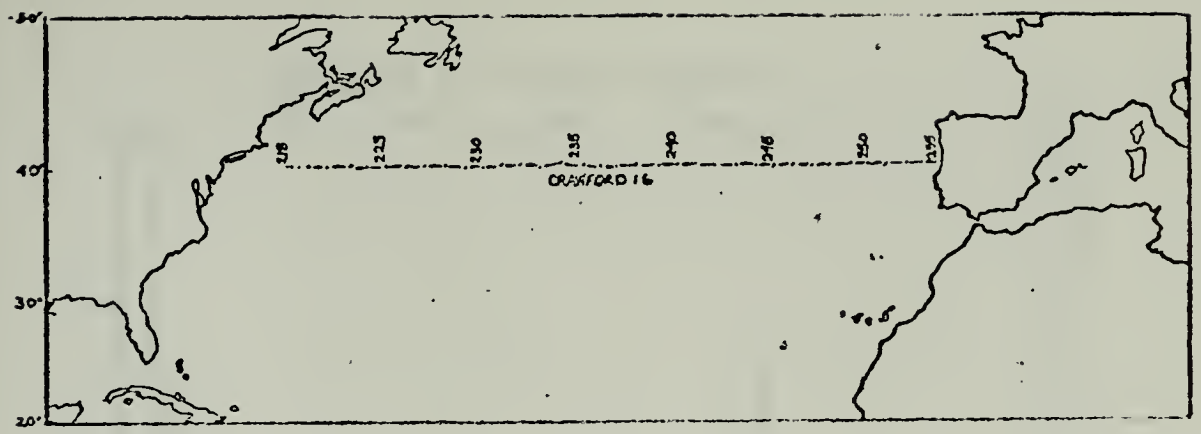

Figure 1. Crawford's transit of the North Atlantic Ocean at 40°N, 2-22 October 1957. Dots indicate stations occupied.

is assumed that the data are completely representative of the thermal and saline distribution occurring that October along this parallel of latitude.

Even though the temperature and salinity data collected by Crawford provides considerable coverage for this cross section of ocean, there are areas along this parallel for which there are no data during the time interval of the Crawford cruise. Two of these regions is that west of station 218 to the North American coast and that east of station 255 to the European coast. The other areas lacking data are the regions between the deepest Crawford observations of temperature and salinity and the ocean floor.

The largest of these areas, that from station 218 to the New Jersey shore, has dimensions of 489 km in the horizontal by 165m in the vertical at station 218 to 0m at the New Jersey shore.

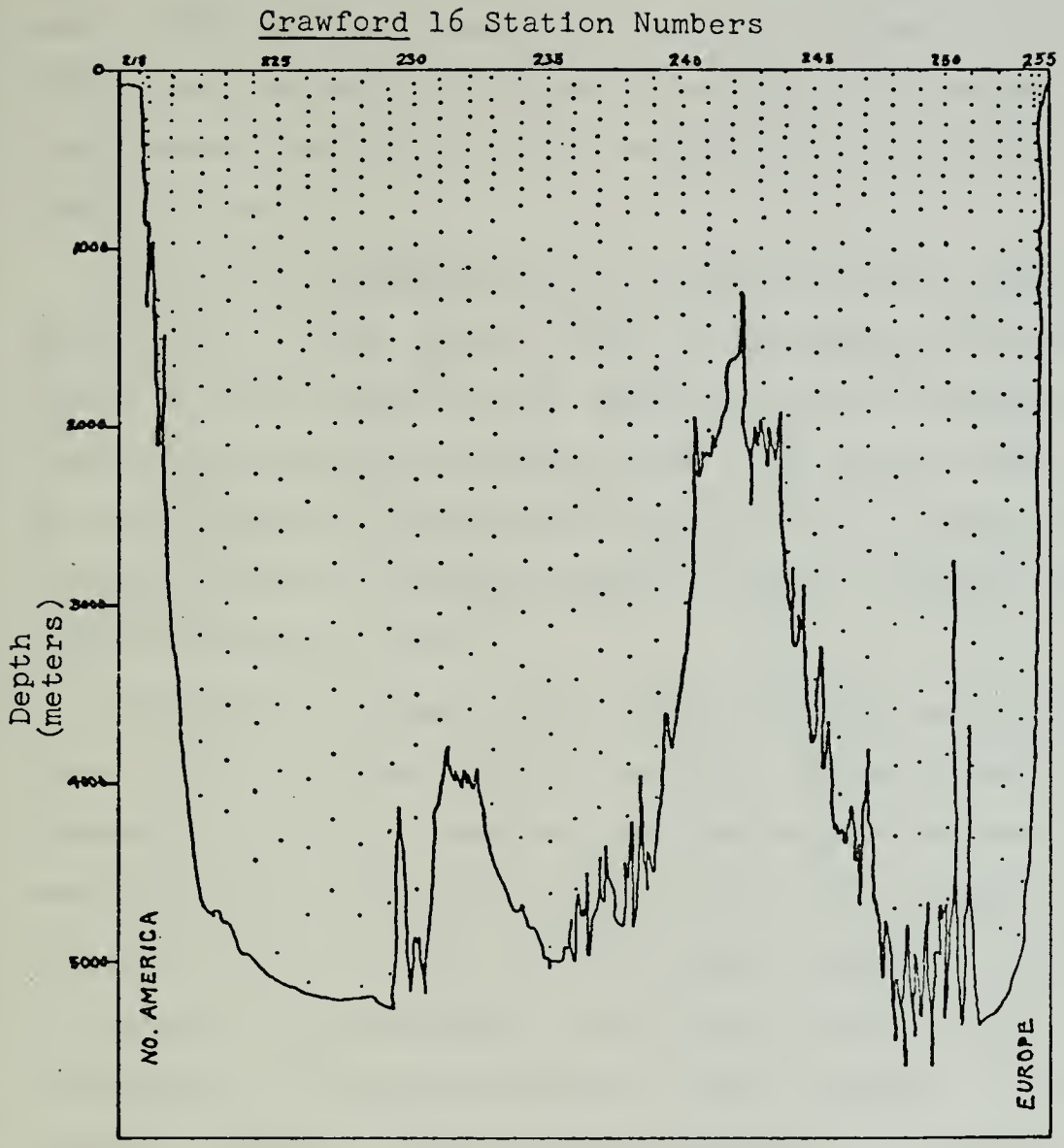

Figure 2. Vertical cross section of the North Atlantic Ocean at 40°N showing the vertical and horizontal extent of temperature and salinity observations. Dots indicate observations of temperature and salinity.

In order to determine the relative importance of the mass, salt, and heat transports for the area west of station 218 it was necessary to arrive at reasonable estimates of the average density, velocity, temperature, and salinity for this area.

The average temperatures for October for this section were taken from the "Serial Atlas of the Marine Environment." Values of the average October temperatures were obtained at one degree longitude increments from 40°N, 69°W to 40°N, 74°W at various depths ranging from 0 to 330 feet. These monthly averages were then averaged again to obtain a single space average value of 13.11°C.

The monthly average of the surface current velocity was taken from the "Pilot Chart of the North Atlantic Ocean" for October 1973. In the section from station 218 westward, the surface current indicated on this chart is in a southerly direction with a velocity of 25.7 cm/sec, which is assumed to approach the geostrophic current due to the east-west orientation of the entire vertical cross section. The geostrophic current at the bottom is assumed to be zero and an average of the surface current and the bottom current is taken to arrive at a single average value of 12.85 cm/sec.

The average value for the salinity of this section was determined from the work of Ketchum and Keen (1955) in which they used depth mean salinities to show a seasonal variation in the concentration of river water on the continental shelf

between Cape Cod and Chesapeake Bay. In this study, their winter depth mean salinities at 20, 30, 40, and 100 fathoms are averaged to arrive at the value of 33.175 ppt for the salinity of the section from station 218 to the coast of New Jersey.

An estimated average density value of 1.02395 g/cm^3 is obtained from the work by Howe (1962). This value is an average of values as read from his graph of Section C, Figure 4.

The average values of temperature, salinity, density, and current velocity obtained in the preceding paragraphs are used to compute estimates of the transport of mass, salt content, and heat in that part of the vertical cross section westward from Crawford station 218 to the New Jersey shore.

The distance from station 255 to the coast of Spain is 67km and the depth of the water is less than 150m. Therefore, it was assumed that the conditions were the same as those between stations 254 and 255. With this assumption, it was possible to take a percentage of the transports of mass, salt, and heat between stations 254 and 255 based on the area eastward of station 255 to the area between stations 254 and 255.

The procedure for obtaining the estimates of the transports of mass, salt, and heat for those areas near the ocean floor is described in a later section.

B. DEVELOPMENT OF THE COMPUTER PROGRAM

An existing computer program, held by the Department of Oceanography of the U.S. Naval Postgraduate School, Monterey, California, which computes absolute current velocities and volume transports between pairs of oceanographic stations was modified so as to compute values for the transport of mass, salt content, and heat. Additional modifications were made to allow the program to perform the necessary summing processes in order to obtain the integrated transports for each pair of stations, and the net transports for the entire cross section. Also the program's capacity for the number of standard depths and stations was increased from 24 to 48 and 48 to 60, respectively.

A copy of the computer program is included in Appendix A.

C. SELECTION OF THE INTERPOLATION METHOD

Since the observed values of temperature and salinity at each station must be interpolated to standard depths for computing the velocity and the various transports in the conventional manner, the problem of selecting an interpolation scheme which comes nearest to approximating the real ocean distribution of temperature and salinity is of major significance.

A comparison was made of four interpolation methods. These methods include linear, mean linear-parabolic[1], mean

---

[1] A mean linear-parabolic interpolation method is a numerical average of one linear plus two parabolic interpolations.

parabolic, and piecewise-cubic polynomial interpolation. The comparison was accomplished with the aid of computer plots of each of these methods at each of the 38 Crawford stations. Visual comparison of the actual temperature and salinity profiles with the interpolated values at 10m increments made it readily apparent that no one method was satisfactory in all cases. It was determined that some combination of a linear and a higher order interpolation method was necessary to give the desired results, especially when there was an isothermal layer near the surface. The results of the comparison of the four different interpolation methods and the specific interpolation method chosen for the rest of this study are included in Section V.A.

D. COMPUTATIONS OF VELOCITIES AND THE TRANSPORTS OF MASS, SALT CONTENT, AND HEAT

With the assumption of geostrophic balance it is possible to use the procedure of computing dynamic heights so as to obtain the velocity estimates for the latitude section. A detailed description of the flow of computations is included in the following paragraphs to aid the reader in understanding the computer program in Appendix A, and the exact procedures used in obtaining the transport values.

The data from Crawford Cruise 16, stations 218 to 255, are at various depths and have to be interpolated to standard depths. This is accomplished by the subroutine "LGTP" (Appendix A) which is the programmed version of the combination

linear and parabolic mean interpolation method. The observed values of temperature and salinity are interpolated to the following standard depths: 0, 50, 100, 150,200, 250, 300, 350, 400, 450, 500, 550, 600, 650, 700, 750, 800, 850, 900, 950, 1000, 1050, 1100, 1150, 1200, 1250, 1300, 1400, 1500, 1600, 1700, 1800, 1900, 2000, 2250, 2500, 2750, 3000, 3250, 3500, 3750, 4000, 4250, 4500, 4750, 5000, 5250, and 5500m.

After obtaining the interpolated values of temperature and salinity at the standard depths, the computer subroutine "SGTSVA" (Appendix A) is called to compute the sigma-t, specific volume anomaly, and specific volume for each standard depth.

With the specific volume anomaly values calculated for each standard depth, the next step is to compute the dynamic heights, D. This process is accomplished in the main computer program. An average specific volume anomaly between each pair of standard depths for each station is computed according to the following equation:

$$\overline{\delta} = \frac{\delta_z + \delta_{(z+\Delta z)}}{2} \qquad (7)$$

where $\overline{\delta}$ is the mean specific volume anomaly, and δ_z and $\delta_{(z+\Delta z)}$ are the specific volume anomalies at the standard depths, z and z+Δz, respectively. The increments, Δz, are in standard depth increments only.

The equivalent of an integration is then accomplished using:

$$\Delta D = \bar{\delta}[z-(z+\Delta z)] \qquad (8)$$

where ΔD is the difference in the dynamic heights (depths) between the standard depths. A vertical summation of the ΔD's is carried out for each station:

$$\Sigma_0^z \Delta D = D \qquad (9)$$

The distance L between stations in (4) is computed with use of the computer subroutine "DSTSTA" (Appendix A) using the following method. The length, in meters, of one degree of latitude and one degree of longitude for each station is computed using the equations based on Clarke's spheroid[2] of 1866. These lengths are functions of the latitude and longitude of each station. The two values for one degree of latitude are averaged as are the two values for one degree of longitude. The difference in the latitudes and the difference in the longitudes of the two stations are computed. The differences in degrees in latitude and longitude of the pair of stations are multiplied by the average values for the length of one degree of latitude and

---

[2]The earth is approximately an oblate spheroid (a sphere flattened at the poles). Its dimensions and the amount of flattening are not known exactly, but the values determined by the English geodesist A.R. Clarke in 1866 as defined by U.S. Coast and Geodetic Survey in 1880 are used for charts of North America.

longitude, respectively. This procedure gives two sides of a right triangle and the third side, the distance L, between the two stations, can be obtained by the use of the Pythagorean relation.

The use of the Pythagorean relation to obtain the third side of a right triangle involves a flat earth assumption. This assumption seems to be reasonable since the maximum distance between any pair of stations is 170km.

With the distance L computed, the computer subroutine "GEOCUR" (Appendix A) computes the relative velocity between pairs of stations at each standard depth according to (4). The relative velocities can be converted to absolute velocities by setting the geostrophic velocity at an assumed level of no motion equal to zero. The computational procedure used for determining the level of no motion from (5) and (6) is discussed later in this section.

The velocity values obtained by the preceding method represent values at standard depths between a pair of stations. The velocity values are averaged in the computer subroutine "GEOCUR" to obtain a velocity in the center of an area bounded by the two stations in the vertical and by a pair of standard depths in the horizontal. This procedure (denoted as Step 1) is illustrated in Figure 3.

Density is computed from the following equation:

$$\rho_{STP} = \frac{1}{\alpha_{STP}} \qquad (10)$$

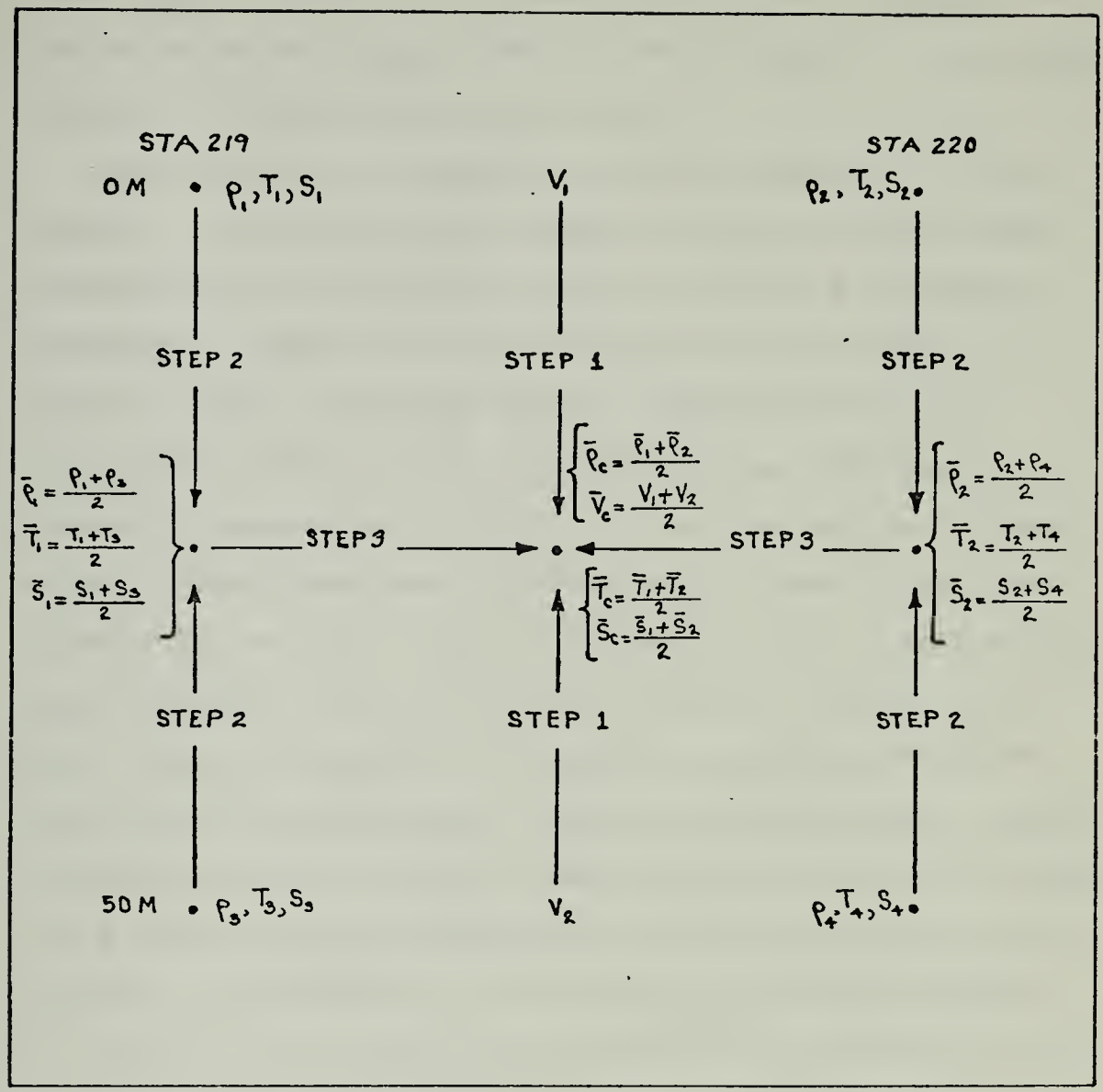

Figure 3. Illustration of the averaging process in order to make values of velocity, density, temperature, and salinity compatible within a sample rectangular area.

where ρ_{STP} is density at a particular salinity, temperature, and pressure, and α_{STP} is the specific volume at a particular salinity, temperature, and pressure.

Since density is computed at standard depths for each station, one has available values for density for the four corners of the rectangular area described in a preceding paragraph. These four values of density are averaged to obtain a value of average density compatible with the average velocity for that rectangular area. The average values of temperature and salinity are obtained in the same manner. This procedure, illustrated in Figure 3, is accomplished in two steps. Step 2 is carried out in the main computer program and the values are stored in a matrix array until they are needed by the computer subroutine "GEOCUR" where Step 3 is performed. This averaging procedure is performed for each rectangular area formed by a pair of stations and a pair of standard depths for the entire vertical cross section. In summary then, the values are either passed to or computed in the subroutine "GEOCUR" for each rectangle are the area, the average density, the average velocity, the average temperature, and the average salinity. The product of the first three gives the mass transport, which when multiplied in turn by each of the remaining averages gives the heat transport and salt transport across a particular rectangular area of the vertical cross section.

The transport values computed for each rectangular area are summed both horizontally and vertically. By summing vertically between each pair of stations, one obtains values for the integrated transports of mass, salt, and heat for that pair of stations. The transport values between each pair of standard depths, for example 0 to 50m, are summed horizontally to give the net transports of mass, salt, and heat in a particular layer of the North Atlantic Ocean at 40°N. These layer values are then summed vertically to give the total net transports of mass, salt, and heat across the entire vertical cross section.

This process is accomplished by the computer program; an example of the method is shown in Figure 4. Wherein it is understood that the transports of mass, salt, and heat have been computed individually for each of the rectangular areas 1 thru 9. For example; the sum of the mass transports for the rectangular areas 1, 4, and 7 gives the integrated mass transport, A, between the pair of stations, 218 and 219. The integrated values for salt and heat transport are computed for each pair of stations in the same manner. Similarly, the mass transport values for the rectangular areas 1, 2, and 3 gives the net mass transport, B, for the layer between 0 and 50m extending from station 218 to station 221.

The computer program computes the transport values for each pair of stations down to the deepest standard depth

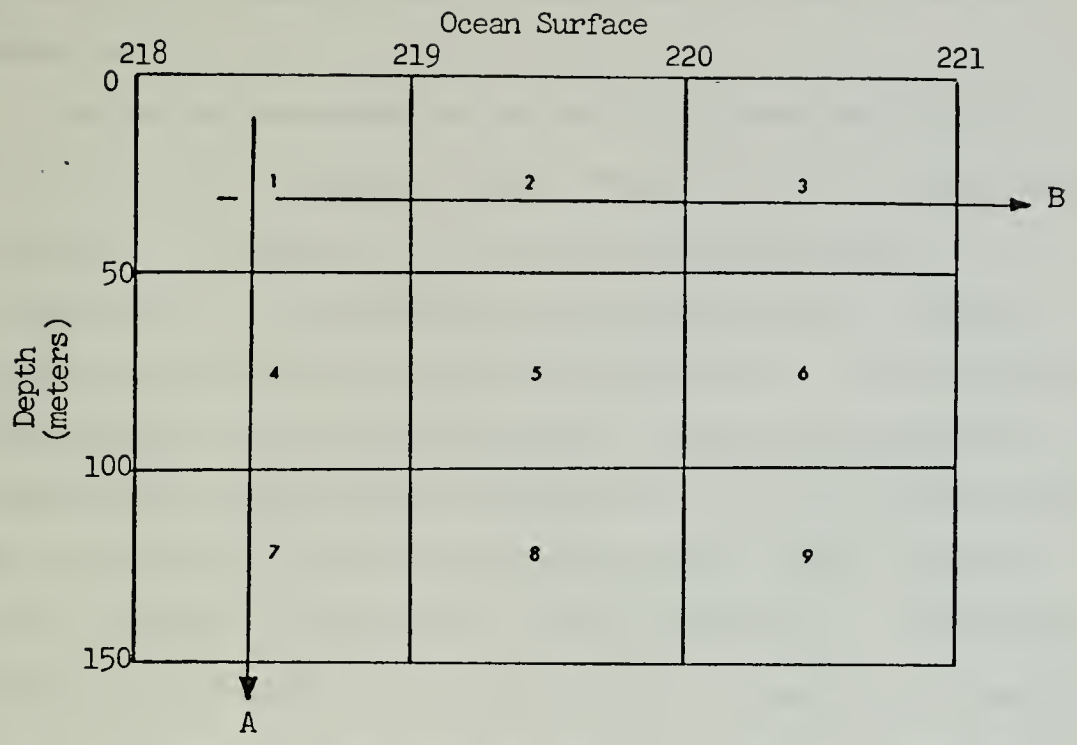

Figure 4. Illustration of the summation process performed in the computer program for a sample cross section of ocean. A represents integrated transport for a pair of stations 218-219. B represents the net transport for the layer 0 to 50m.

common to both stations. Thus, account is not taken for small areas, mentioned previously, of ocean near the bottom where there are no computed values for the transports. The areas in question are represented in Figure 5 as the areas between the bottom of the ocean and the first solid line above the ocean bottom. The solid line above the ocean bottom indicates the deepest depth common to each pair of stations for which the transports are computed. The method for obtaining the estimates of the transports for these

triangles or quadrangles is described in the following paragraph.

Values of temperature and salinity were extrapolated to depths deep enough to cover the entire water area between each pair of stations. In some cases this involved an extrapolation of temperature and salinity into the ocean floor as if the ocean bottom did not exist. The transport values were then computed via the computer program and a percentage value of the water area to the total area present in each rectangle was multiplied by the values of mass, salt, and heat transports for each rectangle. After this process was completed for each of the triangles or quadrangles, a summation was carried out to obtain the estimated net transport values for mass, salt, and heat. The number of areas involved is illustrated in Figure 6. It is recognized that this is only a rough estimate due to the fact that the bottom is not smooth and orderly. Once these values are obtained they are assumed to be constant.

Each time the level of no motion is varied the integrated transports will vary. If the integrated transports are recorded for each level of no motion for each pair of stations, it is possible to determine the amount of change in the integrated transports for a change in the level of no motion. For example, the integrated transports are recorded for the pair of stations, 235-236, with the level of no motion set at 1000m and then at 1050m. The difference between the

Figure 5. Vertical cross section through the North Atlantic Ocean at 40°N showing the deepest level common to a pair of stations for which the transports of mass, salt, and heat are computed. Numbers across the top of the figure represent Crawford stations 218 to 255.

Figure 6. Vertical cross section through the North Atlantic Ocean at 40°N showing the areas for which the estimates of the transports of mass, salt, and heat are made from extrapolated temperature and salinity values. Values of temperature and salinity are extrapolated for every intersection of dashed lines. Darkened areas are considered to have negligible transports of mass, salt, and heat.

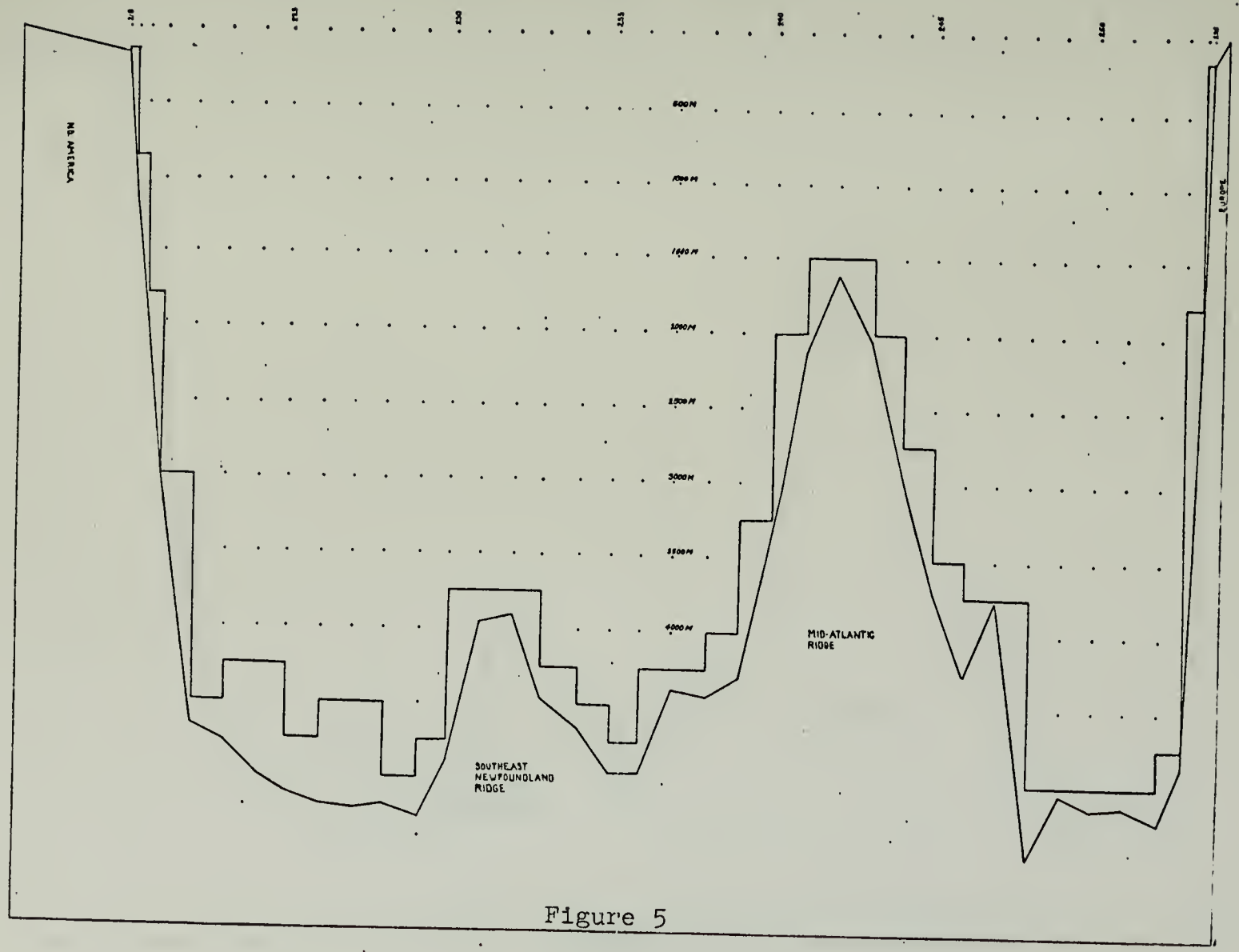
N.B. AMERICA
SOUTHEAST
NEWFOUNDLAND
RIDGE
MID-ATLANTIC
RIDGE

Figure 5

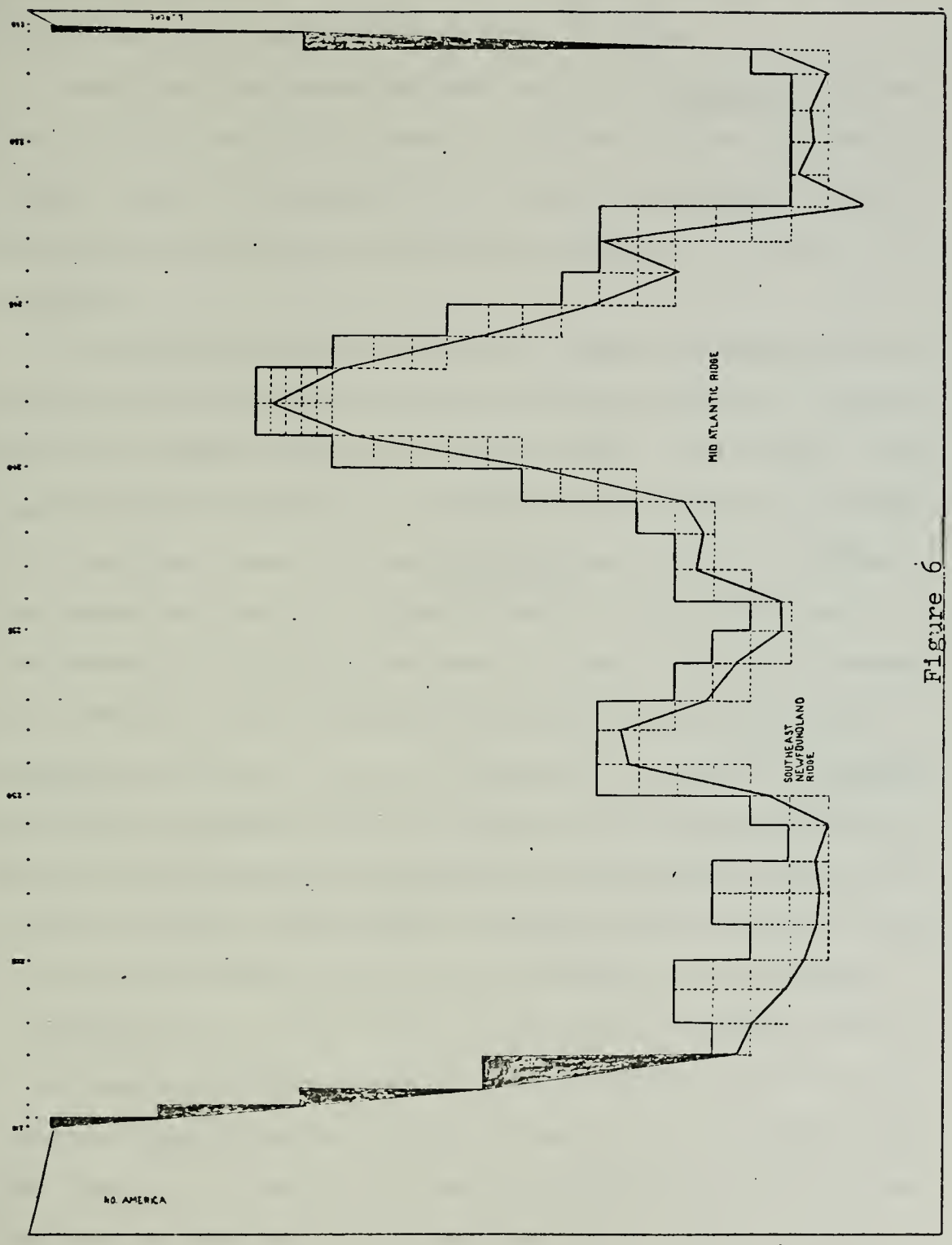
MID ATLANTIC RIDGE
SOUTHEAST NEWFOUNDLAND RIDGE
NO. AMERICA

Figure 6

transport figures is the amount of change when the level of no motion is shifted from 1000m to 1050m.

The above procedure is used only for Crawford stations 222 to 253. The shaded areas in Figure 6 along the continental slope of both the United States and European coasts are considered to have negligible transports of mass, salt, and heat.

To show that the mass and salt balance obtained with the inclusion of the mass and salt transport estimates in the areas for which there are no actual data, causes only slight variations in the level of no motion obtained by a mass and salt balances based only on Crawford data, the following procedure was adopted. First a level of no motion was determined by balancing the mass and salt transports across the portion of the vertical cross section covered by the Crawford data only, i.e., all areas not covered by Crawford data were neglected. Next a level of no motion was determined by balancing the mass and salt transports across the vertical cross section which included those estimates of the transports of mass and salt for the areas not covered by Crawford data. If the level of no motion obtained by the first approach agreed reasonably well with the level of no motion obtained in the second approach, it was assumed that the level of no motion obtained from Crawford data only was the best approximation of the level of no motion for this cross section of ocean since it was based on actual data.

The level of no motion was determined by balancing the mass and salt transports across the entire vertical cross section. This is accomplished by setting a constant level of no motion equal to a standard depth into the computer program, for all pairs of stations and computing the net transports of mass, salt, and heat for the entire cross section of the ocean. This procedure was repeated for a different standard depth until the net transports of mass and salt change sign. In this particular computer program positive values indicate northward movement and negative values southward movement. If a level of no motion specified for any particular pair of stations was deeper than the data for the two stations, the program automatically used the deepest level common to both stations.

Once the net transports of mass and salt have changed sign, the level of no motion is varied (by hand) for pairs of stations until a balance of the mass and salt transports is achieved for the entire vertical cross section of the North Atlantic Ocean at 40°N.

V. DISCUSSION OF RESULTS

A. COMPARISON OF VARIOUS INTERPOLATION METHODS

It was not until this work was completed that the work of Borkowski and Goulet (1971) was discovered. They recommend the use of linear interpolation at the top and bottom of the profile and mean parabolic interpolation otherwise. This recommendation came as a result of a comparison of ten different interpolation methods with values obtained from an *in situ* STD (salinity-temperature-depth) recorder.

The same conclusion was drawn by the author after making a comparison of four different interpolation methods at each of the 38 *Crawford* stations. While comparing these four interpolation methods, it became apparent that two problem areas existed. The first problem area is at stations that have an isothermal layer near the surface; the second problem area exists at all stations that exhibit a permanent thermocline. As a general rule, higher order interpolation methods overestimate the temperatures in the isothermal layer while the linear interpolation method overestimates the temperatures in certain areas of the permanent thermocline.

Crawford Station 221 is specifically singled out for illustration of the comparison process due to the indications of the isothermal layer at the surface and the steep thermocline below this layer. Figures 7, 8, 9, and 10 are computer plots of the vertical temperature profile for this station.

The crosses represent the observed values of temperature while the continuous line represents values of temperature interpolated at every 10m using the various interpolation methods.

Figure 7 is a plot of the linear interpolation method. This method provides satisfactory interpolated values for the isothermal layer between the surface and the 2nd observed values in Figure 7, but does not give as good an approximation of the temperature distribution as some of the other interpolation methods in the area of the 3rd, 4th, and 5th observed temperature values.

Figure 8 is a plot of the mean linear-parabolic interpolation method. This interpolation method is a numerical average of the combination of two parabolic interpolations plus one linear interpolation for a specific standard depth. One of the three-point parabolic interpolations includes the observed values two depths above and the observed value one depth below the standard depth. The other three-point parabolic interpolation includes the observed value one depth above and the observed values two depths below the standard depth. It is obvious from the plot that this interpolation method does not provide satisfactory values for temperature in the region of the isothermal layer between the surface and the 2nd observed temperature value.

In Figure 9, a piecewise-cubic polynomial interpolation method is shown. This interpolation method tends to produce

even higher values of temperature in the isothermal layer, plus a slight exaggeration of the profile between the 3rd, 4th, and 5th observed temperature values. Another disadvantage of the piecewise-cubic polynomial interpolation is that it requires more computer time than the other interpolation methods.

The interpolation method finally adopted for use in this research is a combination of linear interpolation between the first two observed values and the last two observed values with a mean parabolic interpolation method for the rest of the profile. The mean parabolic interpolation was used because the work by Borkowski and Goulet (1971) showed, by statistical means, that the mean parabolic interpolation method was more accurate in the nonlinear portion of the profile. This method is illustrated in Figure 10.

A comparison of the previously discussed interpolation methods, with the exception of the piecewise-cubic polynomial interpolation method, is made to determine the effect of the interpolation method on the net transports of mass, salt content, and heat across the entire vertical cross section. If the level of no motion is held constant then variation in the transport values is entirely due to the different interpolated values of temperature and salinity as obtained by the different interpolation methods.

As can be seen from Table I, there is a considerable difference in the magnitude of the transports computed by

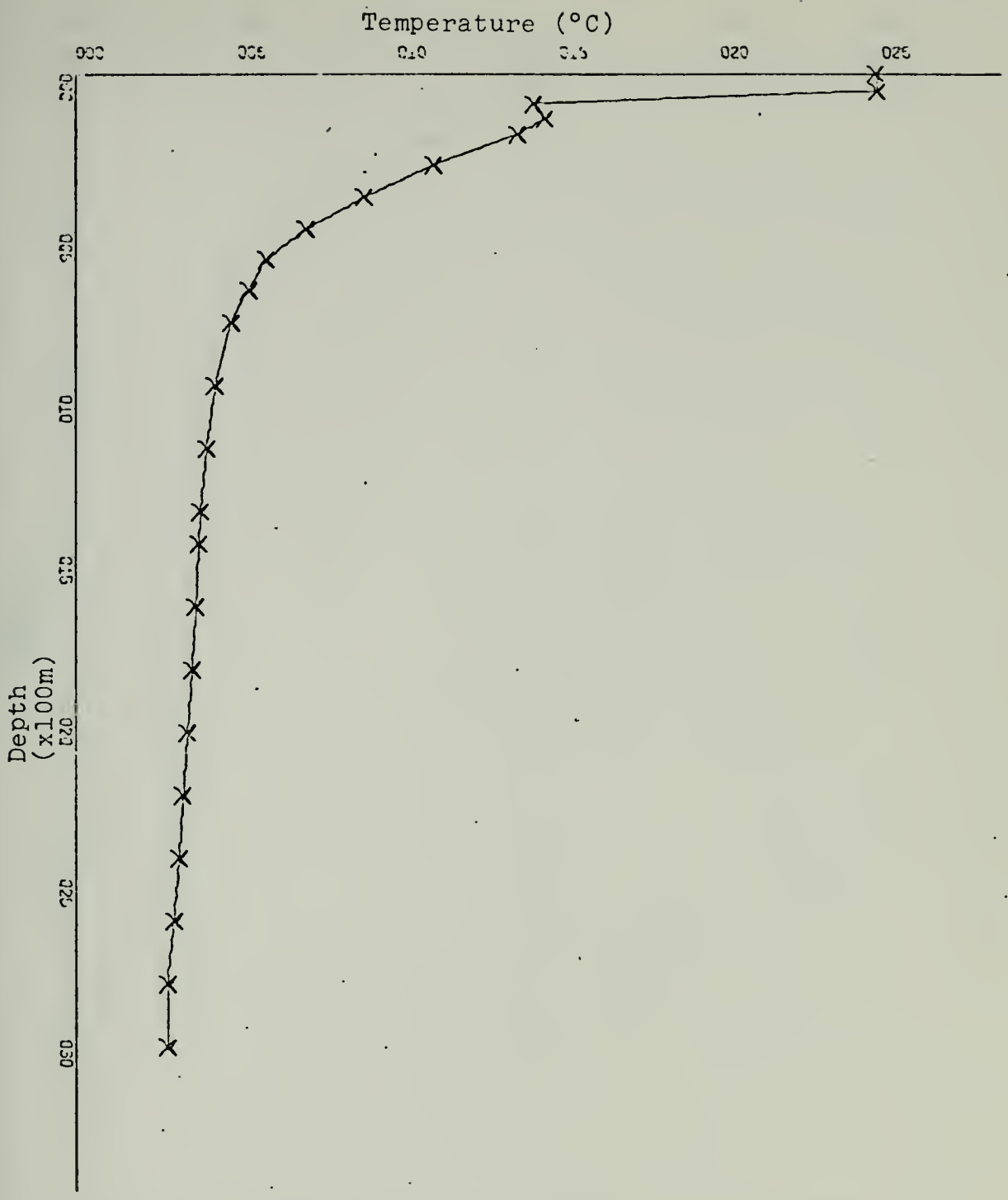

Figure 7. Computer plot of the linear interpolation method for the vertical temperature profile at Crawford Station 221. Crosses represent observed values. Continuous line represents values interpolated every 10m.

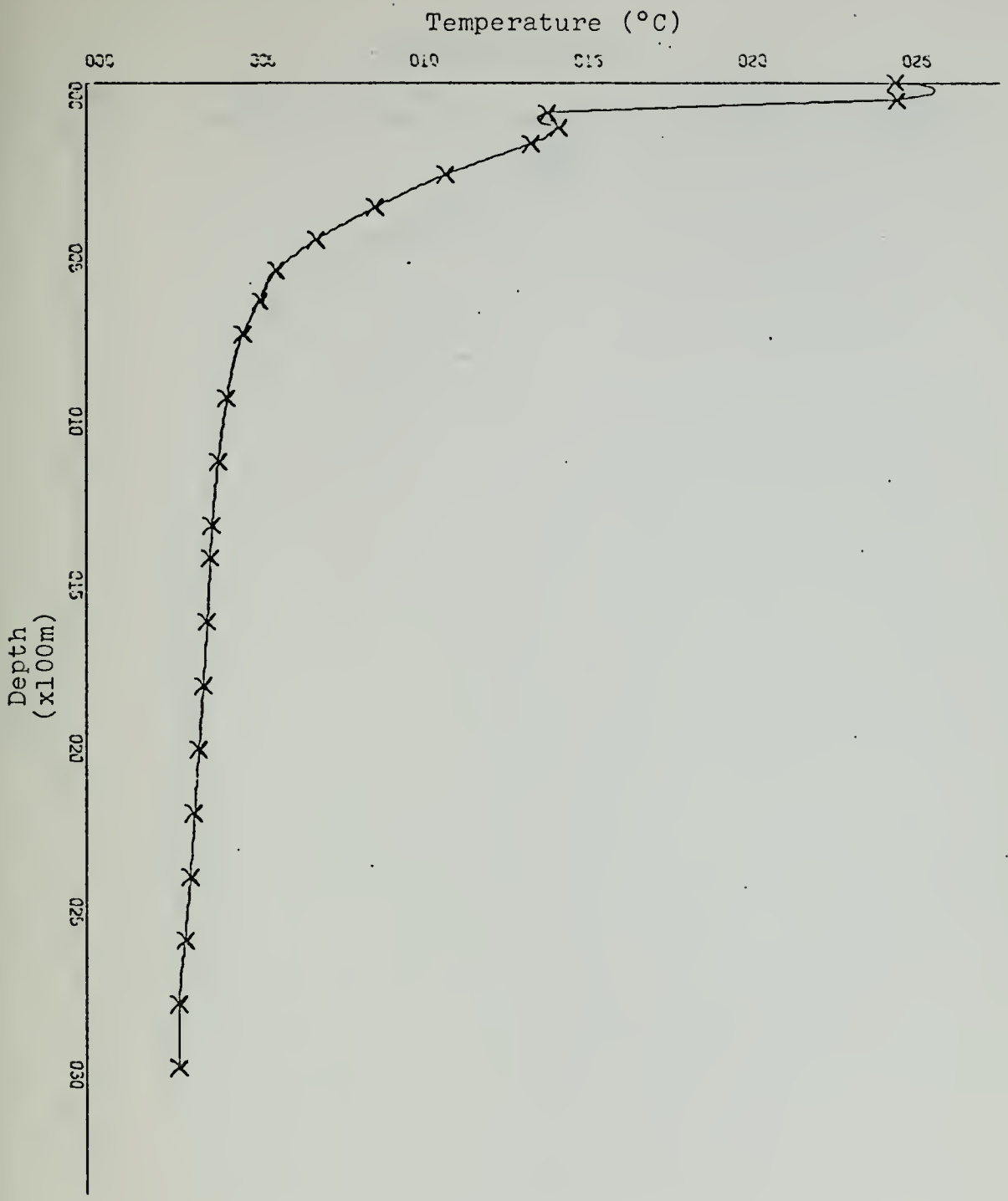

Figure 8. Computer plot of the mean linear-parabolic interpolation method for the vertical temperature profile at Crawford station 221. Crosses represent the observed values. The continuous line represents values interpolated every 10m.

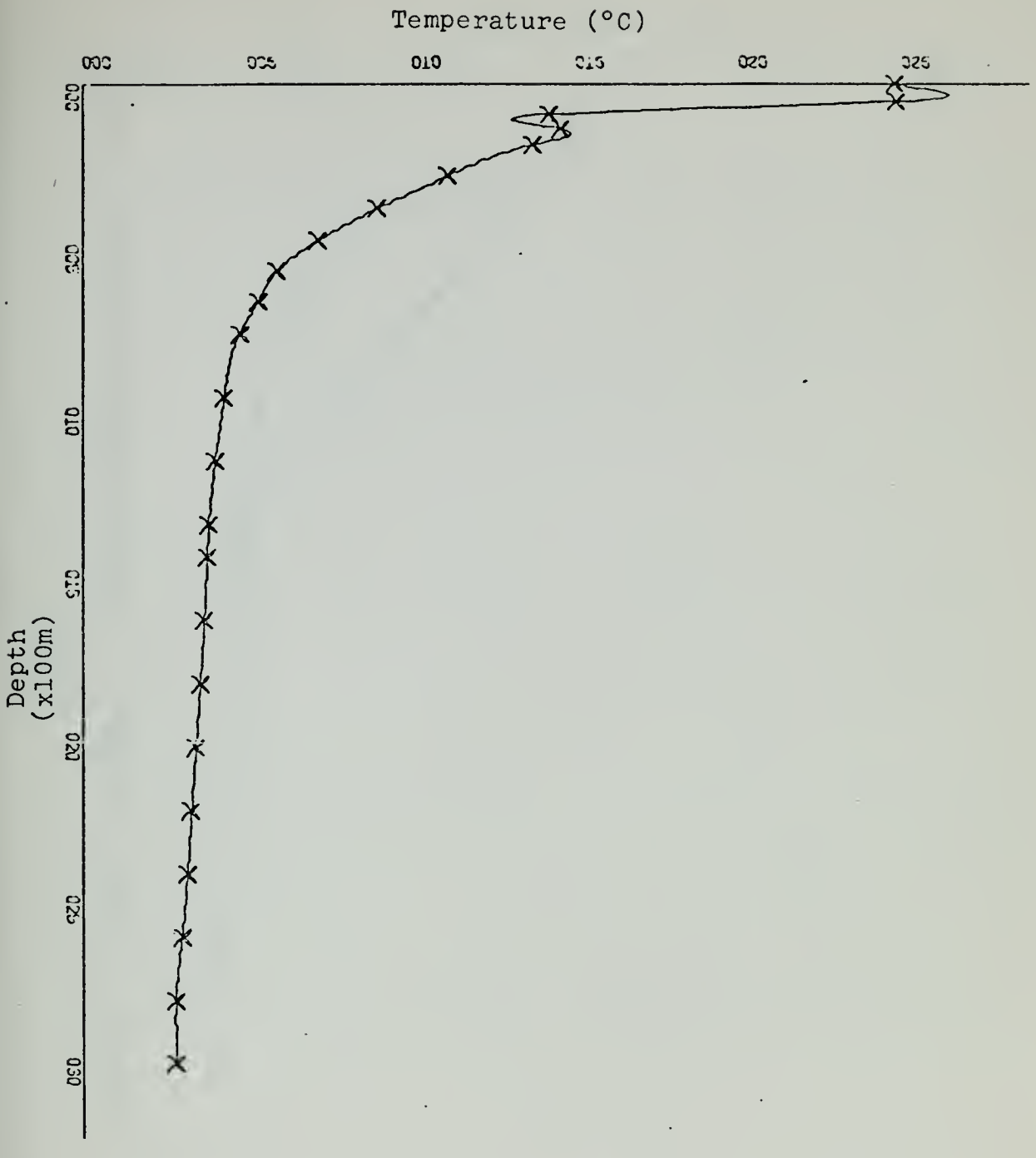

Figure 9. Computer plot of the piecewise-cubic polynomial interpolation method for the vertical temperature profile at Crawford station 221. Crosses represent the observed values. The continuous line represents values interpolated every 10m.

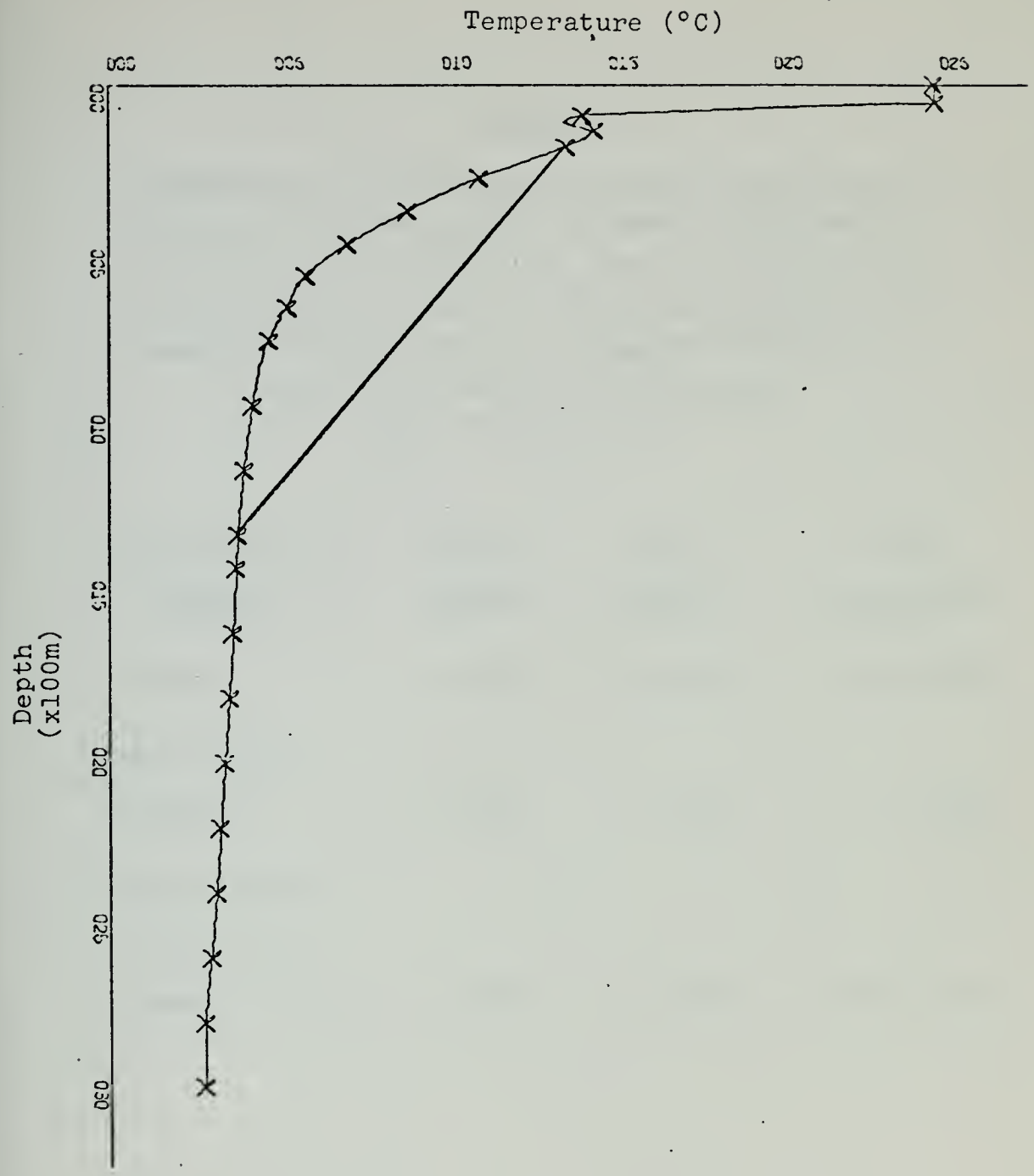

Figure 10. Computer plot of the combination linear and mean parabolic interpolation method for the vertical temperature profile at Crawford station 221. Crosses represent the observed values. The continuous line represents values interpolated every 10m.

TABLE I

Comparison of the Effect of Various Interpolation Methods on the Transports of Mass, Salt Content, and Heat at 40°N within the North Atlantic Ocean. (Positive values indicate northward transport and negative values indicate southward transport.)

Level of No Motion Held Constant

(All Values x 10^{12})

Interpolation Method	Mass gm/sec	Salt gm/sec	Heat gm-cal/sec
Linear	- 1.7543	- 53.9933	- 316.9080
Mean Linear-Parabolic	- 0.4966	- 8.8255	+ 48.1338
Combination of Linear and Parabolic Mean	- 0.2677	- 0.5861	+ 114.4340

the linear interpolation method when compared with the other two. One explanation for this difference can be traced to the observations of temperature and salinity which are missing between the depths of 200m and 1295m at Crawford Station 220. The other 37 stations have observations of temperature and salinity in this depth region at approximately 100m increments; therefore, the use of the linear interpolation method would not have as drastic an effect at these stations. The cause for the large variation is illustrated in Figure 10. Assume that the observations of temperature and salinity are missing between the 5th and 13th observations for station 221, and that one is using the linear interpolation method. The line drawn in Figure 10 illustrates the resulting linear interpolation for this region. Higher temperatures at the standard depths would be obtained and these values, coupled with large negative velocities, would account for the large deviation in the transport values obtained by this method. In this case, the mean parabolic interpolation method would more closely approximate the actual temperature distribution expected in this region.

B. LEVEL OF NO MOTION

The determination of the level of no motion for the entire vertical cross section requires that net transports of mass and salt across that section be equal to zero. The level of no motion for each pair of stations based solely on Crawford data is listed in Table II. This level of no motion is based

TABLE II

Level of No Motion for Each Pair of Crawford Stations at 40°N Within the North Atlantic Ocean

(Values in parentheses represent changes in the level of no motion as a result of taking into consideration all the areas in the vertical cross section of ocean not covered with Crawford data.)

Crawford Stations	Level of No Motion (Meters)	
218-219	150	
219-220	850	
220-221	1150	(1100)
221-222	1200	(1250)
222-223	1200	
223-224	1200	
224-225	1200	
225-226	1250	(1300)
226-227	1200	(1300)
227-228	1300	(1250)
228-229	1200	
229-230	1200	(1300)
230-231	1200	
231-232	1250	
232-233	1200	
233-234	1250	
234-235	1250	
235-236	1200	
236-237	1200	
237-238	1200	
238-239	1250	
239-240	1250	
240-241	1250	
241-242	1200	
242-243	1100	
243-244	1200	
244-245	1150	
245-246	1200	
246-247	1200	
247-248	1200	
248-249	1200	
249-250	1200	
250-251	1200	(1250)
251-252	1200	
252-253	1150	
253-254	1100	
254-255	150	

upon the balance of the integrated mass and salt transports shown in Table III.

The sums of the different columns represent the net transports of mass, salt, and heat across the entire vertical cross section. The near balance of the mass and salt transport columns represents an attempt to balance both of these simultaneously. It should be noted that the balance of either one is not equal to zero exactly. If one rounds each of the integrated mass and salt transports to the nearest whole number x 10^{12} then the salt transport balance is off by +1 x 10^{12} while the mass transport balance is off by -1 x 10^{12} from an exact balance. The balance in Table III represents a compromise between the best mass balance and the best salt balance. If one attempts to balance only the salt transport while ignoring the mass balance then it is possible to make the net salt transport value in Table III closer to zero. The opposite is true if the mass transport is balanced without regard for the salt balance. When this is done the variation in the level of no motion is only 50m at three pairs of stations.

The second approach in determining the level of no motion was to assume that the mass and salt transports of the areas neglected in the first approach were significant. Once the estimates for the transports of mass, salt, and heat were obtained for these areas, the level of no motion was varied between pairs of stations until a balance of the

TABLE III

Integrated Transports of Mass, Salt, and Heat
(Positive values represent northward transport,
negative values represent southward transport)
(All values x 10^{12})

Crawford Stations	Transports Mass gm/sec	Salt gm/sec	Heat gm-cal/sec
218-219	-0.048	-1.679	-13.751
219-220	7.839	276.115	2223.725
220-221	-3.466	-121.334	-967.546
221-222	-0.718	-25.308	-202.166
222-223	2.588	98.986	854.604
223-224	0.144	-0.998	-63.565
224-225	1.328	46.447	367.518
225-226	-8.409	-294.734	-2336.479
226-227	17.277	634.543	5177.051
227-228	-20.877	-759.727	-6188.070
228-229	3.160	111.538	900.428
229-230	.969	32.936	245.045
230-231	9.650	352.005	2859.991
231-232	-9.637	-350.146	-2834.232
232-233	0.215	5.795	3.316
233-234	-.539	-13.904	-1.416
234-235	9.188	342.636	2817.137
235-236	-9.294	-335.634	-2693.083
236-237	5.620	184.374	1394.852
237-238	-6.622	-223.337	-1721.683
238-239	1.301	39.190	278.117
239-240	6.987	251.106	2015.054
240-241	-7.047	-252.019	-2015.903
241-242	0.047	1.534	11.676
242-243	1.881	67.120	536.609
243-244	2.939	105.393	843.956
244-245	-1.114	-40.968	-332.850
245-246	1.232	42.960	339.036
246-247	-1.911	-70.292	-572.699
247-248	0.449	19.228	168.333
248-249	-2.800	-98.216	-776.739
249-250	0.389	12.659	95.273
250-251	-0.389	-14.214	-115.026
251-252	2.076	72.249	569.122
252-253	-1.454	-51.382	-408.233
253-254	-1.137	-40.494	-318.681
254-255	-0.084	-3.014	-24.269
Net Transports	-0.268	-0.586	+114.43

mass transport occurred. It turns out that the level of no motion has to be varied at only 7 pairs out of 37 pairs of stations, the maximum variation at any one pair of stations being 100m. The new levels of no motion for the 7 pairs of stations are shown in Table II in parentheses.

A comparison of the level of no motion obtained by both approaches is shown in Figure 11. The solid line indicates the level of no motion established with the first assumption: that the areas west of station 218, east of station 255, and near the ocean floor make negligible contributions to the transport of mass, salt, and heat. The dashed line indicates the variations to this level of no motion when making the opposite assumption. It can be seen from either Figure 11 or Table II that the maximum variation in the level of no motion using either assumption is 100m, which occurs at two pairs of stations, 226-227 and 229-230. This would indicate that the level of no motion determined solely from actual Crawford data is a good approximation.

Table IV shows the magnitude of the estimates for the various transports in those areas not covered by Crawford data. The estimates in the fourth line of Table IV are the estimates obtained from the computer program when the level of no motion is varied to achieve a mass balance for the entire cross section with those areas not covered by Crawford data included. By summing each column in Table IV, one obtains the net transports across the entire vertical cross section of the North Atlantic Ocean.

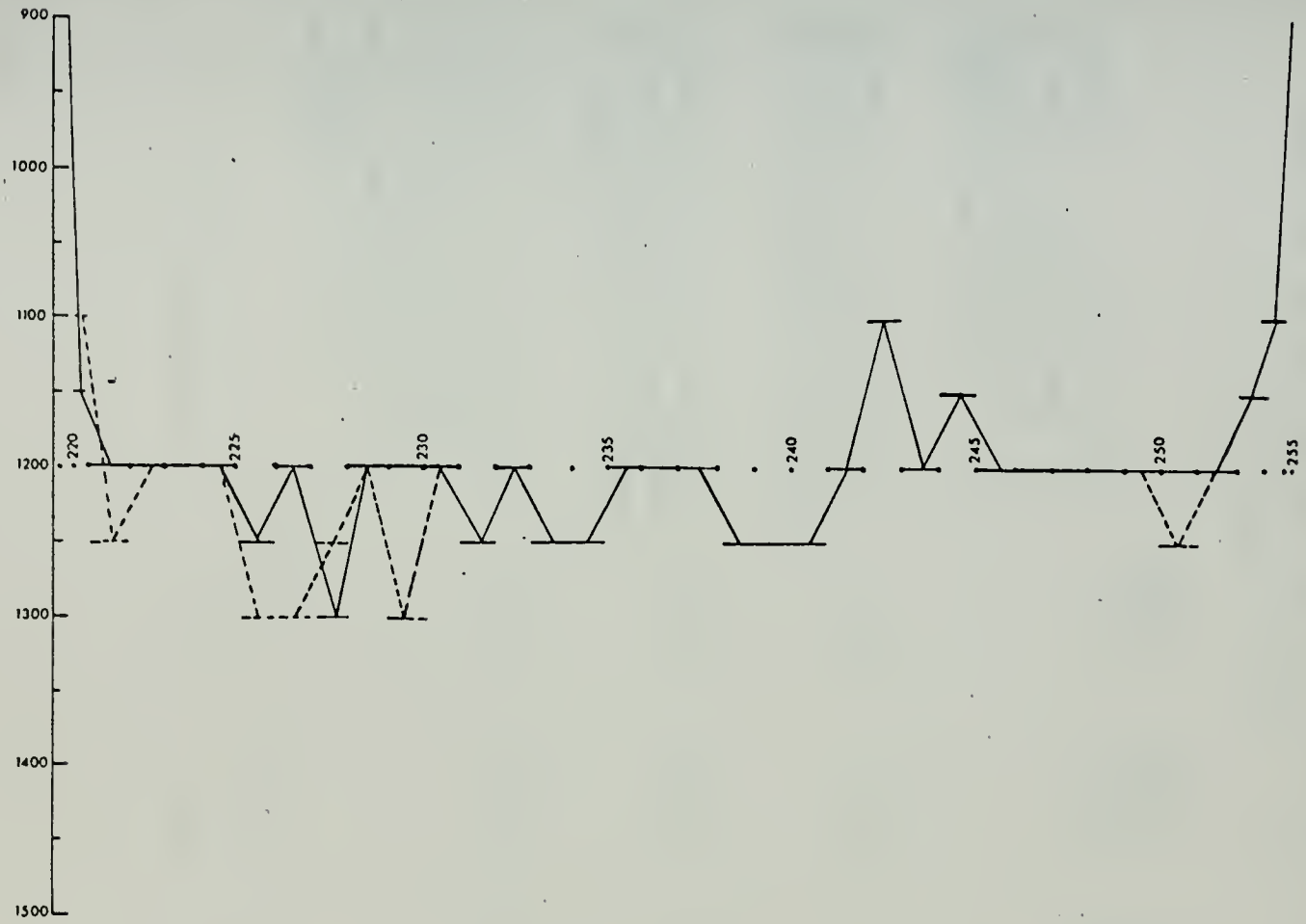

Figure 11. Comparison of the level of no motion determined by two approaches for the cross section at 40°N within the North Atlantic Ocean. Solid line represents the level of no motion determined solely from Crawford data. Dashed lines represent the variations in this level of no motion as a result of including all areas not covered by Crawford data.

TABLE IV

Transports of Mass, Salt, and Heat
Including all Areas Not Covered by Crawford Data

(Positive values indicate northward transport and negative values indicate southward transport.)

(All values x 10^{12})

	Mass gm/sec	Salt gm/sec	Heat gm-cal/sec
Estimates of the transport of mass, salt, and heat for the area westward from Crawford Station 218 to the coast of New Jersey.	-6.439	-213.540	-1842.942
Estimates of the transport of mass, salt, and heat for the area eastward of station 255 to the coast of Spain.	-.128	-4.589	-32.026
Estimates of the transport of mass, salt, and heat for the bottom areas not covered by Crawford data.	+2.571	+81.734	+670.659
Estimates of the transport of mass, salt, and heat based on the level of no motion determined by the mass transport balance including the above estimates.	+4.003	+149.276	+1304.520
Net Transports	+.008	+12.881	+100.211

An attempt to balance only the mass transport was undertaken since it was felt there was less chance of error in the estimates of density than those of salinity. The values of salinity in the region from Crawford station 218 to the United States coast are highly variable due to considerable river runoff from the Hudson and Delaware Rivers. It is important to understand that various transports of mass, salt, and heat obtained for those areas not covered by Crawford data are very rough estimates and that there is no way of checking their validity. The comparison of the two levels of no motion in Figure 11 shows that there is very little variation resulting from the two different approaches. A comparison of the results in Tables III and IV shows there is also very little resulting variation in the net heat transport values for the vertical cross section. Since by comparison of the two approaches, one obtains approximately the same results, the level of no motion obtained by using only the Crawford data is the one upon which the rest of this work is based.

Table V shows the effect on the balance of mass and salt transports, and the net transport of heat by varying the level of no motion for each pair of stations 50m either side of the presently established level of no motion. The level of no motion is not varied between stations 218-219, 219-220, and 254-255 because of their shallow depths; it is assumed that the level of no motion is located at the ocean

TABLE V

Comparison of the Net Transports of Mass, Salt, and Heat for the Vertical Cross Section at 40°N Within the North Atlantic Ocean When the Level of No Motion is Varied 50m Above and Below the Level of No Motion Obtained from Actual Crawford Data

(Positive values indicate northward transport, negative values indicate southward transport.)

(All values x 10^{12})

	Mass gm/sec	Salt gm/sec	Heat gm-cal/sec
50m above	-3.288	-106.994	-728.523
Level of No Motion (Based on Crawford Data)	-0.268	-0.586	+114.434
50m below	+24.923	+911.009	+7509.230

floor for these stations. The differences in the transports are considerable thus providing additional evidence that the level of no motion obtained in this study lies somewhere in between these limits.

C. VELOCITIES

Within the North Atlantic Ocean at latitude 40°N the Gulf Stream Current System begins to meander and is generally considered to have a west to east flow. It is also a region where the system begins to diffuse; and the surface current velocities are generally recognized as gradually becoming weaker as one proceeds from west to east.

Geostrophic velocities were computed for every standard depth that is common to a pair of stations. The geostrophic velocities between each pair of stations at 0, 1000, 2000, 3000, and 4000m are shown in Figures 12, 13, 14, 15, and 16 respectively.

The maximum surface geostrophic velocities occur between stations 226-227 and 227-228: 44.18 cm/sec in the northward direction and -48.45 cm/sec where the minus sign indicates southward flow, respectively. This is probably related to a meander of the Gulf Stream Current that crosses 40°N. The water temperatures in this region are higher than the surrounding water temperatures which is a further indication that these velocities can be associated with the Gulf Stream.

Fuglister (1964) showed the path of the Gulf Stream in the vicinity of 40°N to be complex (see Figure 17). The

Figure 12 Surface Geostrophic Velocities

Figure 13 Geostrophic Velocities at 1000m

Figure 14 Geostrophic Velocities at 2000m

Figure 15 Geostrophic Velocities at 3000m

Figure 16 Geostrophic Velocities at 4000m

(In the figures listed above, the vertical axis is in cm/sec. The horizontal axis represents Crawford stations 218 to 255. Positive velocity values represent a northward flowing current while negative values represent southward flow. The solid arrows represent velocities computed from the level of no motion based only on Crawford data.)

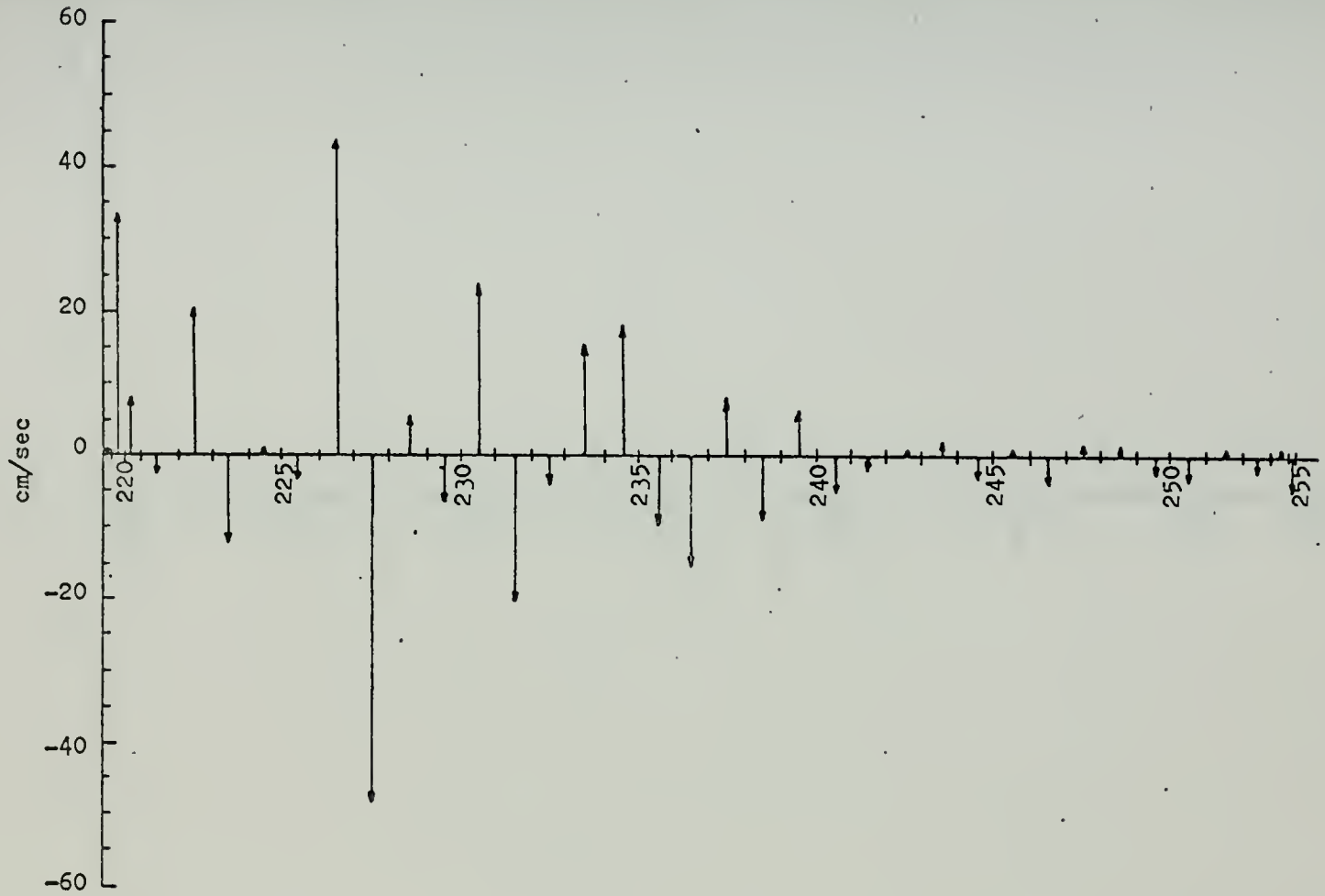

Figure 12

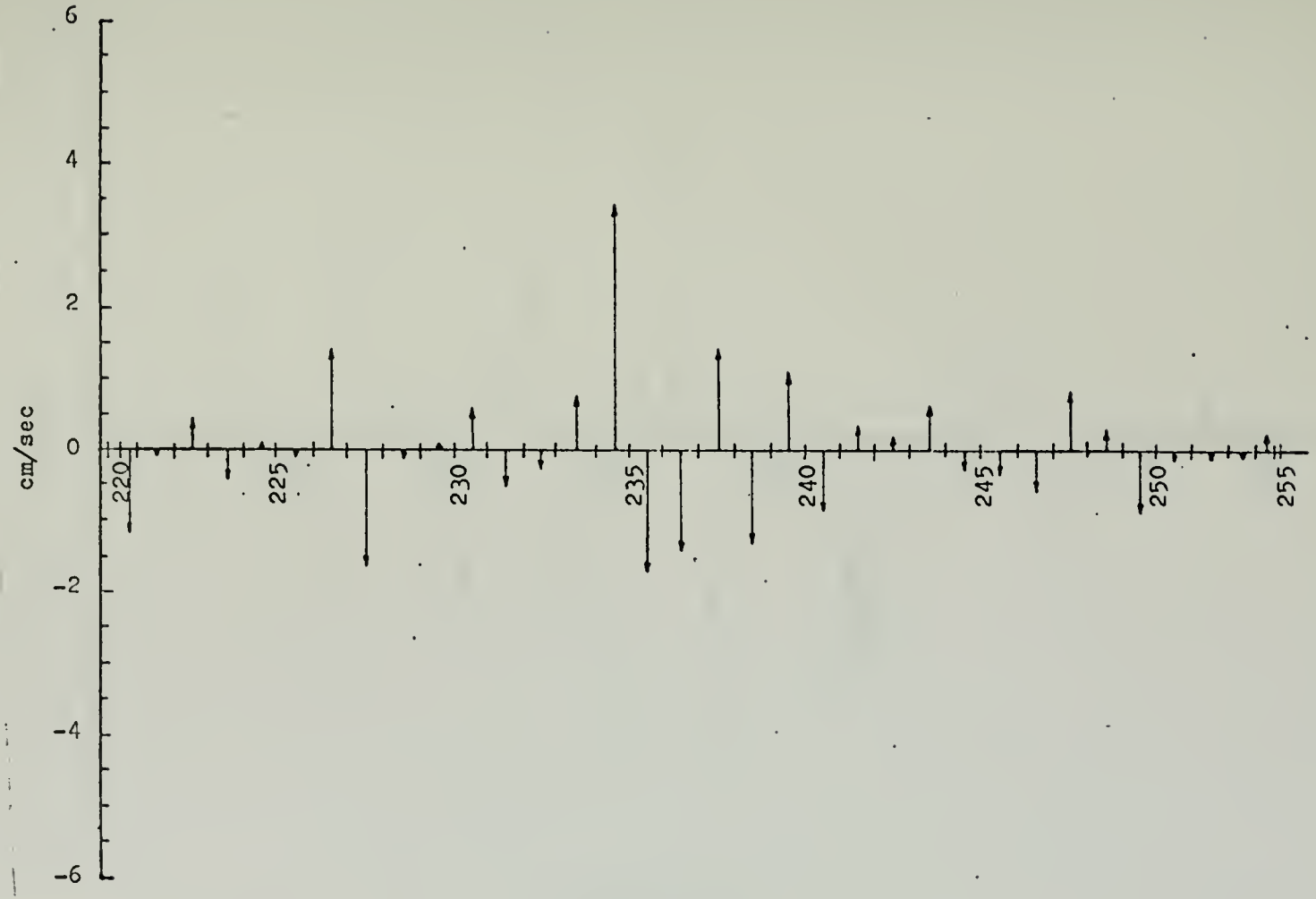

Figure 13

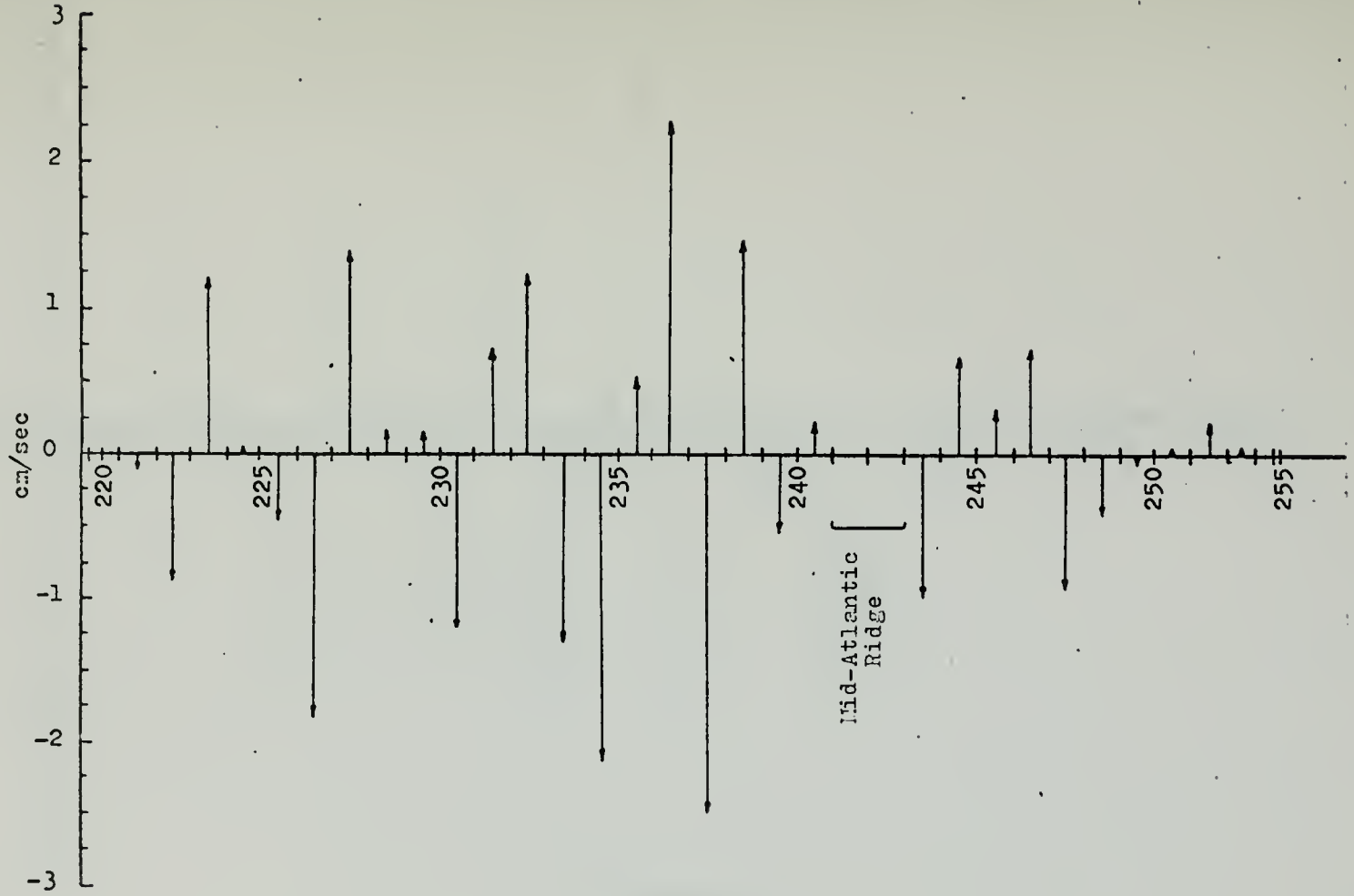
3
2
1
0
-1
-2
-3
cm/sec
220
225
230
235
240
245
250
255
Mid-Atlantic
Ridge

Figure 14

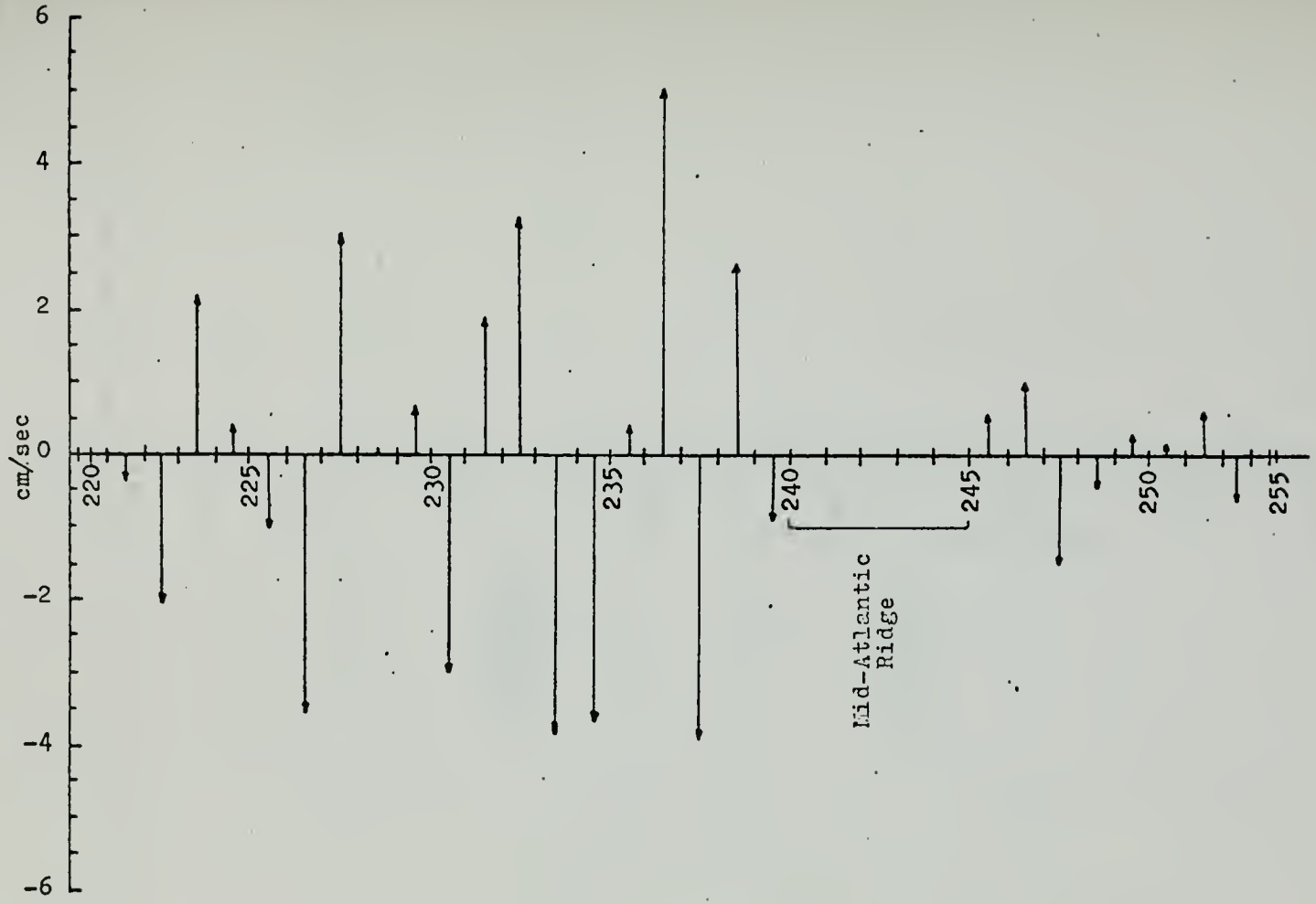
6
4
2
0
-2
-4
-6
cm/sec
220
225
230
235
240
245
250
255
Mid-Atlantic
Ridge

Figure 15

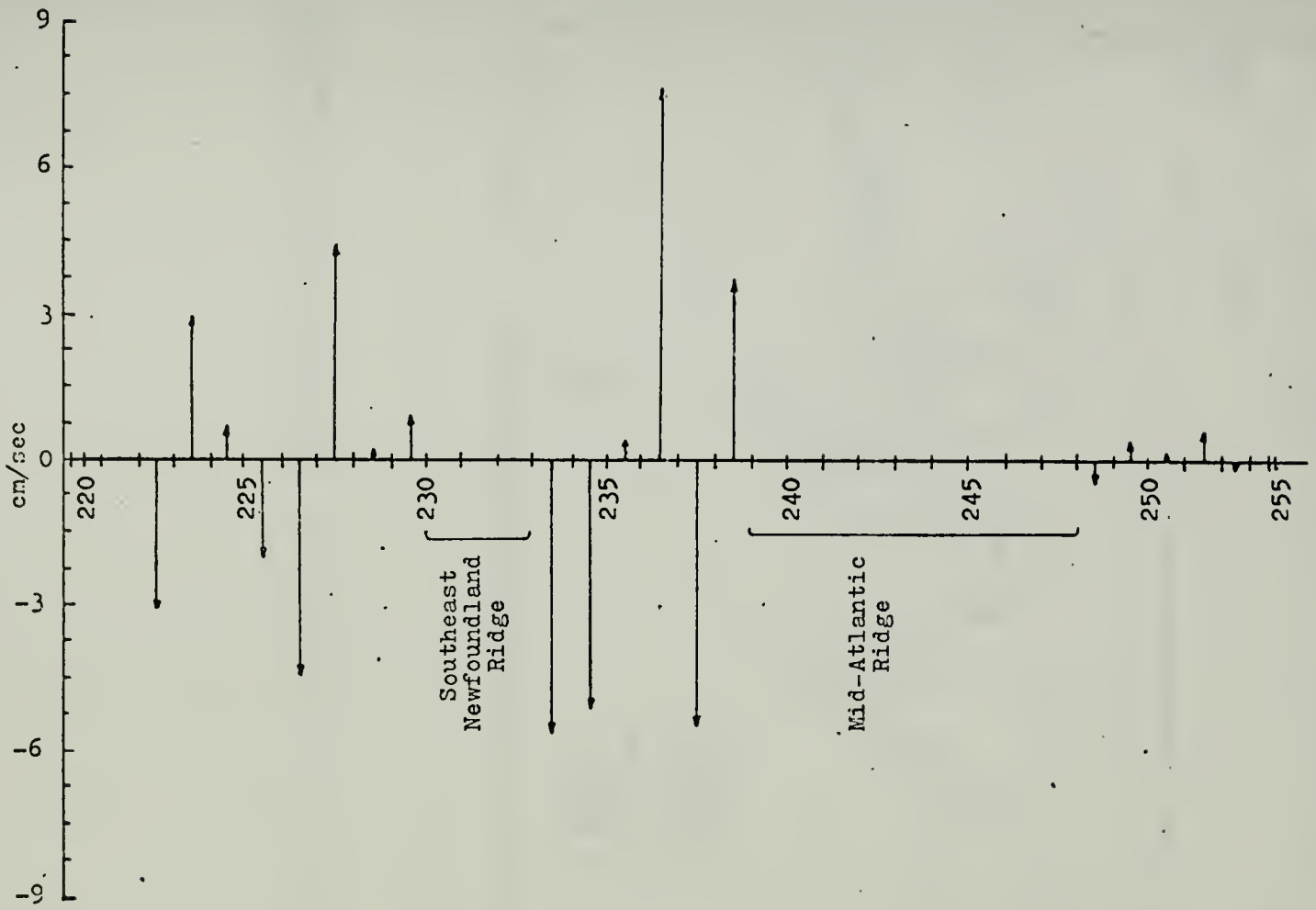
9
6
3
0
-3
-6
-9
cm/sec
220
225
230
235
240
245
250
255
Southeast Newfoundland Ridge
Mid-Atlantic Ridge

Figure 16

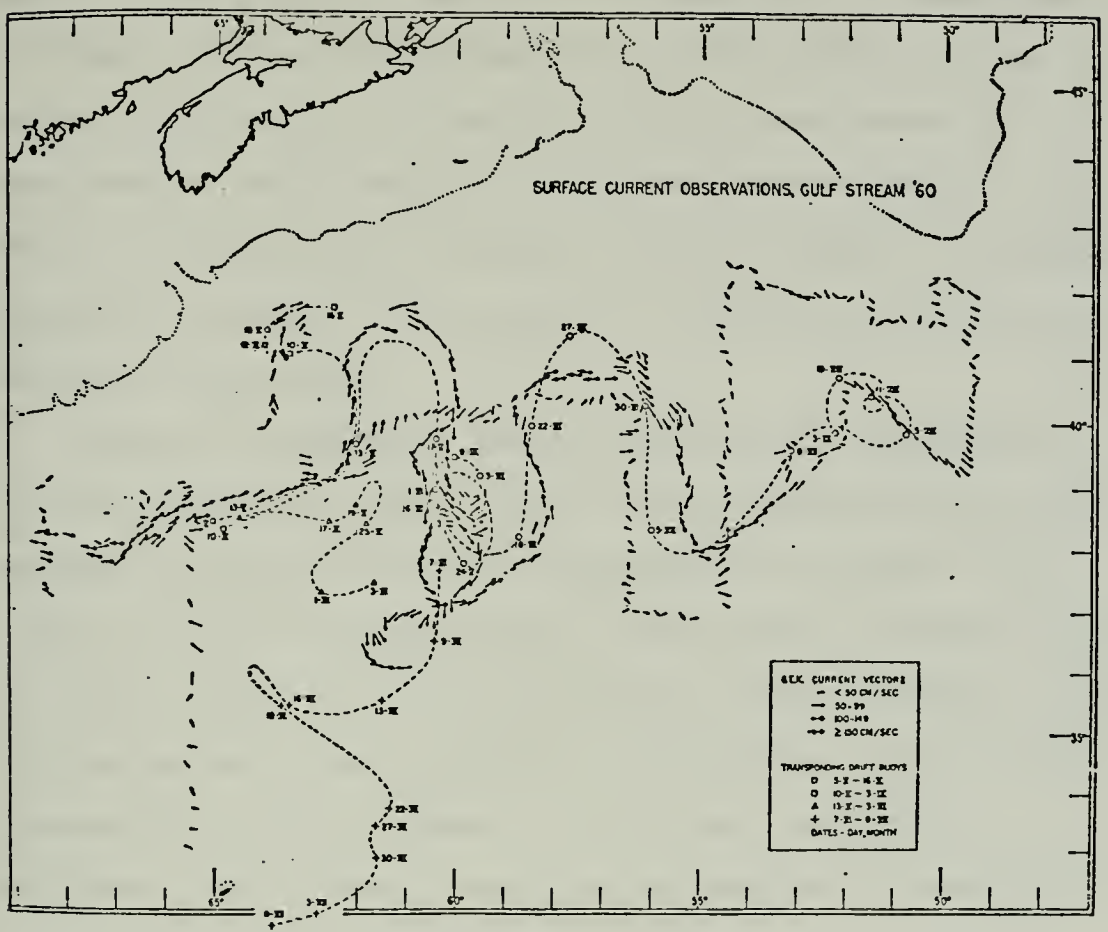

Figure 17. Surface current observations "Gulf Stream '60". [From Fuglister (1964)]

current measurements in his study were obtained with the use of a GEK during 2 April to 15 June 1960. A comparison of Figures 12 and 17 indicates some similarities in the north-south pattern of the Gulf Stream even though his measurements were taken in a different season and year than those of this study. His 1960 study was chosen for comparison because it happens to be nearer to the time that the IGY data were collected.

One major difference between his current pattern and the one obtained in this study is the presence of the large meander shown in his pattern between 60°W and 63°W. The path of the Gulf Stream plotted from various cruises conducted in 1947, 1948, 1950, and 1960 shows a quasi-stationary pattern with an abrupt change near 62°W. Some years this meander crosses 40°N and in others, it does not. According to Fuglister, this sudden change in the pattern of meanders is a permanent feature of the Gulf Stream.

The geostrophic velocities below the level of no motion as determined in this study are shown in Figures 14, 15, and 16. The maximum geostrophic velocity of about +7 cm/sec below the level of no motion occurs at a depth of 4000m between stations 236 and 237. In most cases, for this vertical cross section of the North Atlantic Ocean, the deep ocean velocities are less than 3 cm/sec for the areas below the level of no motion. In general, the stronger geostrophic velocities at depth can be associated with the stronger velocities at the surface.

The weak geostrophic velocities below the level of no motion could be another indication that the level for this cross section of ocean has been chosen properly.

D. TRANSPORTS OF MASS, SALT, AND HEAT

The integrated transports of mass, salt, and heat for each pair of stations are shown in Figures 18, 19, and 20, respectively. These figures closely resemble the geostrophic velocity figures since the transports are directly related to the velocity. One item to note in Figures 18 and 19 is that the transports of mass and salt for one pair of stations tends to be balanced by another pair of stations in close proximity. For example, in Figure 18, the integrated northward mass transport value for stations 226 to 227 tends to be balanced by the integrated southern mass transport value for stations 227 to 228.

This is in conformity with the assertion of Sverdrup et al. (1942): "If the section is taken across an ocean, the mass transport to the north must equal the mass transport to the south but the heat transport may differ because the temperature of the water transported in one direction may be higher or lower than that of the water which is transported in the opposite direction."

Two methods are available for measuring the meridional heat transport in the oceans. Heat balance computations are used in one method. The addition of geothermal heat through the ocean floor is relatively small, and the heat transport

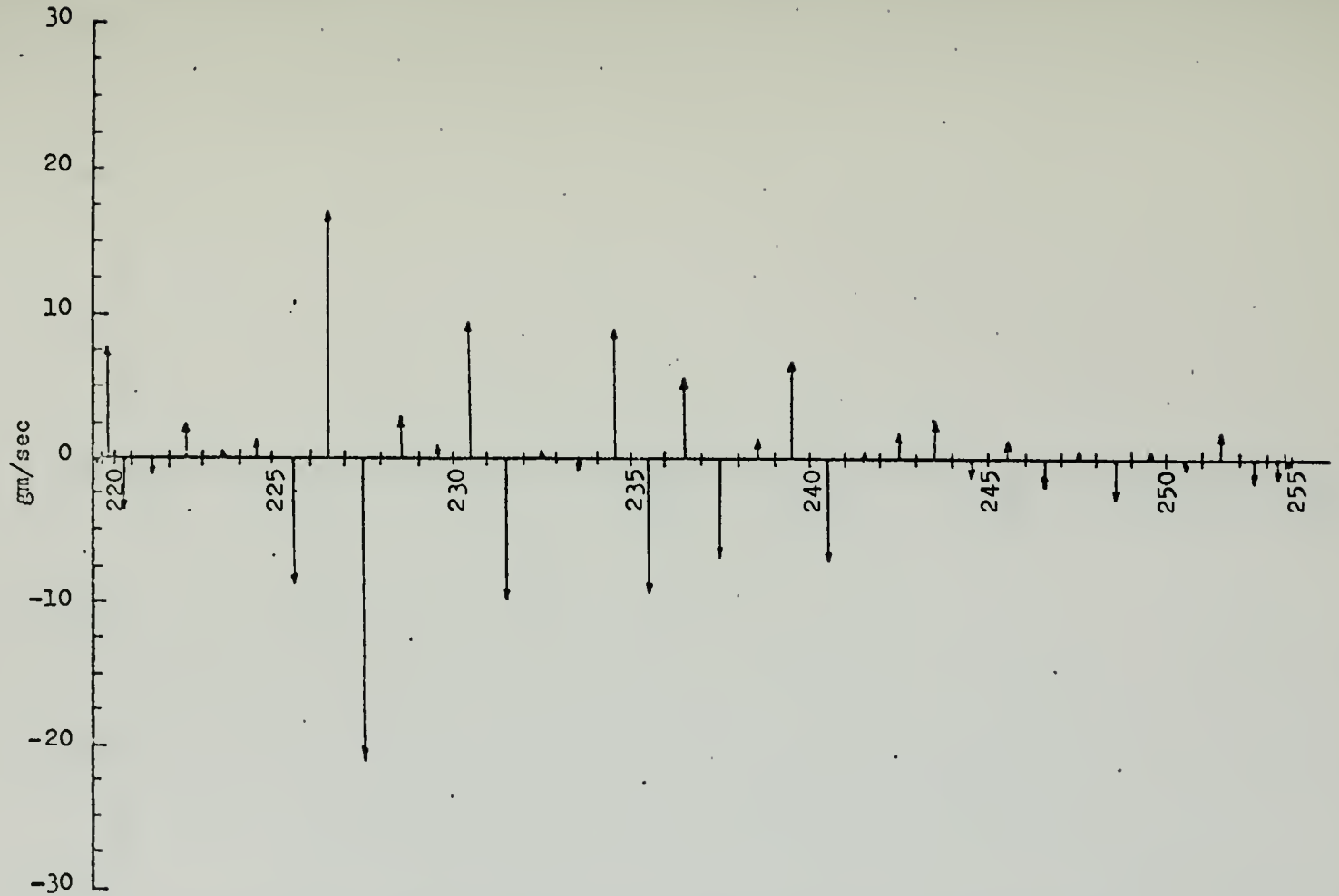

Figure 18. Integrated transport of mass for Crawford stations 218-255.

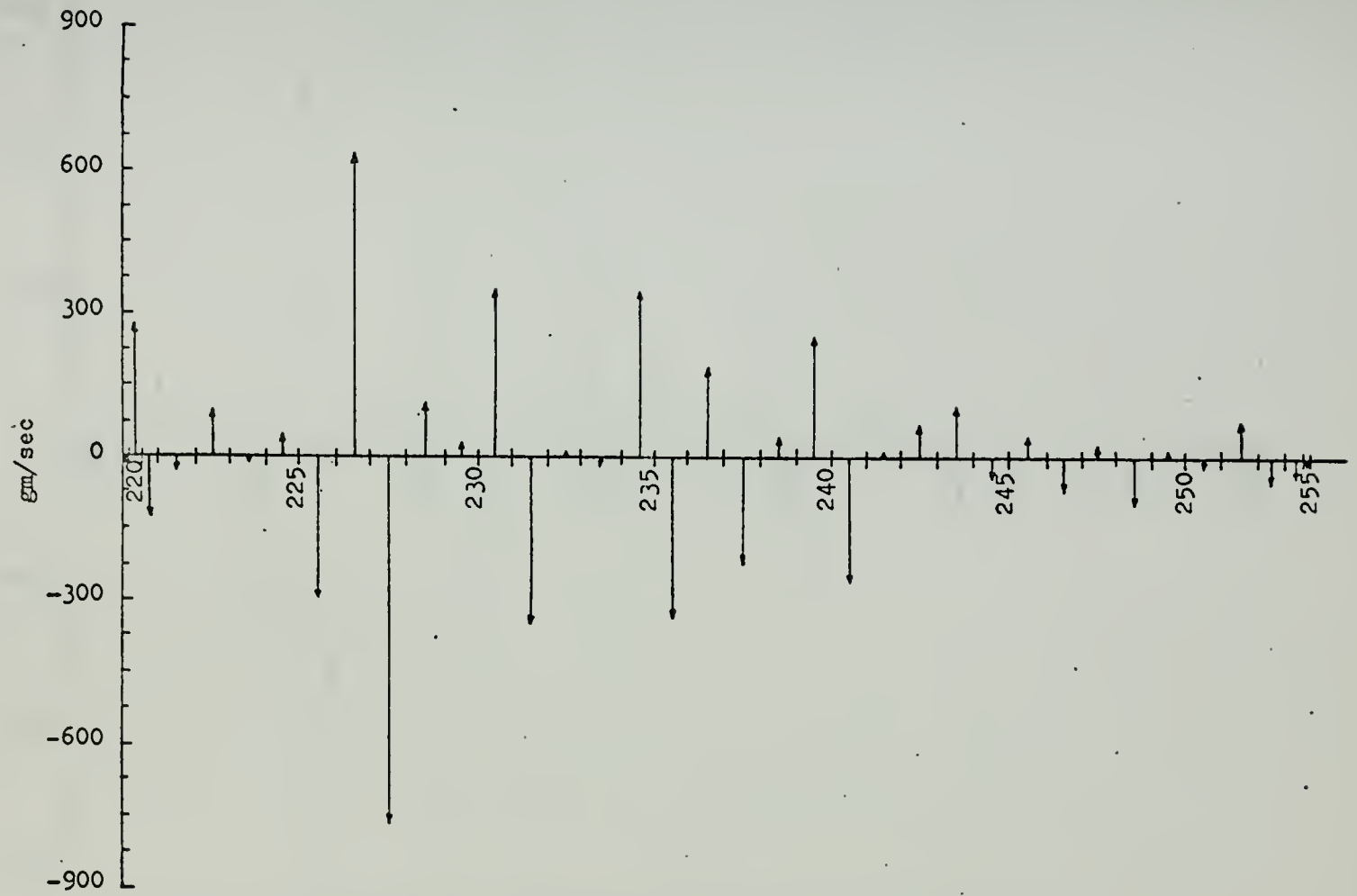

Figure 19. Integrated transport of salt for Crawford stations 218-255.

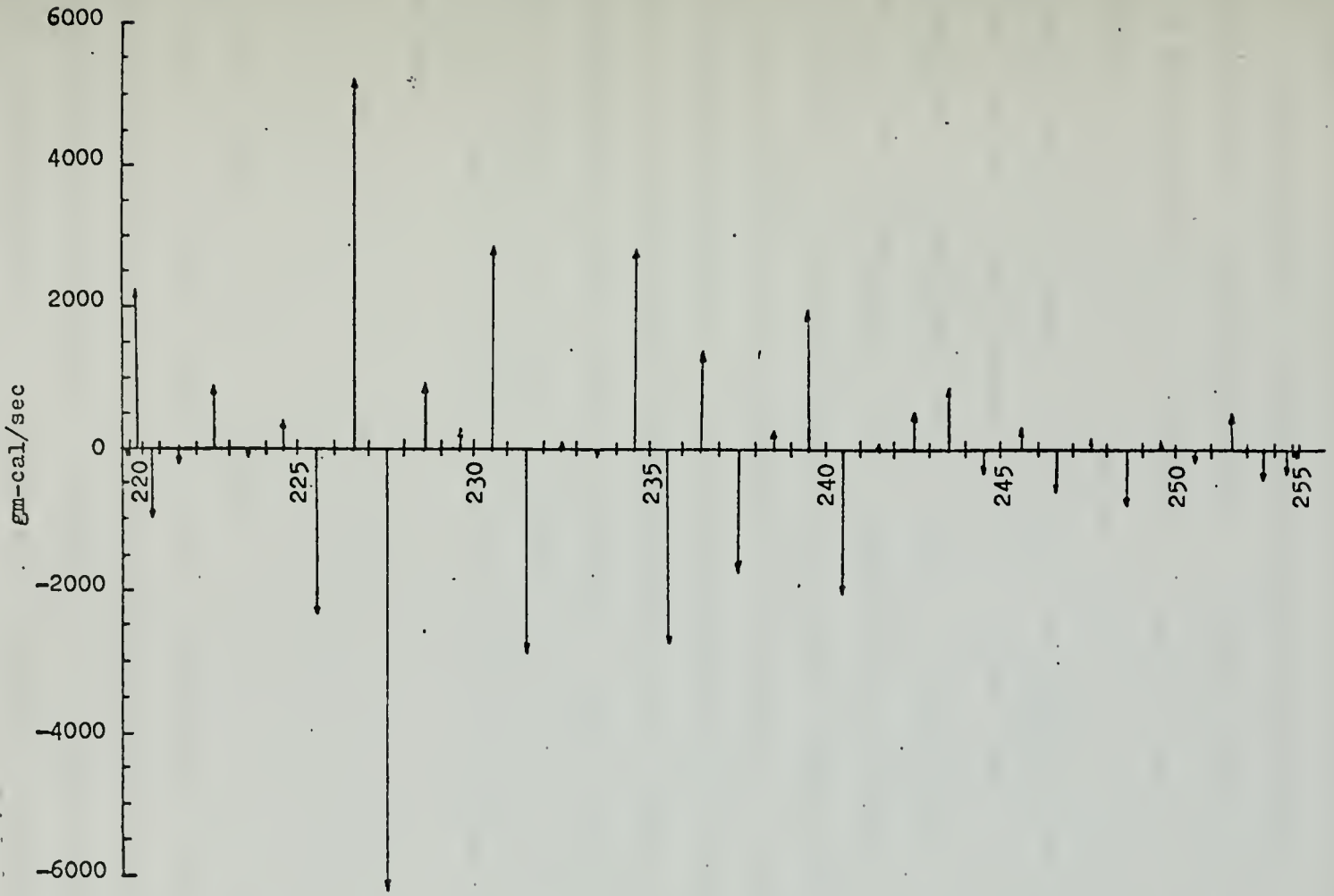

Figure 20. Integrated transport of heat for Crawford stations 218-255.

can be computed from the distribution of heat sources and sinks at the surface. The second method consists of direct computation based on measurements of velocity and temperature.

Sverdrup's heat transport estimates were obtained by utilization of the first method. Budyko constructed maps of the heat balance for the entire earth's surface from which he obtained his estimates. Jung (1955) utilized the second approach based on data from the Meteor expedition and The Naval Hydrographic Office. Bryan (1962) used a completely independent method based on geostrophic calculations from hydrographic data, measuring the integral of covariance of the meridional velocity and temperature of an entire vertical section across an ocean basin. This method included the division of the heat transport into two parts. One part is calculated from hydrographic data alone and is independent of the level of no motion. The other part of the integral does contain information about the level of no motion, and is calculated from the field of surface wind stress.

A comparison of the heat transport values determined in this study is made in Table VI with the values obtained by Jung, Budyko, Sverdrup and Byran. Of note is the discrepancy between the author's value and that determined by Bryan. Both studies for this cross section are based on the same IGY data, but the methods are different. The only explanation for the discrepancy is that Bryan's method is limited by the existing knowledge of the distribution of the wind stress.

TABLE VI

Comparison of Heat Transport Values
(Positive values indicate northward transport.)
(All values x 10^{13} gm-cal/sec)

Greeson	Jung (1955)		Budyko (1956)	Sverdrup (1957)	Bryan (1962)
40°N	36°N	45°N	40°N	40°N	40°N
+11.4	+13.5	+9.5	+18.0	+14.5*	+0.0

*Interpolated value.

The methods of Sverdrup and Budyko eliminated seasonal effects by using annual heat balance computations while Jung eliminated them by averaging all data for the cross section. Since the data used in the present study were collected during one month, it should reflect a seasonal variation if one exists; therefore, there is no reason why the values of Sverdrup, Budyko, and Jung should compare favorably. However, due to the favorable comparison of author's heat transport value with those obtained by Sverdrup, Budyko, and Jung, it might be suggested that the meridional transport of heat for this cross section of ocean is quasi-stationary.

E. WATER MASSES AND THEIR RELATIVE LOCATION TO THE LEVEL OF NO MOTION

Figure 21 is a representation of the distribution of the water masses present at 40°N within the North Atlantic Ocean The basis for this figure are the T-S diagrams of Crawford stations 218-255 included as Appendix B. The horizontal discontinuous line through Regions III and IV represents the level of no motion as determined by the balance of mass and salt transports through the vertical cross section.

Sverdrup et al. (1942) defined the North Atlantic Central Water (Region II) as water that is characterized by a nearly straight T-S curve between the points T=8°C, S=35.10 ppt, and T=19°C, S=36.70 ppt, and North Atlantic Deep and Bottom Water (Region V) as characterized by temperatures between 3.5°C and 2.2°C, and salinities between 34.97 and 34.90 ppt.

According to Sverdrup, between these two typical water masses are found other water masses, most of which have not been formed in the North Atlantic Ocean but which exercise a considerable influence upon the distribution of temperature and salinity at mid-depths.

The regions depicted as II and V in Figure 21 represent the area for which values of temperature and salinity fall within the limits defined by Sverdrup for the North Atlantic Central Water and the Deep and Bottom Water.

Region I represents the surface area that experiences highly variable temperatures and salinities due to evaporation and precipitation. Regions III and IV represent areas where the temperatures and salinities fall outside the limits that define the North Atlantic Central, and Deep and Bottom water masses. The reason for dividing this intermediate water region into two areas is that a good portion of it is affected by the high temperature and high salinity water of the Mediterranean Sea, Region III representing the Mediterranean influence. The limits of the region were determined from the T-S diagrams in Appendix B. While it is understood that the limits of the region can not be defined precisely by this method, it does give a good relative picture of the influence of the Mediterranean water at this particular latitudinal cross section. The asterisks indicate the salinity maximum determined from the T-S diagrams.

Figure 21. Relative position of the level of no motion to the various water masses within the North Atlantic Ocean at 40°N.

I. Surface Water

II. North Atlantic Central Water

III. Intermediate Water with Mediterranean Influence

IV. Intermediate Water with no Mediterranean Influence

V. Deep and Bottom Water.

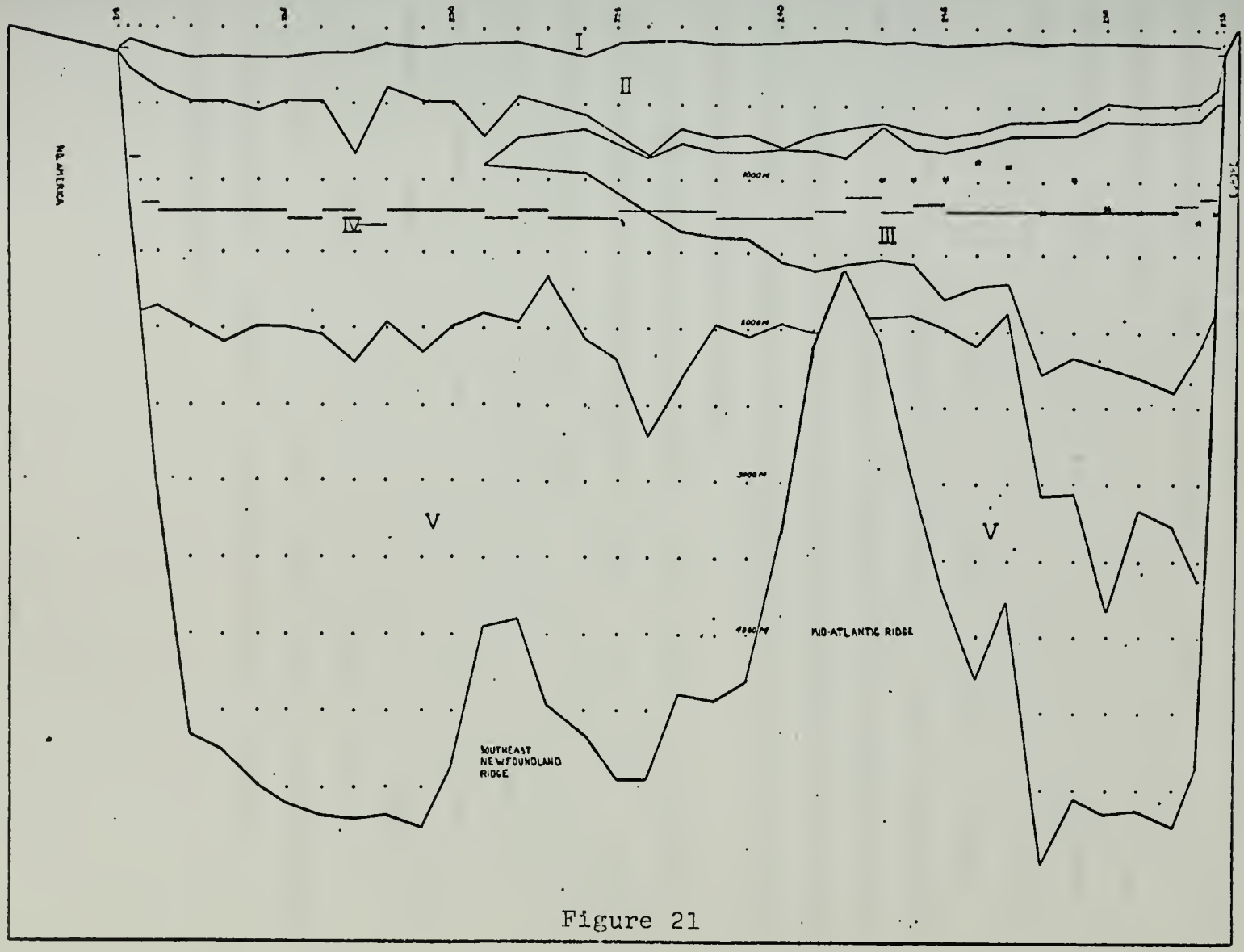
I
II
III
IV
V
V
NO. AMERICA
1000 M
2000 M
3000 M
4000 M
MID-ATLANTIC RIDGE
SOUTHEAST
NEWFOUNDLAND
RIDGE

Figure 21

Region IV is the intermediate water area that falls outside the limits of the North Atlantic Central, and Deep and Bottom water masses, and shows no influence of the Mediterranean water. There is a slight indication of the presence of Arctic Intermediate Water in the T-S diagrams for Crawford stations 236, 231, 227, 222, and 220; but this is not indicated in Figure 21. Regions III and IV could probably be more appropriately described as the areas where more than two water masses are mixed and are represented on a T-S diagram as the nonlinear portion that lies between the North Atlantic Central and the Deep and Bottom water masses of the North Atlantic Ocean.

As can be seen from Figure 21, the level of no motion lies in the intermediate water regions, III and IV. These regions probably represent areas of considerable vertical mixing vice lateral mixing since the level of no motion established in these areas requires no horizontal water movement. Weak horizontal velocities would be prevalent in the close proximity of this level. The author knows no reason why the level of no motion should fall in this region except that this is where the balance of the transports of mass and salt occurs.

VI. CONCLUSIONS AND RECOMMENDATIONS

This study represents the first attempt to determine mass, salt, and heat transports based strictly upon the dynamic method from data which are completely homogeneous and consistent. The results indicate that the transport of heat is quasi-stationary; but this requires additional investigation based upon data taken during different seasons. Agreement between the heat transport of this study and those of other authors is surprisingly good even though the methods and the data were completely different.

A level of no motion has been determined that gives a reasonable geostrophic velocity picture for the entire cross section. It was further established that this level is not necessarily related to any characteristic of the water nor to a specific water mass and is shown to lie in a region where the water masses appear to have been thoroughly mixed.

The volume of calculations for this type of study can be accommodated easily with the aid of high speed computers. Through the use of the computer program in Appendix A, the remainder of the IGY data at other latitudinal cross sections of the North Atlantic Ocean can be used to piece together a complete picture of the heat transport. Not only can the heat transport picture be established in the North Atlantic, but in other oceans as well. Furthermore, the

velocity picture and the level of no motion can be established where there are latitudinal cross sections with data such as the data collected during the IGY.

```
      REAL *8 ITL(12),INFO(30,8)
      DIMENSION Z(48),VEL(48),R(4)
      DIMENSION IT(50),IS(50),IO(50)
      DIMENSION D(50),T(50),S(50),O2(50),ADD(48),BDD(48)
      DIMENSION SD(48),ST(48),SS(48),SGT(48),SV(48),SVA(48)
      DIMENSION SGP(48),DH(48),BDH(48),DD(60,48),SLEV(60),BSVA(48)
      DIMENSION NPA(60),NPB(60),NO(60),NSTA(60,3),ALT(60),ALM(60)
      DIMENSION ALN(60),ANM(60),IDATE(60,3),DHT(60,48),ADH(48)
      DIMENSION XDENS(48,60),XSAL(48,60),XTEMP(48,60),YDE(47,60)
      DIMENSION YTT(47,60),YSL(47,60),TEMSUM(47),XMSUM(47),SSUM(47)
    5 FORMAT(4F7.0)
    6 FORMAT(15X,'VELOCITIES COMPUTED ARE RELATIVE TO ',F5.0,' METERS')
    7 FORMAT(1H1,'VELOCITIES BETWEEN STATION ',3A4,' LATITUDE ',I2,F5.1,
     1'N LONGITUDE ',I3,F5.1,'W  DATE ',3A4/24X,'AND ',3A4,' LATITUDE ',
     2I2,F5.1,'N LONGITUDE ',I3,F5.1,'W  DATE ',3A4//)
    8 FORMAT (1H1,'STATION,',3A4,' LATITUDE ',I2,F5.1,'N LONGITUDE ',
     1I3,F5.1,'W  DATE ',3A4/5X,' TO,',3A4,' LATITUDE ',I2,F5.1,
     2'N LONGITUDE ',I3,F5.1,'W  DATE ',3A4//)
    9 FORMAT(8(1X,2I2,F5.0))
   10 FORMAT(1H1,'STATION ',3A4,' LATITUDE = ',I2,F5.1,'N LONGITUDE =',
     1I4,F5.1,'W  DATE ',3A4//)
   12 FORMAT(10X,'* INDICATES ADJUSTED VALUE')
   13 FORMAT(I4,3A4,F3.0,2F5.1,F4.1,3A4)
   15 FORMAT(F10.3,F9.2,A1,F10.3,A1,F8.2,A1,8X,4A8)
   16 FORMAT(10X,'DEPTH  TEMPERATURE  SALINITY  SIGMA-T  OXYGEN'//)
   17 FORMAT(20X,'OBSERVED VALUES'//)
   18 FORMAT(//20X,'INTERPOLATED VALUES'//)
   19 FORMAT(10X,'DEPTH  TEMPERATURE  SALINITY  SIGMA-T   SPEC VOL  SPEC
     1 V ANOM  MEAN SVA   DELTA D   DYNAMIC HEIGHT'//)
   20 FORMAT(10X,F5.0,F10.2,F12.3,F9.3,F11.4,F13.6,23X,F12.5/70X,F11.6,F
     111.5)
   21 FORMAT(10X,F5.0,F10.2,A1,F11.3,A1,F8.3,F9.2,A1,4X,4A8/)
      DATA SD/0.,50.,100.,150.,200.,250.,300.,350.,400.,450.,500.,550.,
     1600.,650.,700.,750.,800.,850.,900.,950.,1000.,1050.,1100.,1150.,
     21200.,1250.,1300.,1400.,1500.,1600.,1700.,1800.,1900.,2000.,
     32250.,2500.,2750.,3000.,3250.,3500.,3750.,4000.,4250.,4500.,4750.,
     45000.,5250.,5500./
      DO 2000 I=1,47
      XMSUM(I)=0.
      TEMSUM(I)=0.
      SSUM(I)=0.
 2000 CONTINUE
      DO 4 I=1,48
    4 Z(I)=-SD(I)
C
C   MAX NUMBER OF STANDARD DEPTHS IS 48
      NSD=48
C   READ THE NO. OF GEOSTROPHIC CURRENTS AND TRANSPORTS TO BE CALCULATED
```

```
C
      READ (5,13) NGC
      IF(NGC.EQ.0) GO TO 410
      READ(5,5)(R(I),I=1,4)
      READ (5,9) (NPA(I),NPB(I),SLEV(I),I=1,NGC)
  410 NPA(NGC+1)=0
      DO 41 L=1,60
C
C          READ HEADING CARD, CHECK FOR  END OF DATA, THEN
C          READ NOV DATA CARDS.
C
      READ (5,13,END=32) NOV,(NSTA(L,K),K=1,3),ALT(L),ALM(L),ALN(L),
     1ANM(L),(IDATE(L,K),K=1,3)
      IF (NOV) 32,32,24
   24 DO 25 I=1,NOV
      READ (5,15) D(I),T(I),IT(I),S(I),IS(I),O2(I),IO(I),
     1(INFO(I,J),J=1,4)
C
C          SGTSVA IS SUBROUTINE TO COMPUTE SIGMA-T, SPECIFIC VOLUME
C          AND SPECIFIC VOLUME ANOMALY.
C
   25 CALL SGTSVA (T(I),S(I),D(I),SGP(I),SVNO,SVNO)
C
C          LGTP IS SUBROUTINE TO COMPUTE INTERPOLATED VALUES
C
      CALL LGTP(NOV,D,T,NSD,SD,ST,NA)
      CALL LGTP(NOV,D,S,NSD,SD,SS,NB)
      NO(L)=NA
      DO 27 I=1,NA
      CALL SGTSVA (ST(I),SS(I),SD(I),SGT(I),SV(I),SVA(I))
   27 CONTINUE
      DO 2500 I=1,NA
      XDENS(I,L)=1./SV(I)
      XTEMP(I,L)=ST(I)+273.15
      XSAL(I,L)=SS(I)
 2500 CONTINUE
      II=NA-1
      DO 2510 I=1,II
      YDE(I,L)=(XDENS(I,L)+XDENS(I+1,L))*.5
      YTT(I,L)=(XTEMP(I,L)+XTEMP(I+1,L))*.5
      YSL(I,L)=(XSAL(I,L)+XSAL(I+1,L))*.5
 2510 CONTINUE
      NLT=ALT(L)
      NLN=ALN(L)
      WRITE (6,10) (NSTA(L,K),K=1,3),NLT,ALM(L),NLN,ANM(L),
     1(IDATE(L,K),K=1,3)
      WRITE(6,17)
      WRITE (6,16)
```

```
      DO 29 I=1,NOV
   29 WRITE (6,21) D(I),T(I),IT(I),S(I),IS(I),SGP(I),O2(I),IO(I),
     1(INFO(I,J),J=1,4)
      WRITE(6,12)
      WRITE (6,18)
      WRITE (6,19)
      NA=NA-1
      DH(1)=0.
      DO 30 I=1,NA
      BSVA(I)=(SVA(I)+SVA(I+1))*.5
      DD(L,I)=BSVA(I)*(SD(I+1)-SD(I))
   30 DH(I+1)=DH(I)+DD(L,I)
      DO 31 I=1,NA
      DHT(L,I)=DH(I)
   31 WRITE (6,20) SD(I),ST(I),SS(I),SGT(I),SV(I),SVA(I),DH(I),
     1BSVA(I),DD(L,I)
      I=NA+1
      DHT(L,I)=DH(I)
      WRITE (6,20) SD(I),ST(I),SS(I),SGT(I),SV(I),SVA(I),DH(I)
   41 CONTINUE
   32 IF(NGC.EQ.0) GO TO 33
      DO 42 L=1,60
      IF (NPA(L).EQ.0) GO TO 3999
      BASE=SLEV(L)
      N1=NPA(L)
      N2=NPB(L)
      NU1=NO(N1)
      NU2=NO(N2)
      DO 43 I=1,NU1
      ADD(I)=DD(N1,I)
   43 ADH(I)=DHT(N1,I)
      DO 44 I=1,NU2
      BDD(I)=DD(N2,I)
   44 BDH(I)=DHT(N2,I)
      NLT=ALT(N1)
      NLN=ALN(N1)
      MLT=ALT(N2)
      MLN=ALN(N2)
      WRITE (6,8) (NSTA(N1,K),K=1,3),NLT,ALM(N1),NLN,ANM(N1),
     1(IDATE(N1,K),K=1,3),(NSTA(N2,K),K=1,3),MLT,ALM(N2),MLN,
     2ANM(N2),(IDATE(N2,K),K=1,3)
      ALAT=ALT(N1)+ALM(N1)/60.
      ALON=ALN(N1)+ANM(N1)/60.
      BLAT=ALT(N2)+ALM(N2)/60.
      BLON=ALN(N2)+ANM(N2)/60.
      CALL DSTSTA (ALAT,ALON,BLAT,BLON,X2,DIST)
      CALL GEOCUR (NU1,ADH,NU2,BDH,SD,BASE,X2,VEL,NNN,DIST,YDE,YTT,YSL,
     1XMSUM,TEMSUM,SSUM,L)
```

```
      WRITE (6,7) (NSTA(N1,K),K=1,3),NLT,ALM(N1),NLN,ANM(N1),
     1(IDATE(N1,K),K=1,3),(NSTA(N2,K),K=1,3),MLT,ALM(N2),MLN,
     2ANM(N2),(IDATE(N2,K),K=1,3)
      CALL UTPLOT(VEL,Z,NNN,R,1,0)
      XS=(R(1)-R(2))/80.
      YS=(R(3)-R(4))/60.
      WRITE(6,100) XS,YS
  100 FORMAT( 15X,'X-SCALE:  "*"=',F4.1,' CM/SEC'//
     1        15X,'Y-SCALE:  "*"=',F5.2,' METERS'//)
      WRITE(6,6) BASE
   42 CONTINUE
 3999 TSSUM=0.0
      THSUM=0.0
      TMSUM=0.0
      WRITE (6,6002)
 6002 FORMAT (///20X,'DEPTH',10X,'TOTAL MASS',10X,'TOTAL SALT',10X,'TOTA
     1L HEAT'/35X,'TRANSPORT',11X,'TRANSPORT',11X,'TRANSPORT')
      DO 5000 J=1,47
      TMSUM=TMSUM+XMSUM(J)
      THSUM=THSUM+TEMSUM(J)
      TSSUM=TSSUM+SSUM(J)
      WRITE (6,6003) J,SD(J),XMSUM(J),SSUM(J),TEMSUM(J)
 6003 FORMAT ('0',10X,I4,6X,F5.0/29X,E16.6,4X,E16.6,4X,E16.6)
 5000 CONTINUE
      IX=48
      WRITE (6,6003) IX,SD(IX)
      WRITE (6,6004)
 6004 FORMAT (' ',37X,'--------',12X,'--------',12X,'--------')
      WRITE (6,6001) TMSUM,TSSUM,THSUM
 6001 FORMAT ('0',29X,E16.6,4X,E16.6,4X,E16.6)
   33 STOP
      END
```

```
      SUBROUTINE GEOCUR (NA,ADH,NB,BDH,SD,BASE,X2,VEL,NNN,DIST,
     1YDE,YTT,YSL,XMSUM,TEMSUM,SSUM,L)
      DIMENSION AMASST(47),ASALTT(47),AHEATT(47),XMSUM(47),TEMSUM(47),
     1SSUM(47),YDE(47,60),YTT(47,60),YSL(47,60),AVDENS(47),AVTEMP(47),
     2AVSAL(47)
      DIMENSION ADH(NA),BDH(NB),SD(48),RVEL(48),VEL(48),AMB(48),AVT(48)
   10 FORMAT (13X,'DEPTH     DYN HT    DYN HT     DIFF HT    REL VEL    ABS V
     1EL     AVERAGE     AVERAGE ABS     AVERAGE'/15X,'M        STA A     STA
     2B        B-A        CM/SEC     CM/SEC      DENSITY    TEMPERATURE     SAL
     3INITY'/)
   11 FORMAT (12X,F5.0,2X,3(F9.5,1X),2(F8.2,2X)/67X,F12.5,3X,F10.2,4X,F1
     10.3)
   12 FORMAT ('***** LEVEL OF NO MOTION MUST BE EQUAL TO A STANDARD DEPT
     1H *****')
   14 FORMAT(' ',10X,'TOTAL VOLUME TRANSPORT IS COMPUTED BY SUMMING INCR
     1EMENTAL TRANSPORTS ABOVE LEVEL OF NO MOTION:'//5X,'TOTAL TRANSPORT
     2 PERPENDICULAR TO THE PLANE OF THE STATIONS IS ',F7.3,' SVERDRUPS
     3RELATIVE TO ',F5.0,' METERS')
   15 FORMAT(//'  * VALUES IN THIS COLUMN REPRESENT TRANSPORTS IN LAYER
     1INCREMENTS'//)
   16 FORMAT (//13X,'DEPTH',10X,'ABS VOL',8X,'ABS MASS',7X,'ABS SALT',7X
     1,'ABS HEAT'/15X,'M',12X,'TRANSPORT',6X,'TRANSPORT',6X,'TRANSPORT',
     26X,'TRANSPORT',8X,'MASS',11X,'SALT',11X,'HEAT'/)
   17 FORMAT (12X,F5.0/22X,7(F15.5))
   18 FORMAT ('0',32X,'*',14X,'*',14X,'*',14X,'*',20X,'CUMULATIVE TOTALS
     1')
      IF(NA.LE.NB) GO TO 51
      N=NB
      GO TO 52
   51 N=NA
   52 DO 53 I=1,N
      AMB(I)=BDH(I)-ADH(I)
   53 RVEL(I)=AMB(I)*X2
      DO 54 I=1,48
      IF(BASE.EQ.SD(I))GO TO 55
   54 CONTINUE
      WRITE (6,12)
      GO TO 70
   55 NM=I
      IF(NM.GT.N) NM=N
      BASE=SD(NM)
      DO 56 I=1,N
   56 VEL(I)=RVEL(NM)-RVEL(I)
      DO 600 I=2,N
      J=I-1
      AVDENS(J)=(YDE(J,L)+YDE(J,L+1))*.5
      AVSAL(J)=(YSL(J,L)+YSL(J,L+1))*.5
      AVTEMP(J)=(YTT(J,L)+YTT(J,L+1))*.5
```

```
  600 CONTINUE
      STMASS=0.0
      STSALT=0.0
      STHEAT=0.0
      DO 553 I=2,N
      J=I-1
      AVEL=(VEL(I)+VEL(J))*0.005
      AVT(J)=AVEL*DIST*(SD(I)-SD(J))*1.0E-03
      AMASST(J)=AVT(J)*AVDENS(J)
      ASALTT(J)=AMASST(J)*AVSAL(J)
      AHEATT(J)=AMASST(J)*AVTEMP(J)
      XMSUM(J)=XMSUM(J)+AMASST(J)
      TEMSUM(J)=TEMSUM(J)+AHEATT(J)
      SSUM(J)=SSUM(J)+ASALTT(J)
      STMASS=STMASS+AMASST(J)
      STSALT=STSALT+ASALTT(J)
      STHEAT=STHEAT+AHEATT(J)
  553 CONTINUE
      NM=NM-1
      VT=0.
      DO 57 I=1,NM
   57 VT=VT+AVT(I)
C
C   IF STATION B IS EAST OF STATION A, A NEGATIVE SIGN IN THE "ABS VEL"
C   COLUMN IMPLIES A SOUTHWARD FLOWING CURRENT.
C
   58 WRITE (6,10)
      N=N-1
      DO 60 I=1,N
   60 WRITE (6,11) SD(I),ADH(I),BDH(I),AMB(I),RVEL(I),VEL(I),AVDENS(I),
     1AVTEMP(I),AVSAL(I)
      N=N+1
      I=N
      WRITE (6,11) SD(I),ADH(I),BDH(I),AMB(I),RVEL(I),VEL(I)
      WRITE (6,16)
      WRITE (6,18)
      N=N-1
      DO 62 I=1,N
   62 WRITE (6,17) SD(I),AVT(I),AMASST(I),ASALTT(I),AHEATT(I),XMSUM(I),S
     1SUM(I),TEMSUM(I)
      N=N+1
      I=N
      WRITE (6,17) SD(I)
      WRITE (6,1001)
 1001 FORMAT (' ',41X,'-----------',4X,'-----------',4X,'-----------')
      WRITE (6,1000) STMASS,STSALT,STHEAT
 1000 FORMAT ('0',2X,'NET TOTALS',24X,3(F15.5))
      NNN=N
```

```
      WRITE(6,15)
      WRITE(6,14)VT,BASE
70    RETURN
      END
```

```
      SUBROUTINE DSTSTA (SATI,ONGI,SATII,ONGII,X2,DIST)
      IMPLICIT REAL*4 (K)
      REAL*8 A,E
      DATA A/111132.09/,B/566.05/,C/1.20/,D/.002/
      DATA E/111415.13/,F/94.55/,G/.012/
   10 FORMAT (10X,'MEAN LATITUDE = ',F6.2/15X,'DISTANCE = ',F6.2,
     1' KILOMETERS'/)
      CON=2*3.1416/360
      AATI=SATI*CON
      AATII=SATII*CON
      $MERI=A-B*COS(2*AATI)+C*COS(4*AATI)-D*COS(6*AATI)
      PARI=E*COS(AATI)-F*COS(3*AATI)+G*COS(5*AATI)
      $MERII=A-B*COS(2*AATII)+C*COS(4*AATII)-D*COS(6*AATII)
      PARII=E*COS(AATII)-F*COS(3*AATII)+G*COS(5*AATII)
      ALLAT=($MERI+$MERII)/2
      ALLON=(PARI+PARII)/2
      DLAT=SATI-SATII
      DLON=ONGI-ONGII
      KLAT=DLAT*ALLAT/1000
      KLONG=DLON*ALLON/1000
      KDIX=SQRT(KLAT**2+KLONG**2)
      DIST=KDIX
      W2=1.458E-4
      PSI=(SATI+SATII)*0.5
      PSJ=(2.*3.14159/360.)*PSI
      SPSI=SIN(PSJ)
      IF(SPSI.LT.0.1) SPSI=0.1
      X2=1./(W2*SPSI*KDIX)
      WRITE(6,10) PSI,KDIX
      RETURN
      END
```

```
      SUBROUTINE SGTSVA (T,S,D,SGT,SV,SVA)
      ST=-(((T-3.98)**2)/503.57)*((T+283.)/(T+67.26))
      SO=-0.093+0.8149*S-.000482*S**2+6.8E-6*S**3
      AT=T*(4.7867-.098185*T+.0010843*T**2)*1.E-3
      BT=T*(18.030-.8164*T+.01667*T**2)*1.E-6
      SGT=ST+(SO+.1324)*(1.-AT+BT*(SO-.1324))
      AFST=1./(1.+SGT*1.E-3)
      A=D*AFST*1.E-9
      B=4886./(1.+1.83E-5*D)
      C=227.+28.33*T-.551*T**2+.004*T**3
      E=D*1.E-4
      G=(SO-28.)/10.
      H=147.3-2.72*T+.04*T**2
      U=105.5+9.5*T-.158*T**2
      V=1.5*D**2*T*1.E-8
      W=32.4-.87*T+.02*T**2
      X=4.5-.1*T
      Y=1.8-.06*T
      SV=AFST-A*(B-C+E*U-V-G*(H-E*W)+G**2*(X-E*Y))
      AZ=.972643
      YA=-227.+.01055*D
      YB=.01296*(147.3-.00324*D)
      YC=16.E-7*(4.5-D*.00018)
      AP=AZ-D*AZ*(B+YA-YB+YC)*1.E-9
      SVA=SV-AP
      RETURN
      END
```

```
      SUBROUTINE LGTP(N,D,V,M,SD,CV,NN)
      DIMENSION D(N),V(N),CV(M),SD(M)
      JJJ=0
  111 DO 188 J=1,M
  112 DO 186 I=1,N
      IF(SD(J)-D(N))113,115,190
  115 CV(J)=V(N)
      JJJ=JJJ+1
      GO TO 190
  113 IF(SD(J)-D(I))114,114,116
  114 CV(J)=V(I)
      GO TO 170
  116 IF(SD(J)-D(I+1))120,118,186
  118 CV(J)=V(I+1)
      GO TO 170
  120 IF(((D(1).LT.SD(J)).AND.(SD(J).LT.D(2))).OR.
     $    ((D(N-1).LT.SD(J)).AND.(SD(J).LT.D(N)))) GO TO 134
      XA=(SD(J)-D(I))*(SD(J)-D(I+1))*V(I-1)/
     1((D(I-1)-D(I))*(D(I-1)-D(I+1)))
      XB=(SD(J)-D(I-1))*(SD(J)-D(I+1))*V(I)/
     1((D(I)-D(I-1))*(D(I)-D(I+1)))
      XC=(SD(J)-D(I-1))*(SD(J)-D(I))*V(I+1)/
     1((D(I+1)-D(I-1))*(D(I+1)-D(I)))
      ANSU=XA+XB+XC
      YA=(SD(J)-D(I+1))*(SD(J)-D(I+2))*V(I)/
     1((D(I)-D(I+1))*(D(I)-D(I+2)))
      YB=(SD(J)-D(I))*(SD(J)-D(I+2))*V(I+1)/
     1((D(I+1)-D(I))*(D(I+1)-D(I+2)))
      YC=(SD(J)-D(I))*(SD(J)-D(I+1))*V(I+2)/
     1((D(I+2)-D(I))*(D(I+2)-D(I+1)))
      ANSD=YA+YB+YC
      CV(J)=(ANSU+ANSD)/2.
      GO TO 170
  134 ZA=(SD(J)-D(I+1))*V(I)/(D(I)-D(I+1))
      ZB=(SD(J)-D(I))*V(I+1)/(D(I+1)-D(I))
      ANSL=ZA+ZB
      CV(J)=ANSL
      GO TO 170
  186 CONTINUE
  170 JJJ=JJJ+1
  188 CONTINUE
  190 NN=JJJ
      RETURN
      END
```

APPENDIX B

T-S DIAGRAMS FOR CRAWFORD STATIONS 218-255

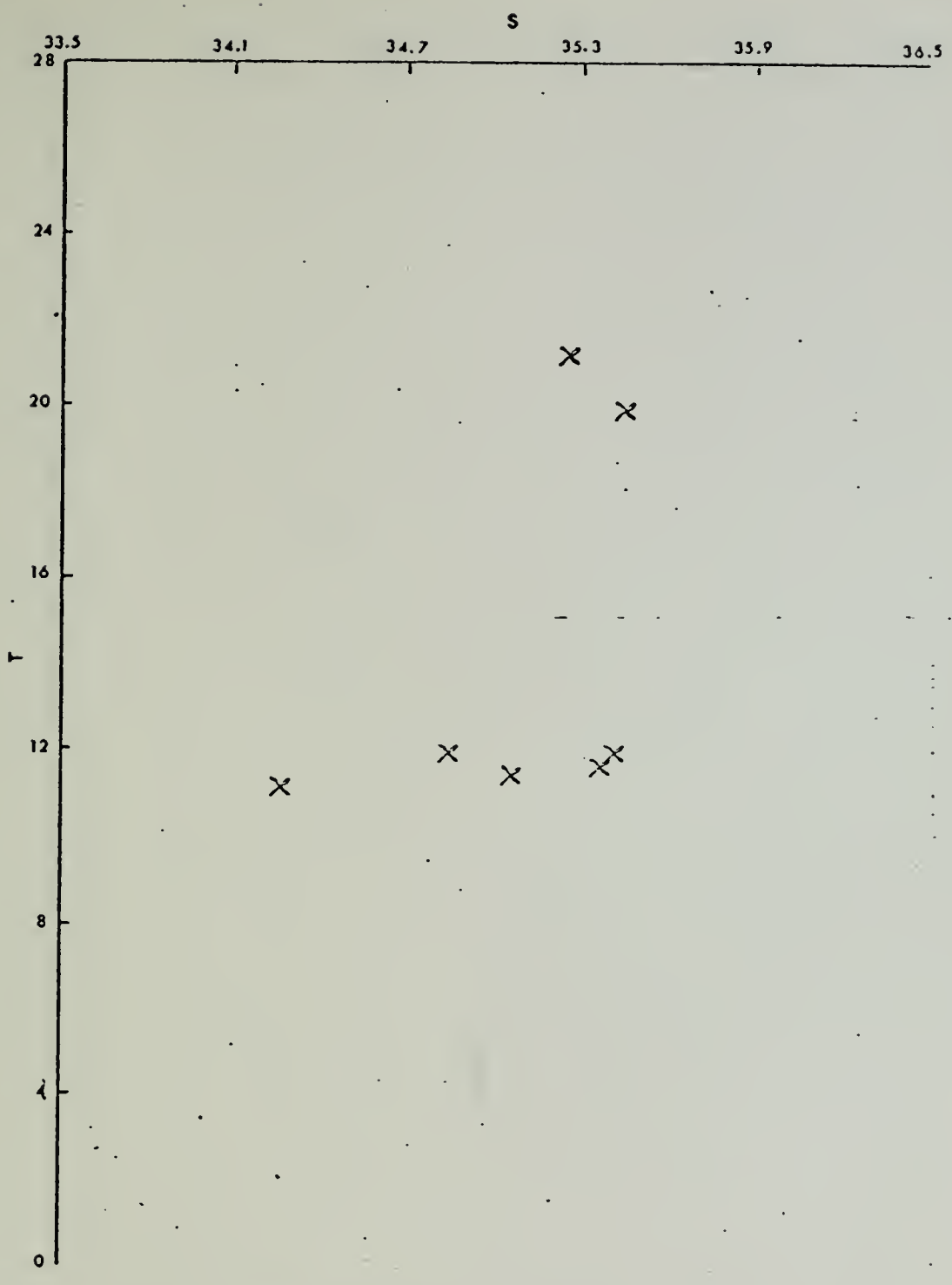

Crawford station 218

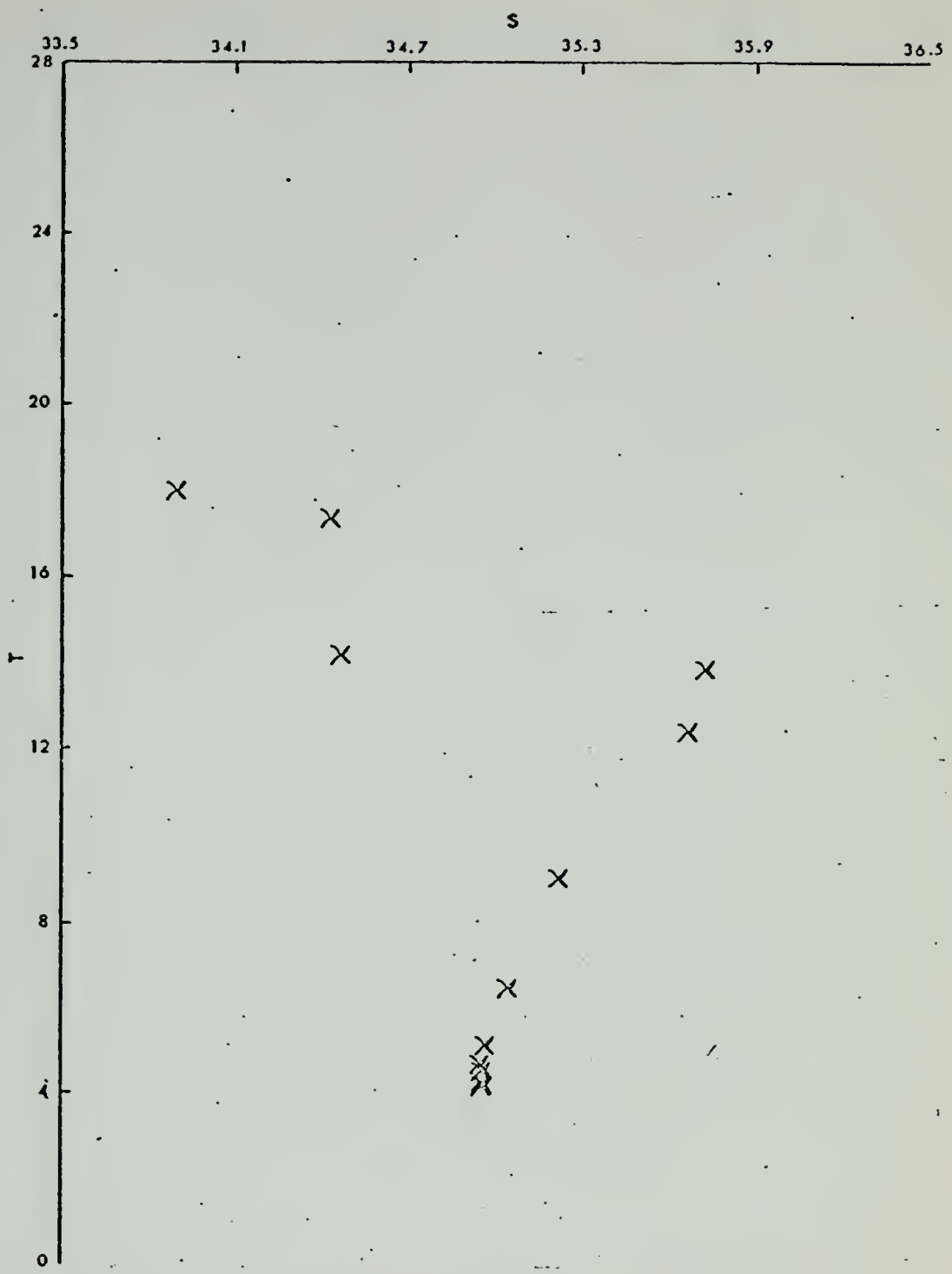

Crawford station 219

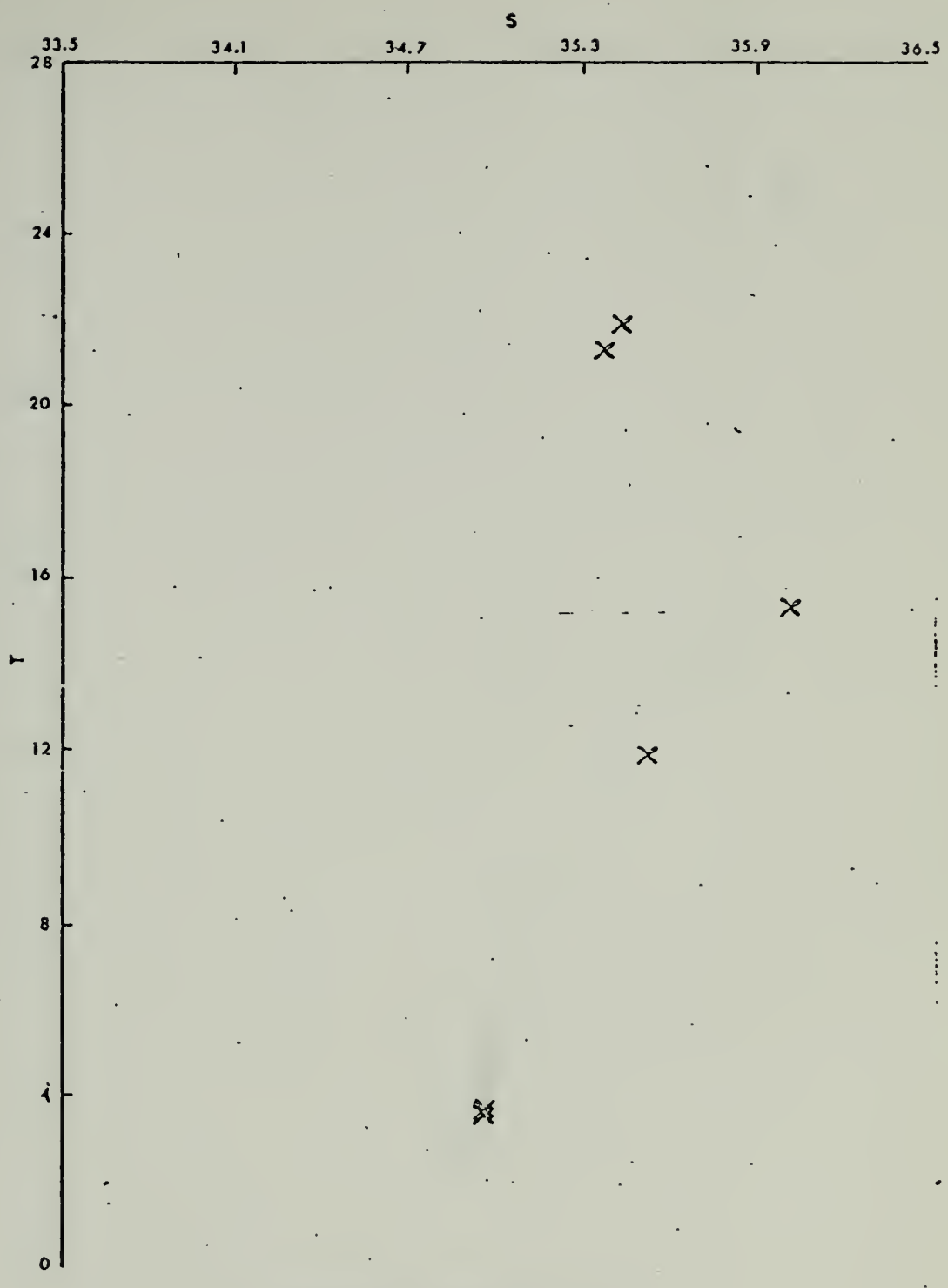

Crawford station 220

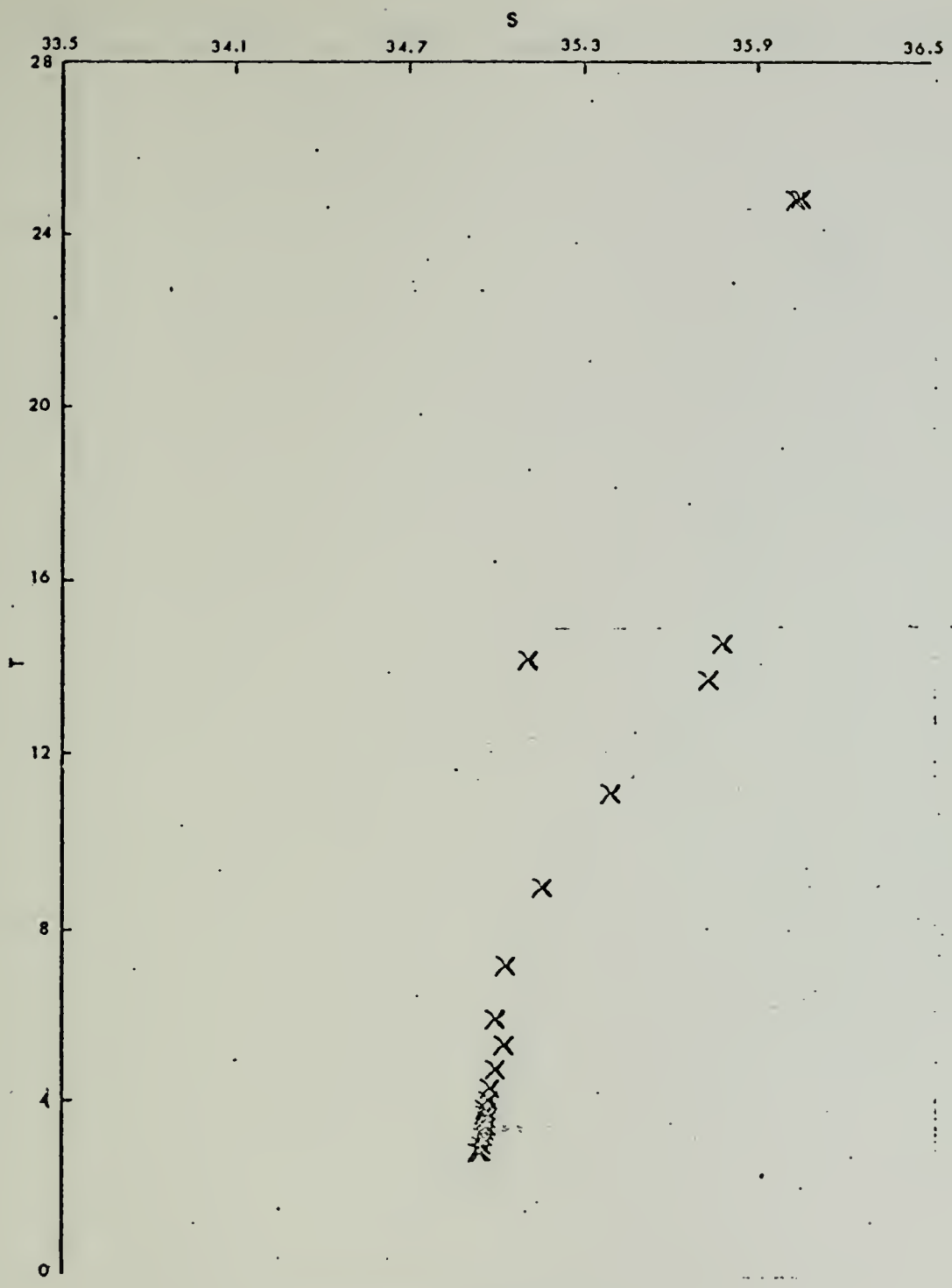

Crawford station 221

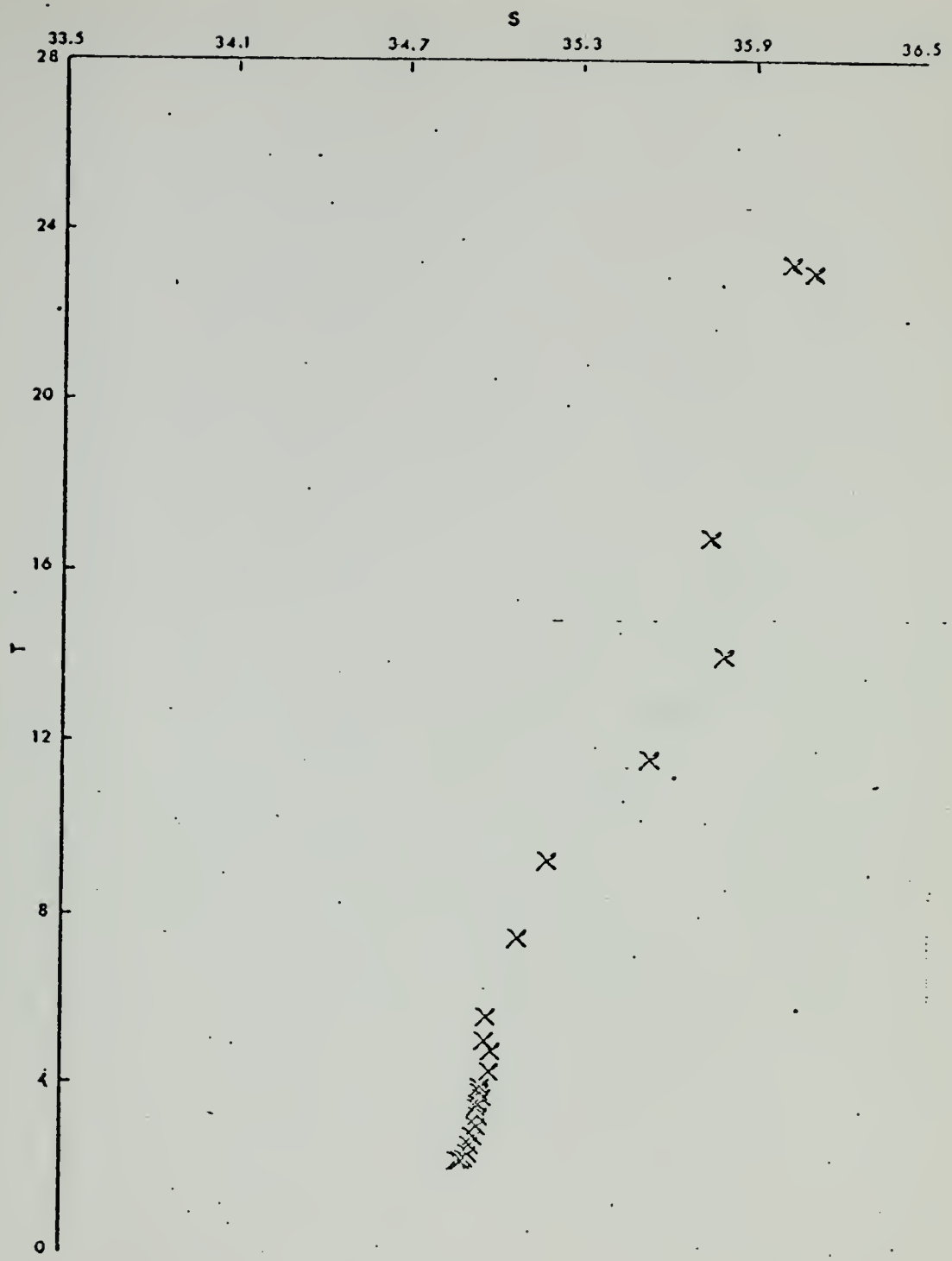

Crawford station 222

Crawford station 223

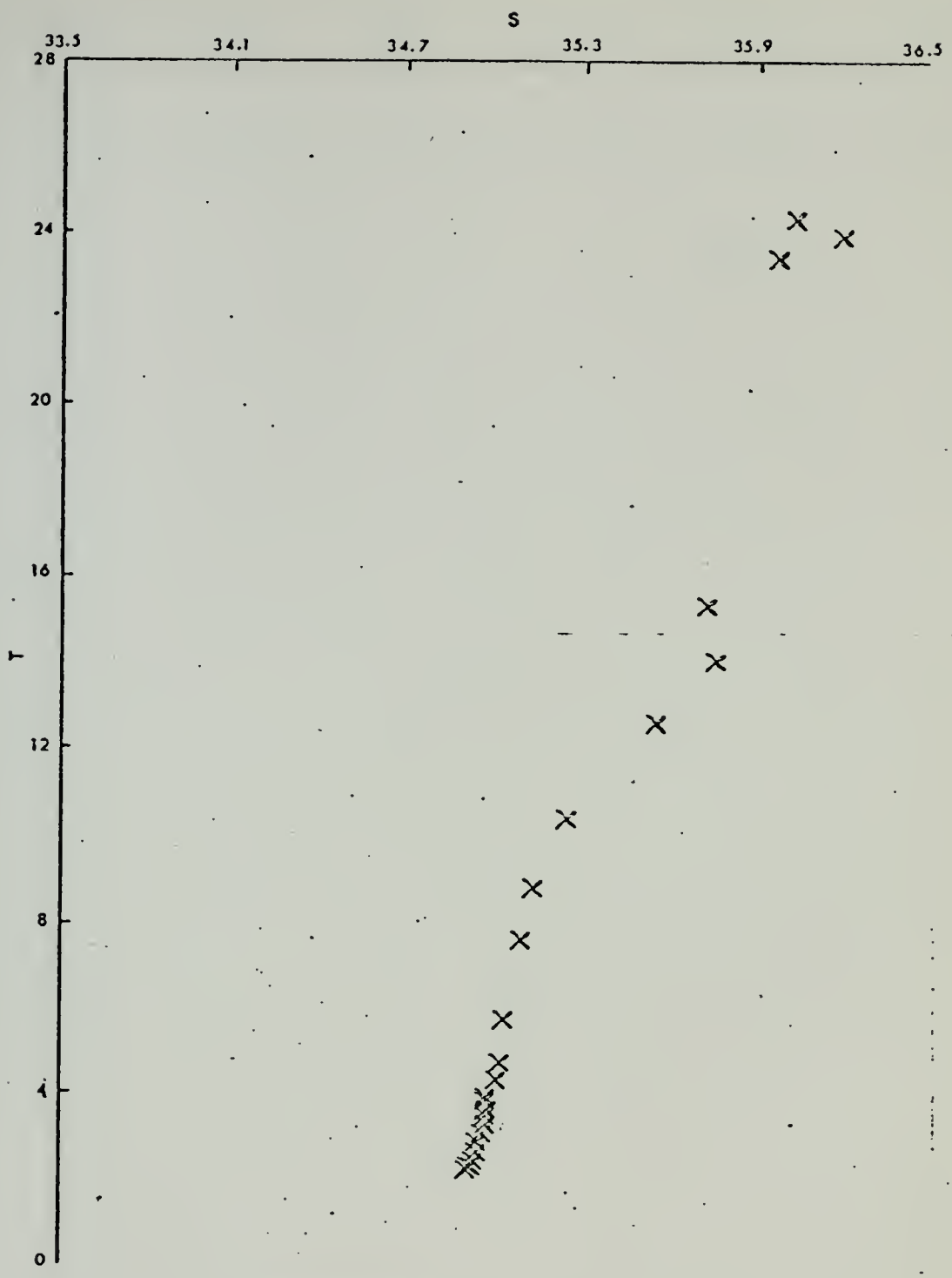

Crawford station 224

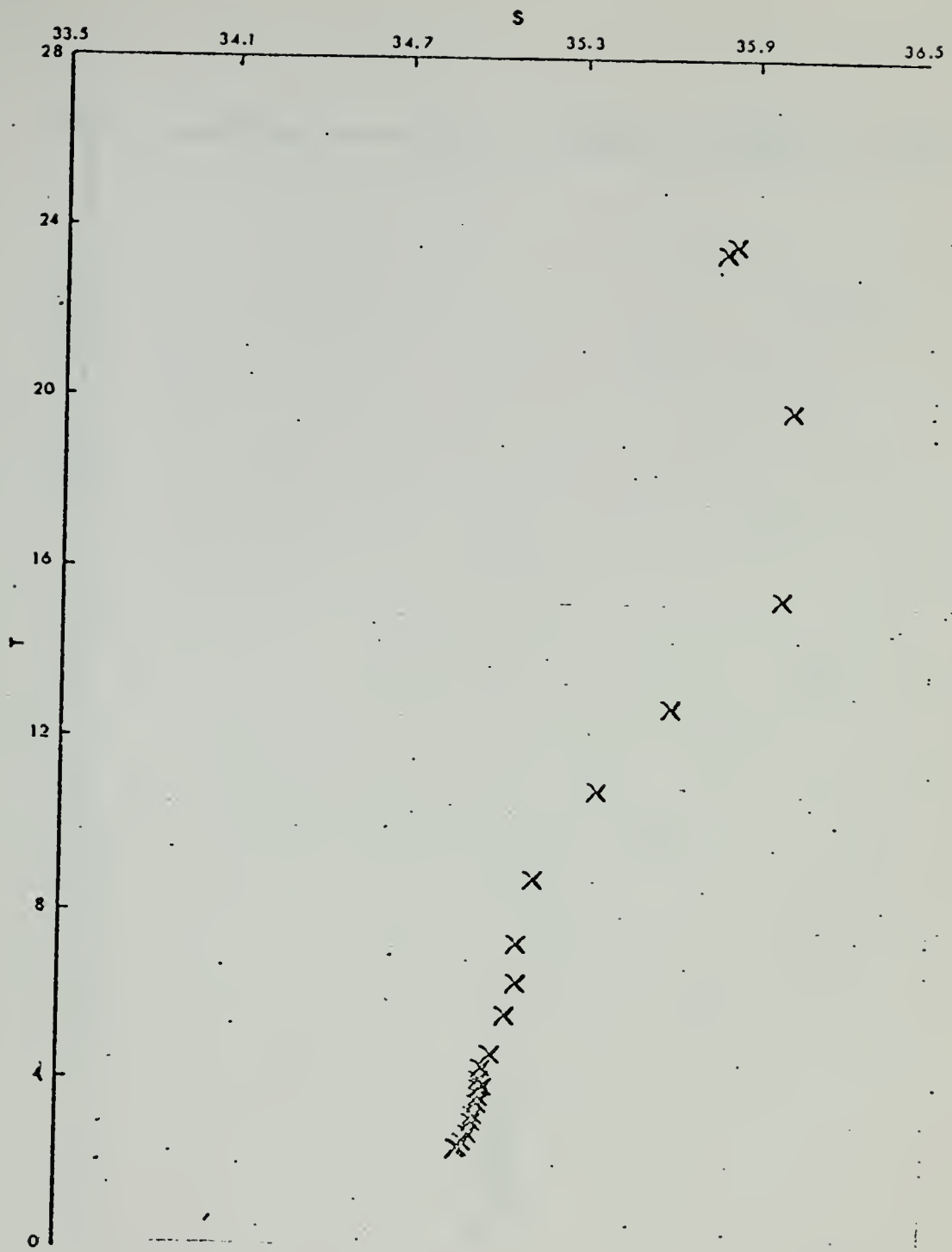

Crawford station 225

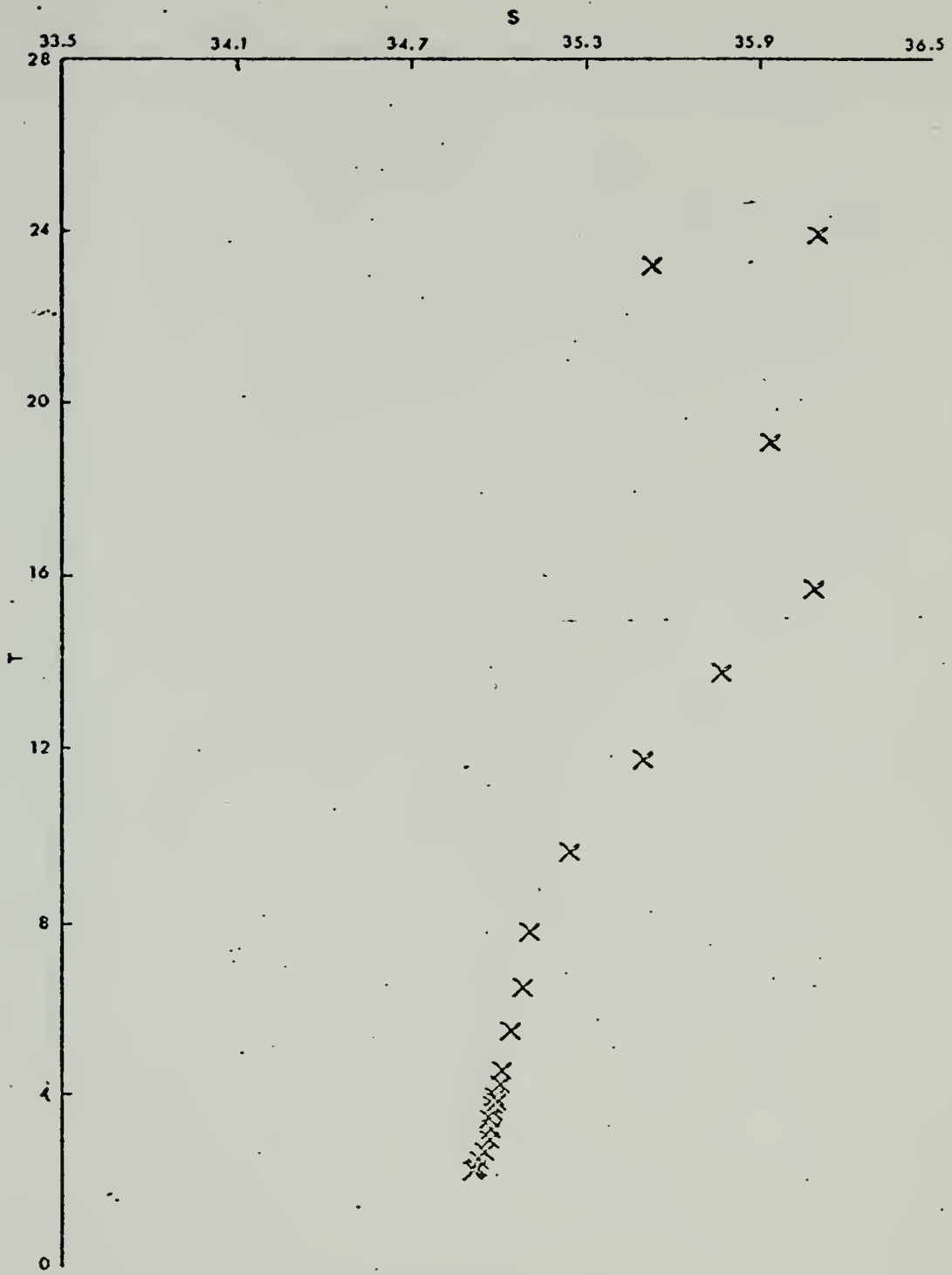

Crawford station 226

Crawford station 227

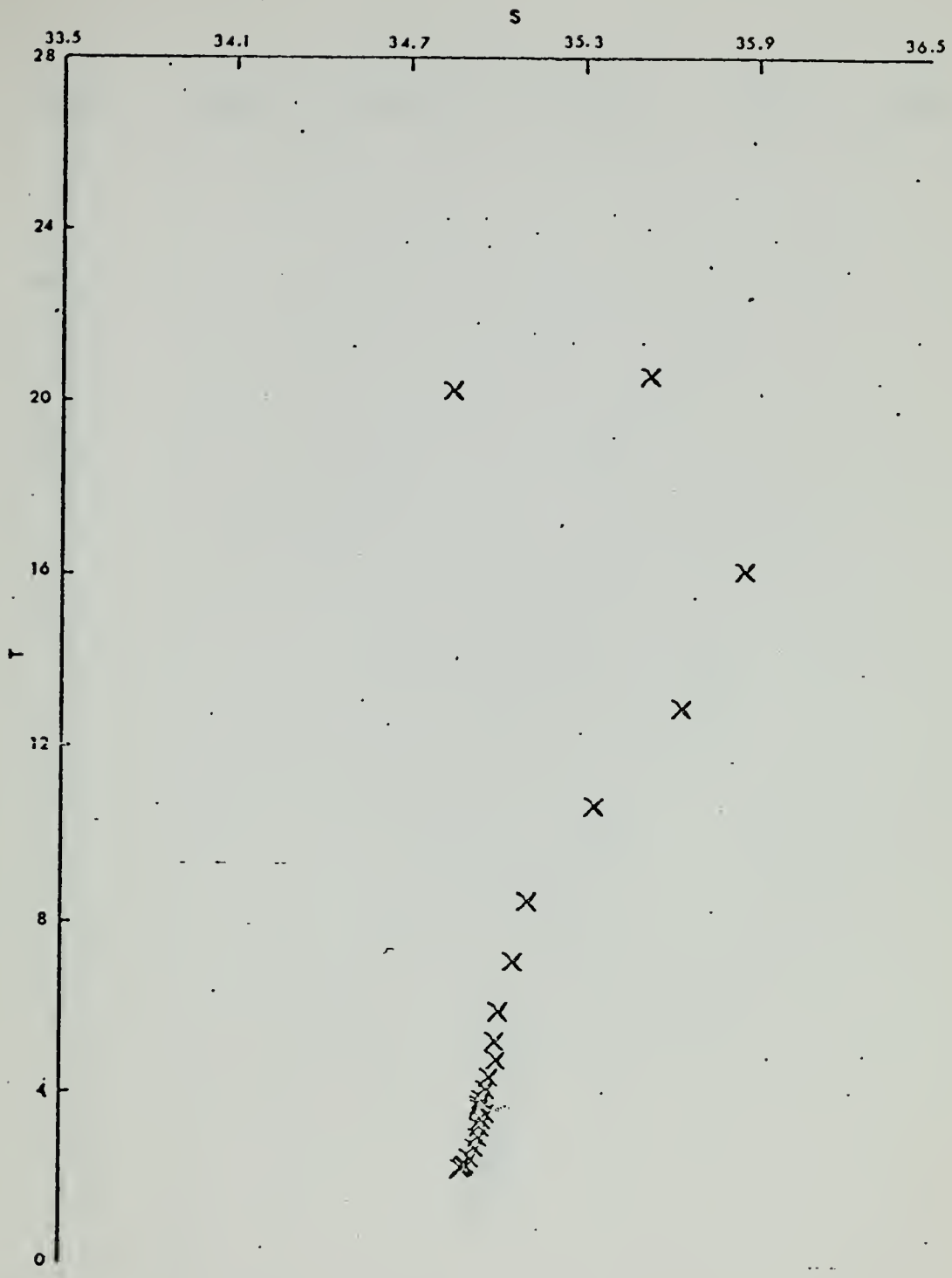

Crawford station 228

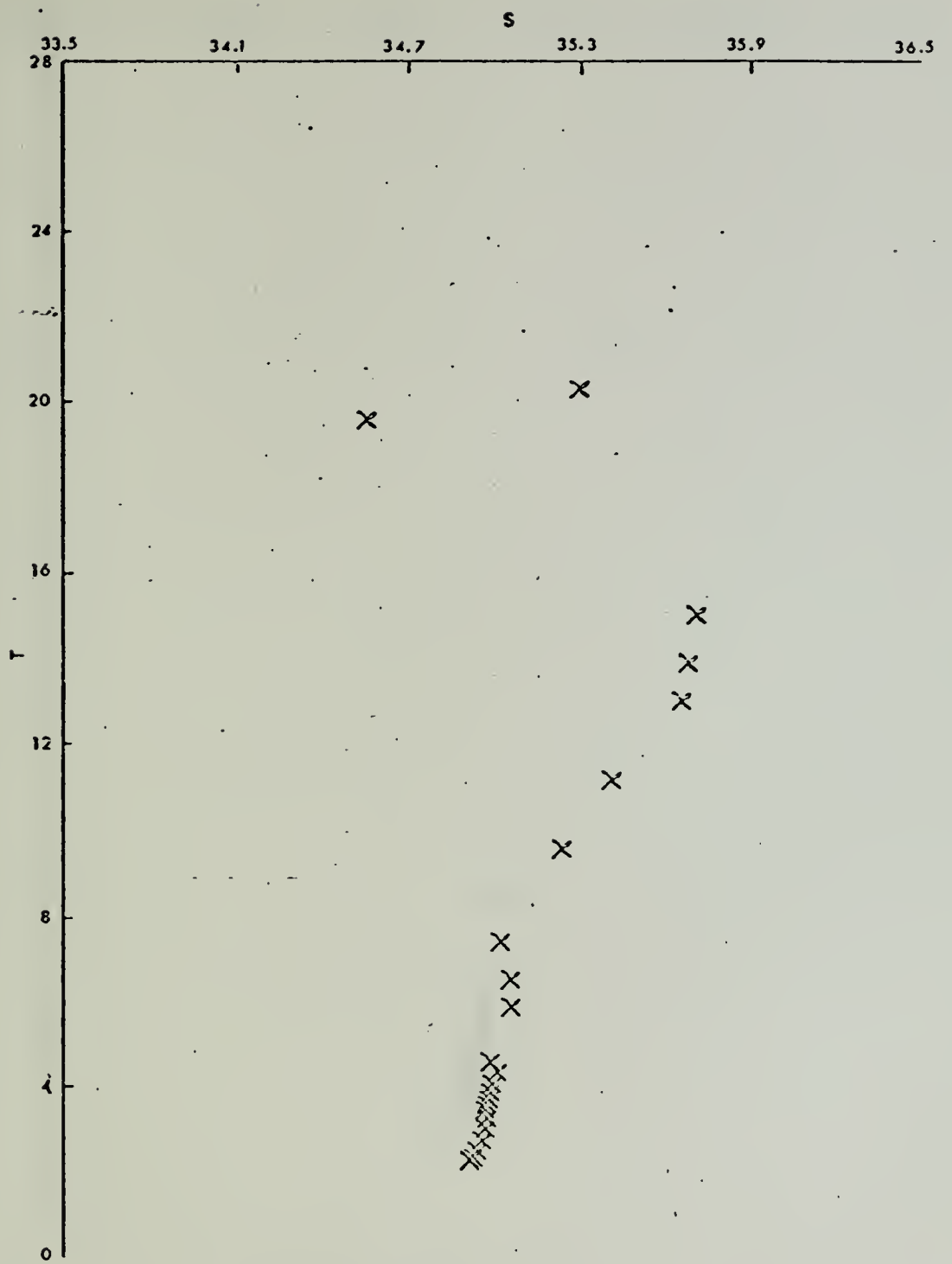

Crawford station 229

Crawford station 230

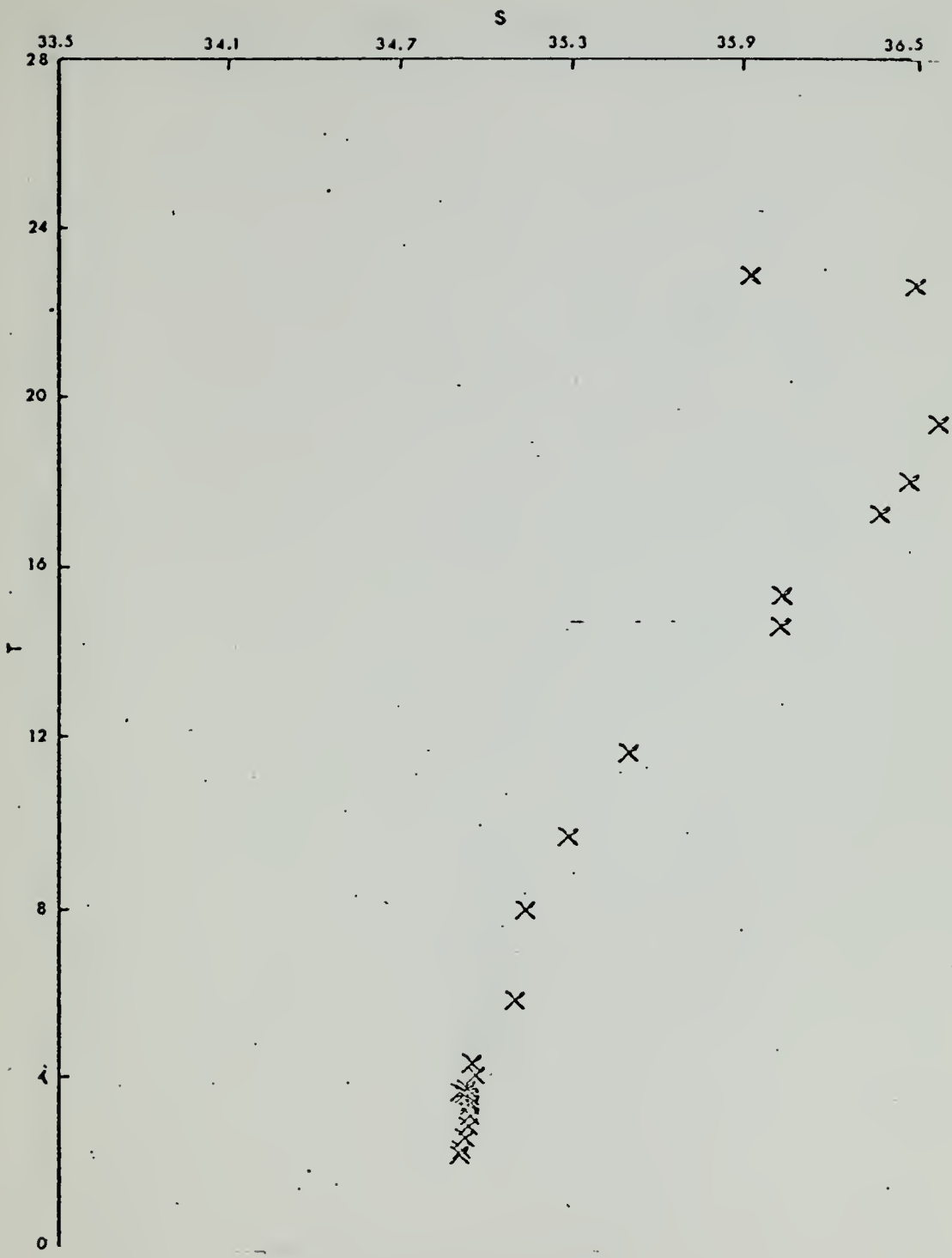

Crawford station 231

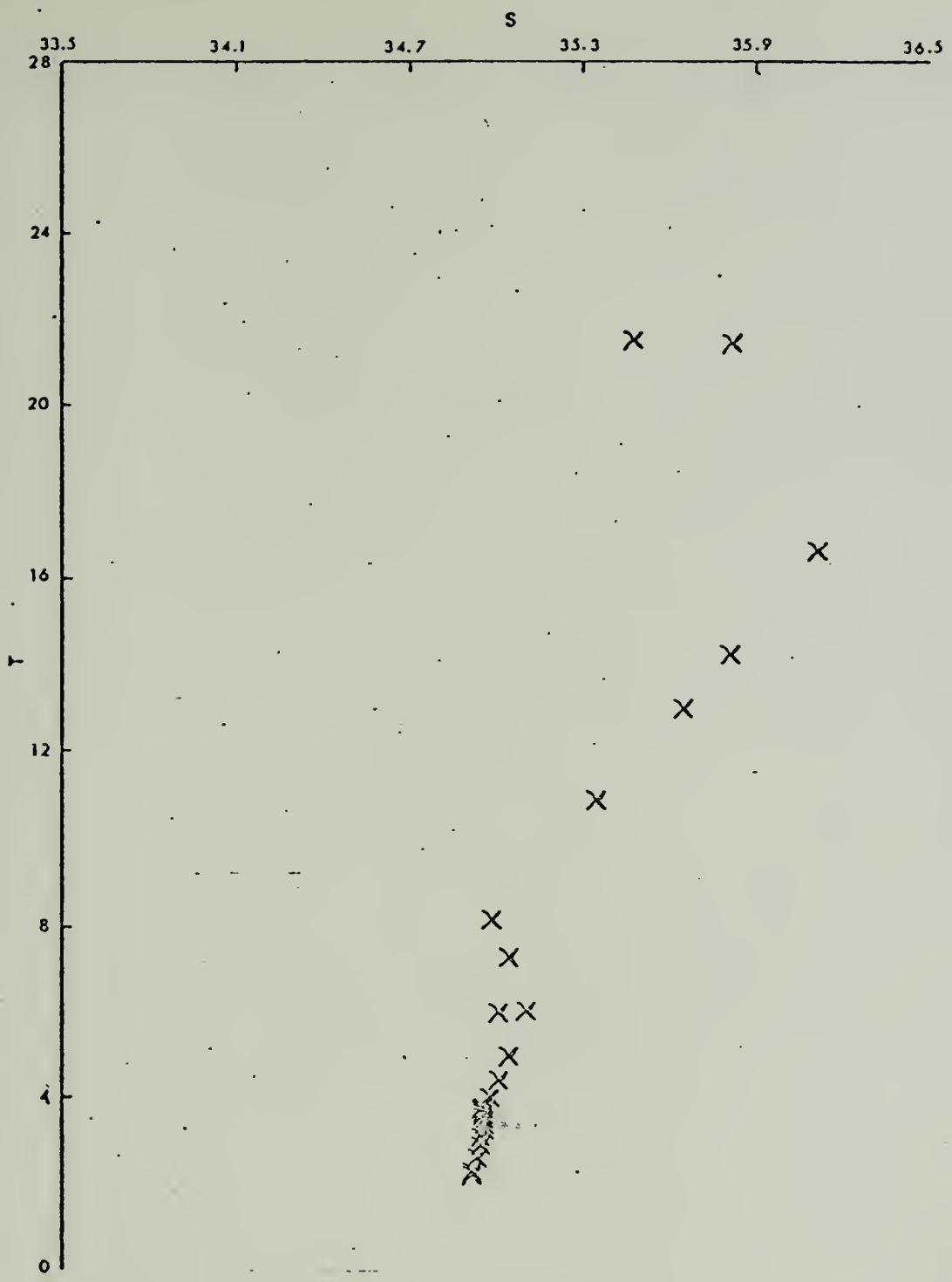

Crawford station 232

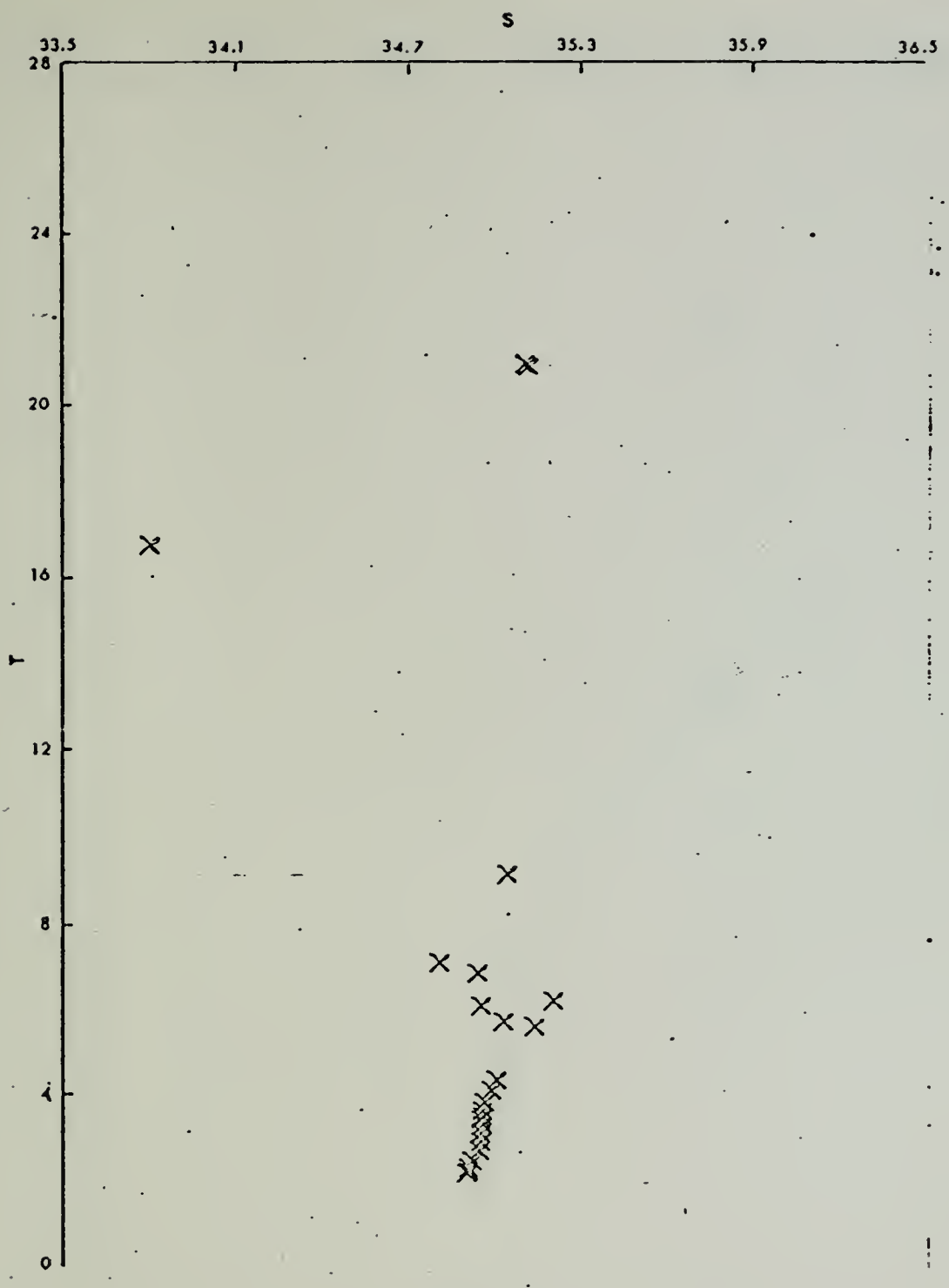

Crawford station 233

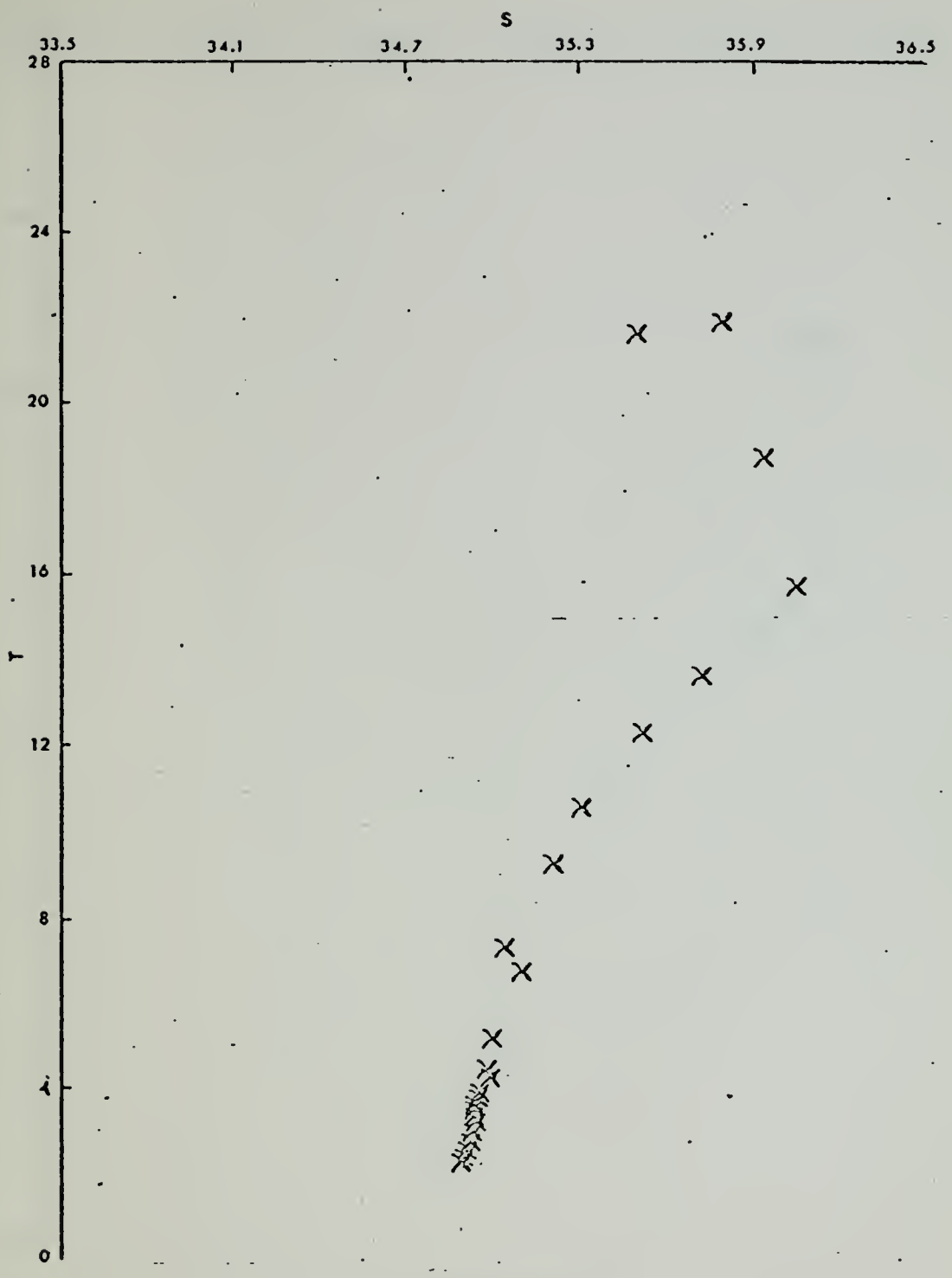

Crawford station 234

Crawford station 235

Crawford station 236

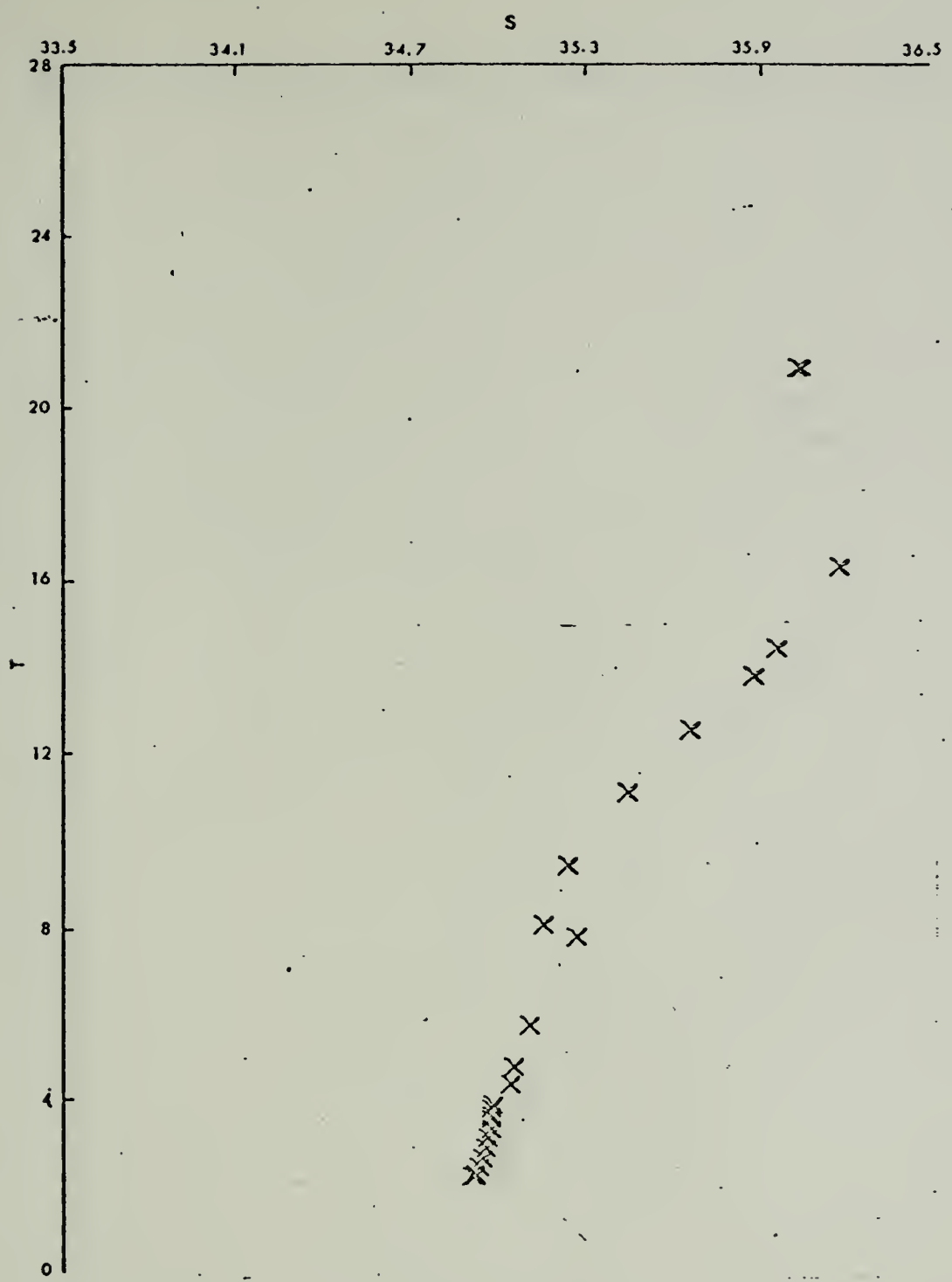

Crawford station 237

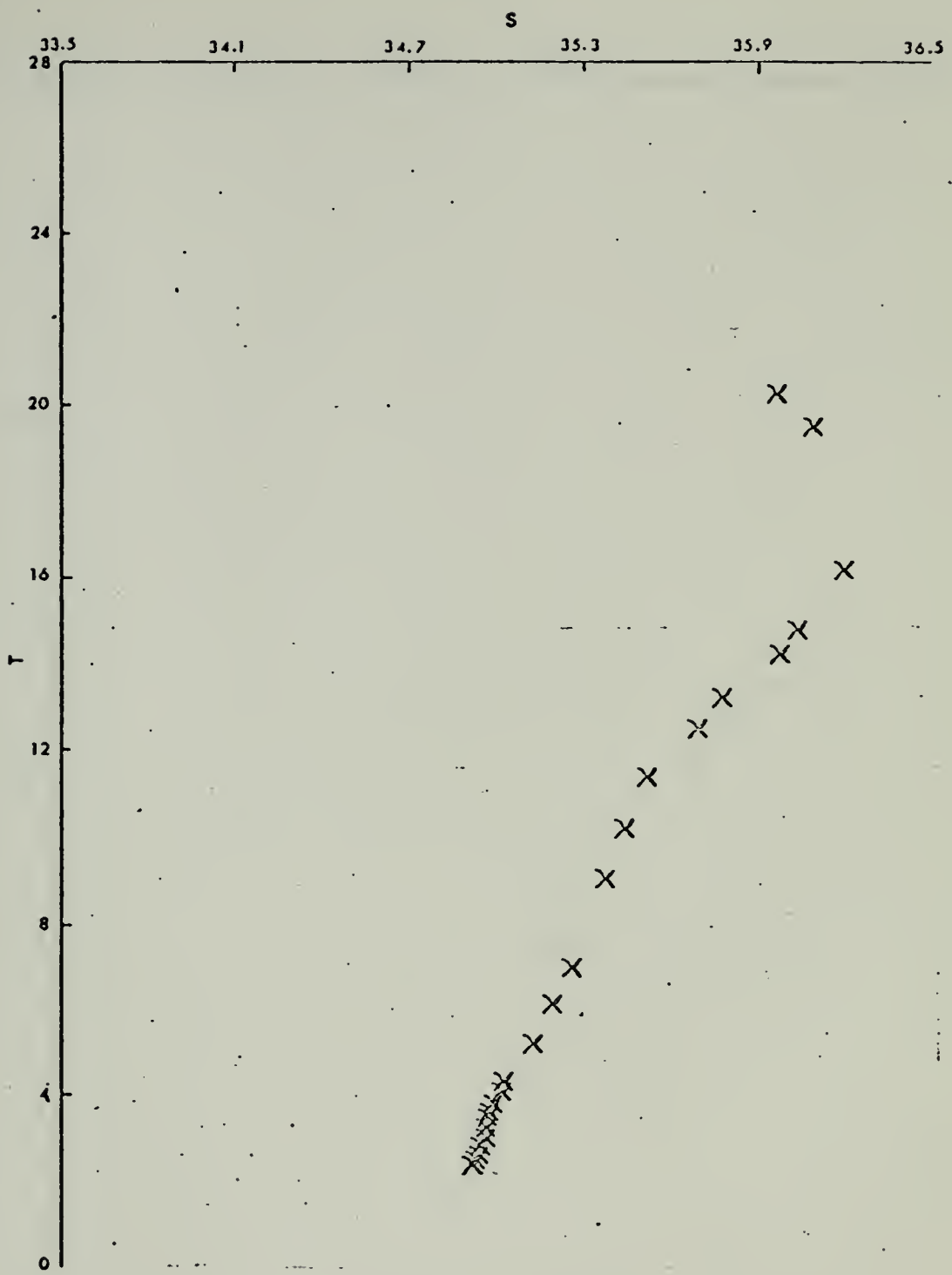

Crawford station 238

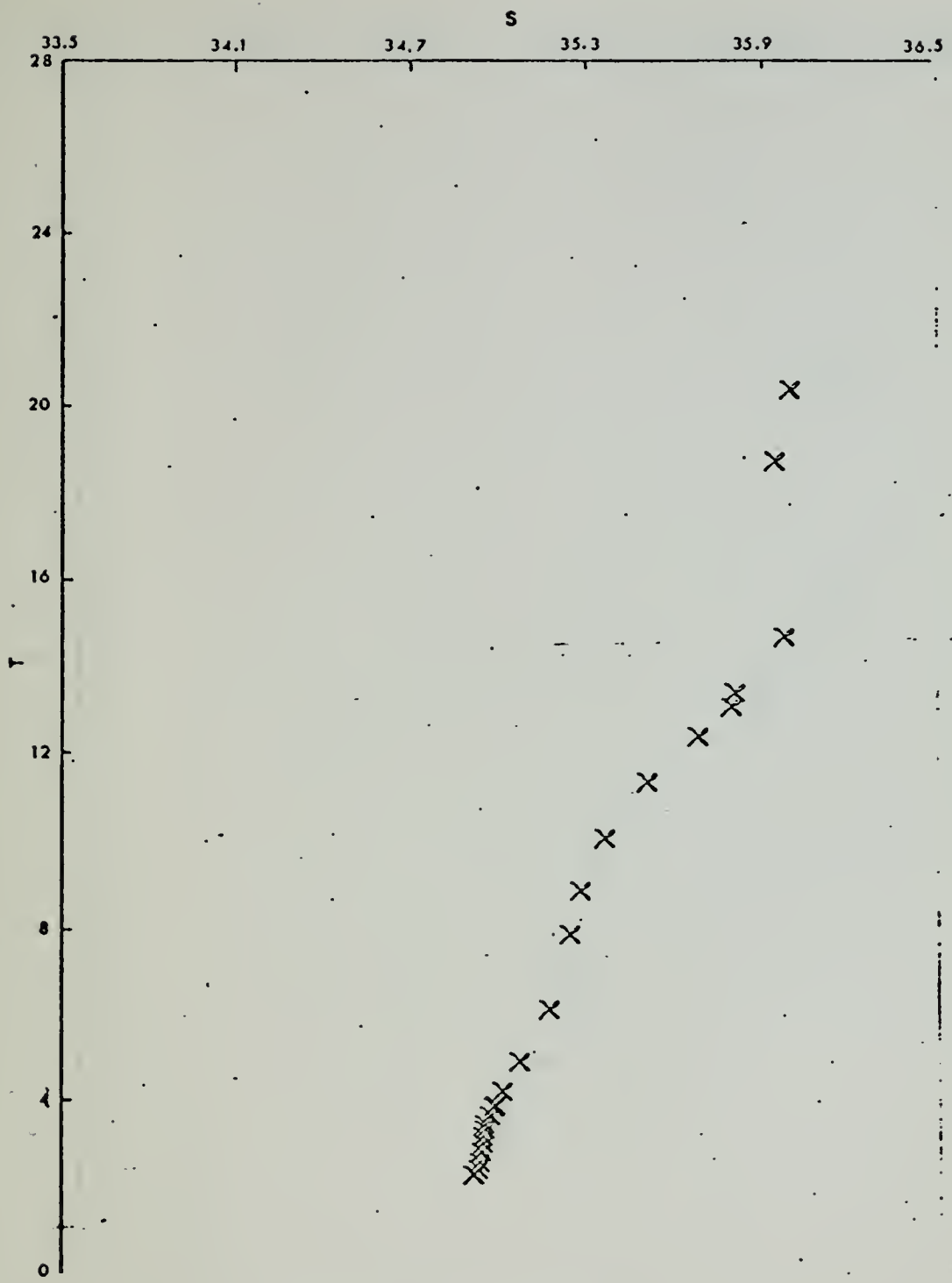

Crawford station 239

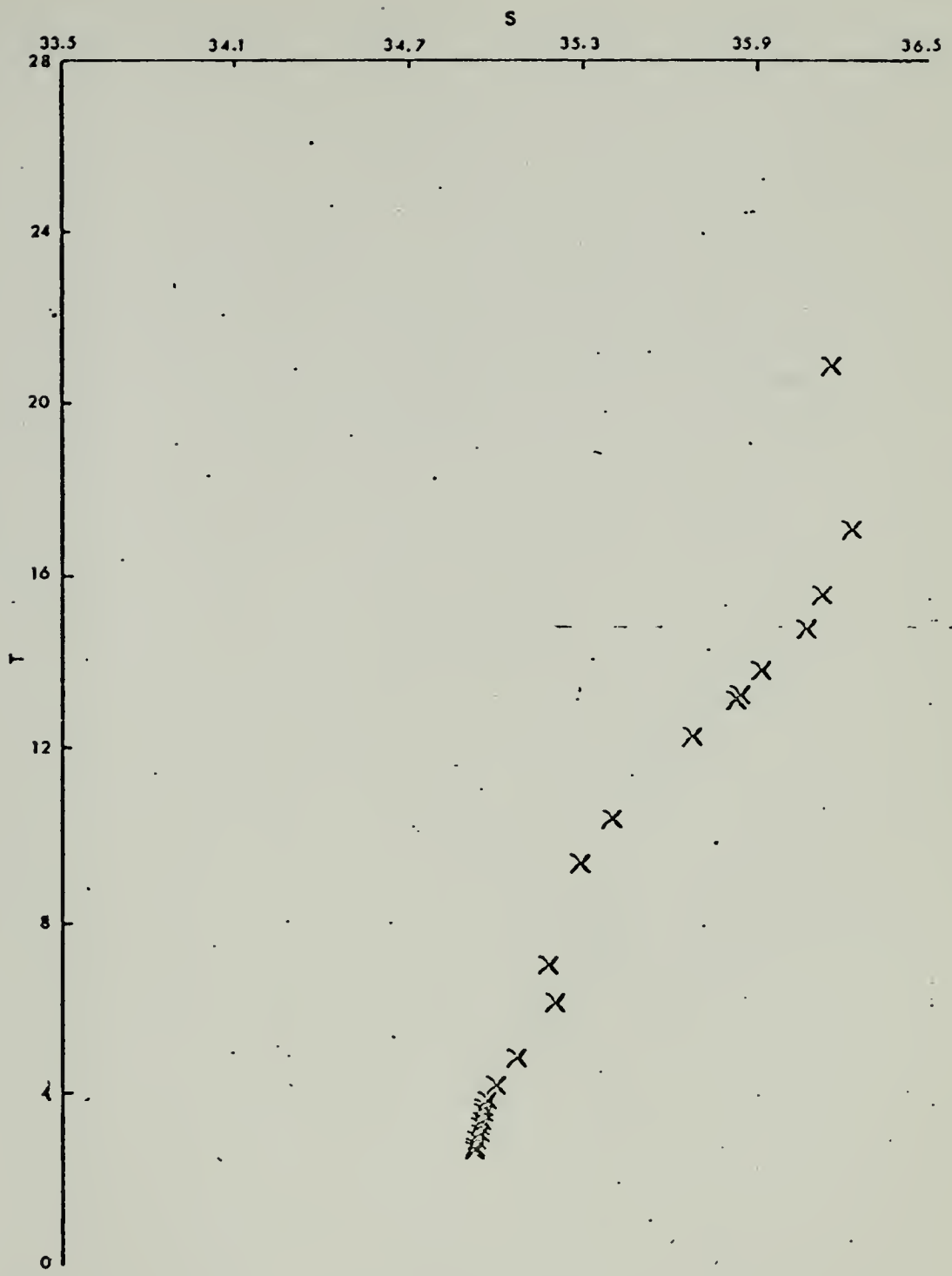

Crawford station 240

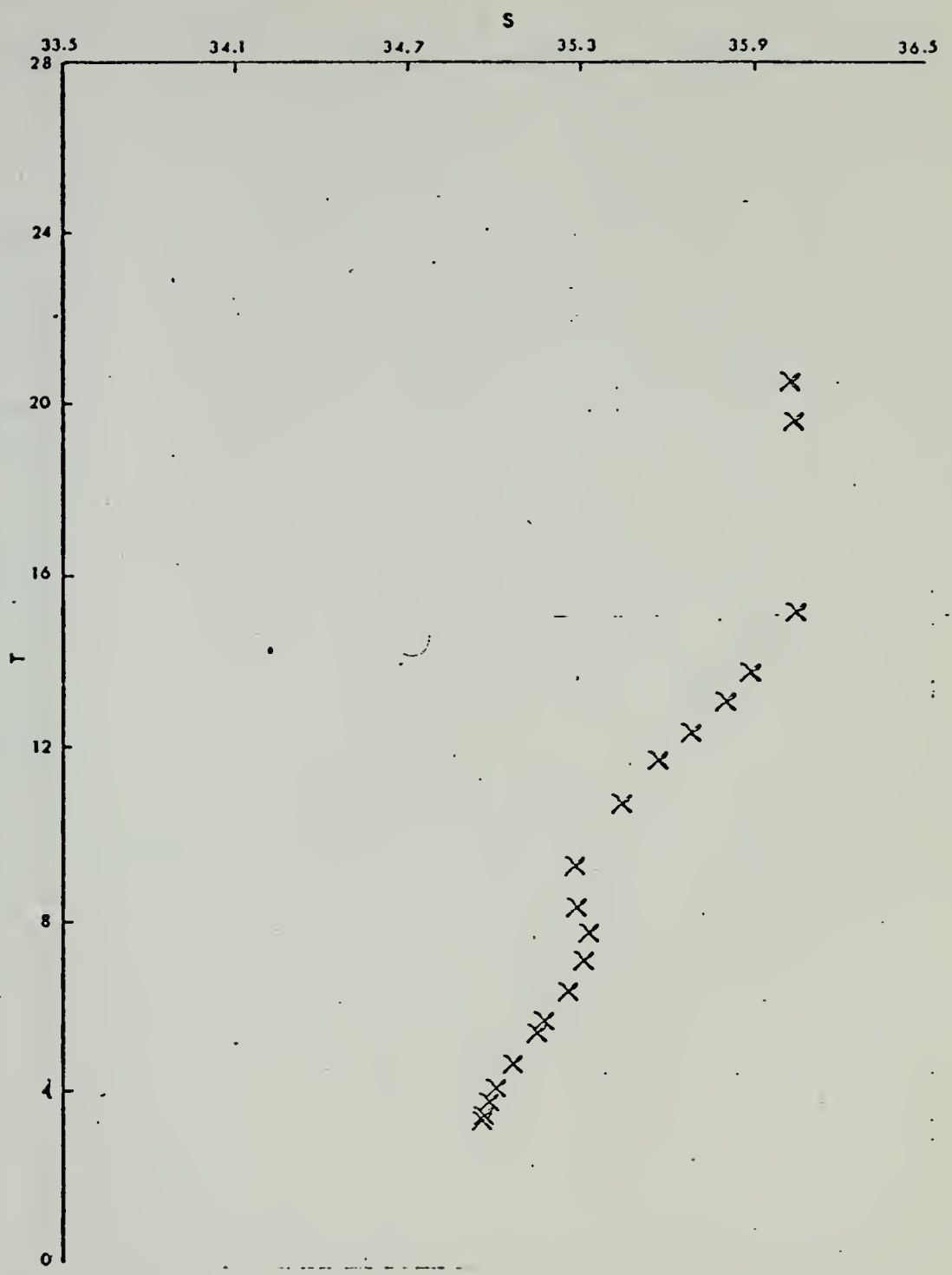

Crawford station 241

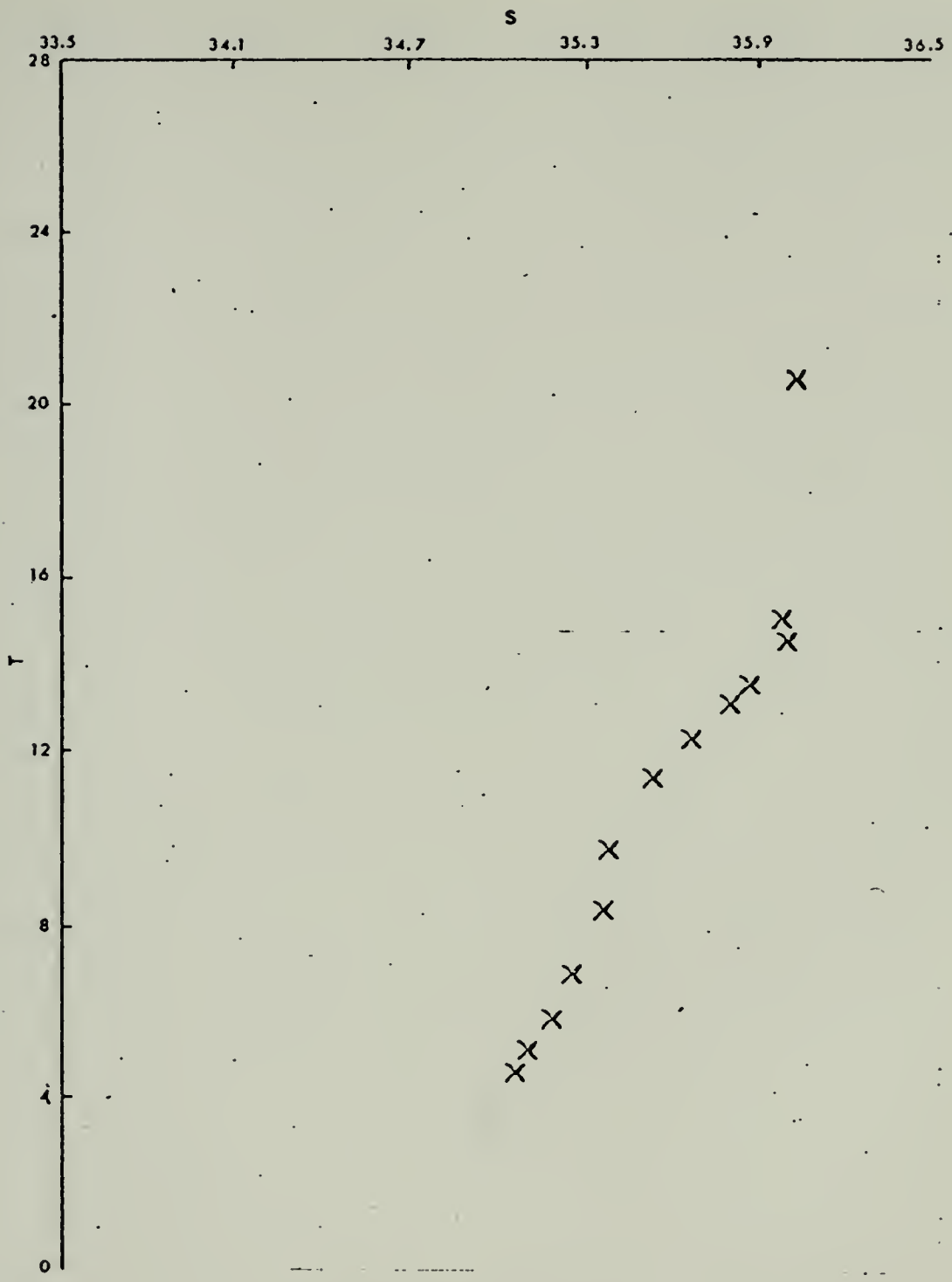

Crawford station 242

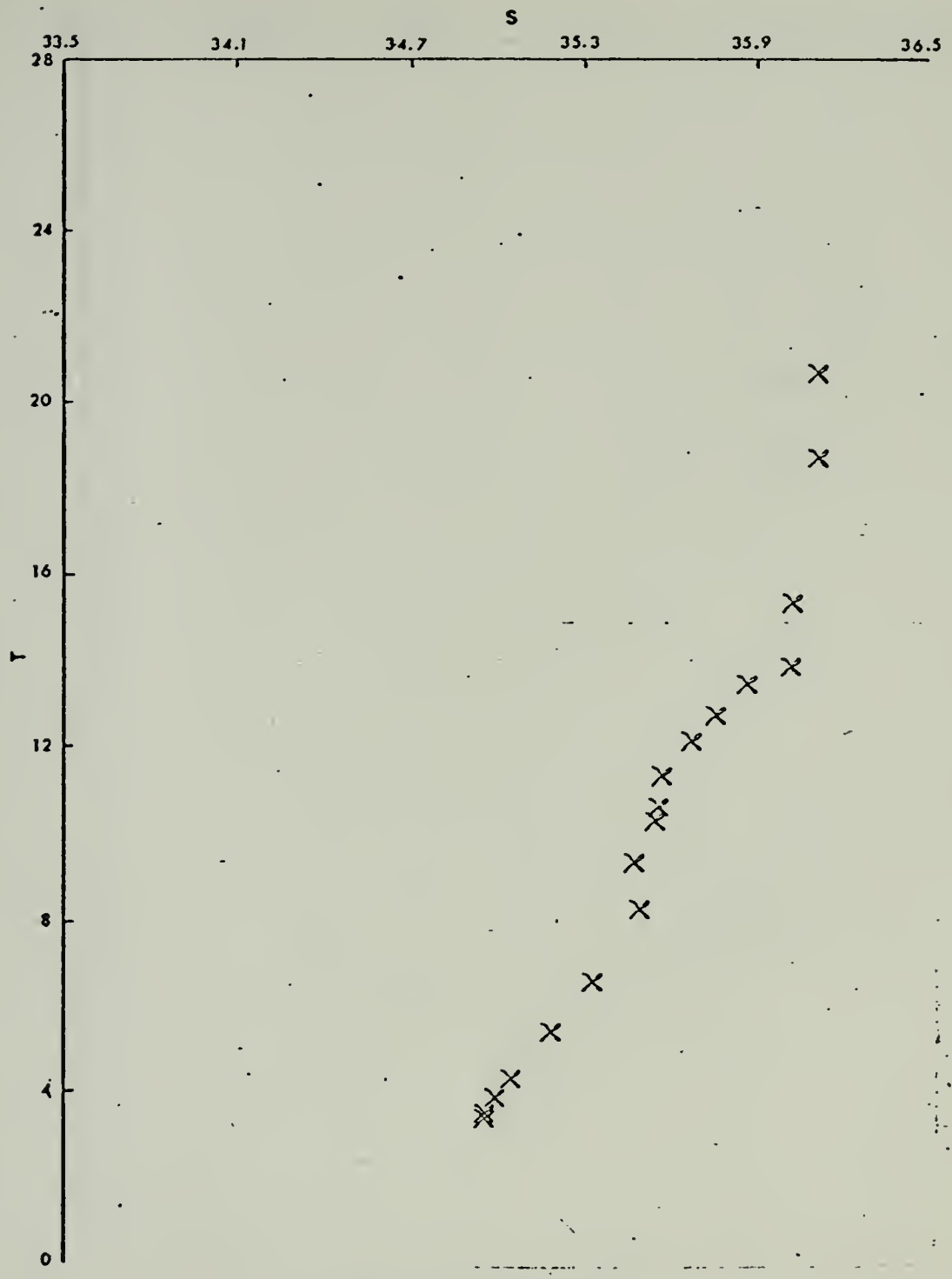

Crawford station 243

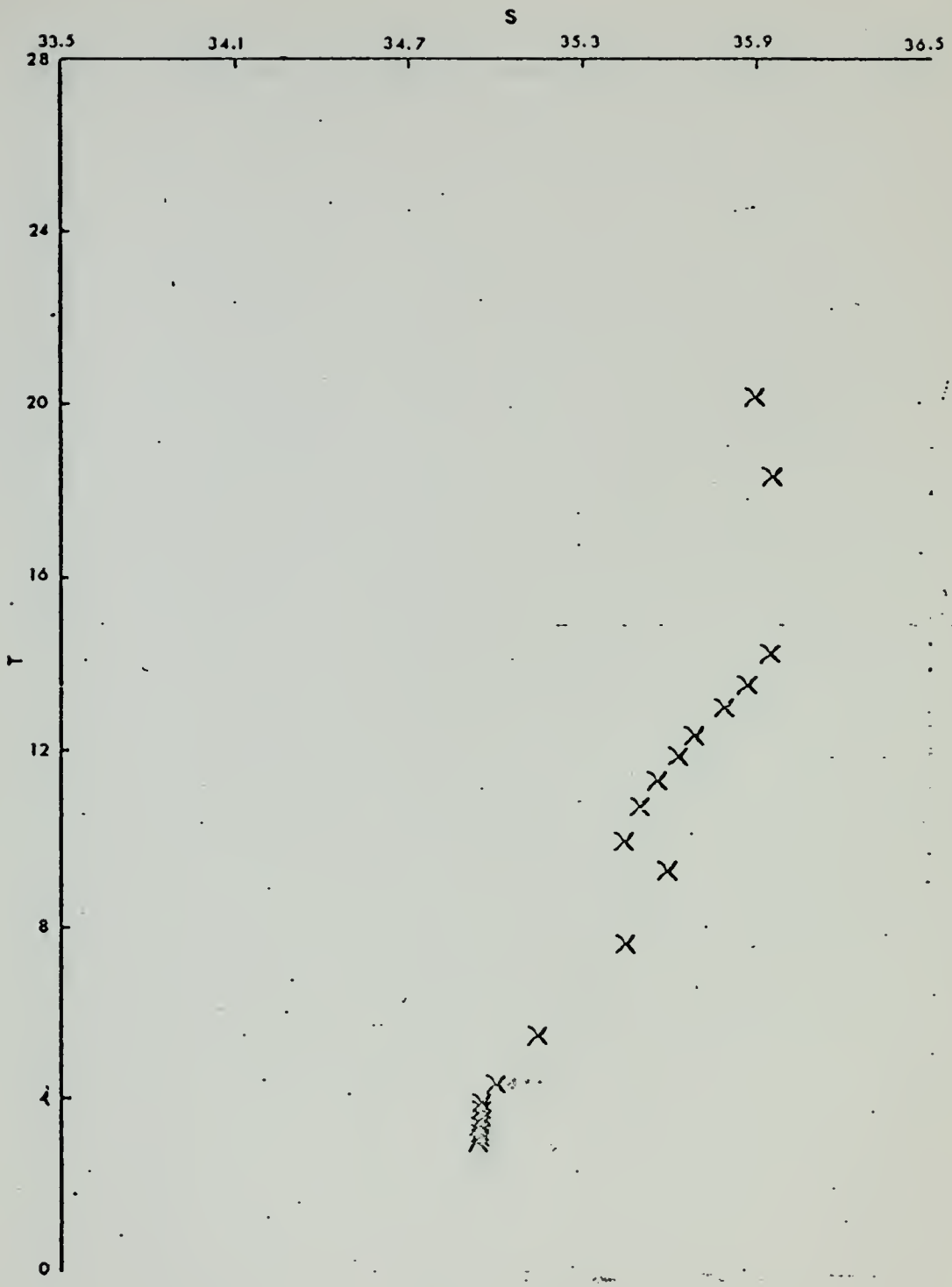

Crawford station 244

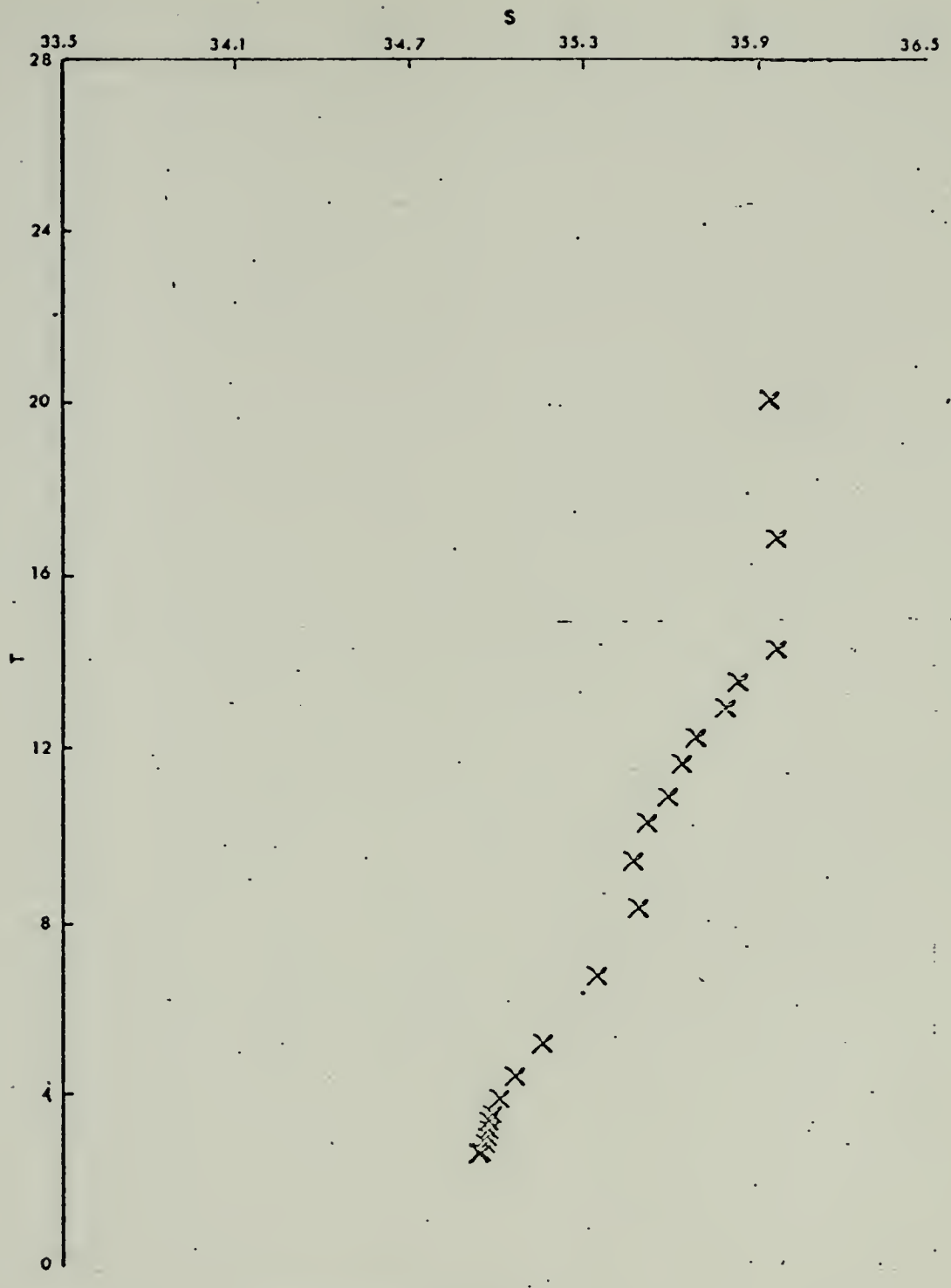

Cramford station 245

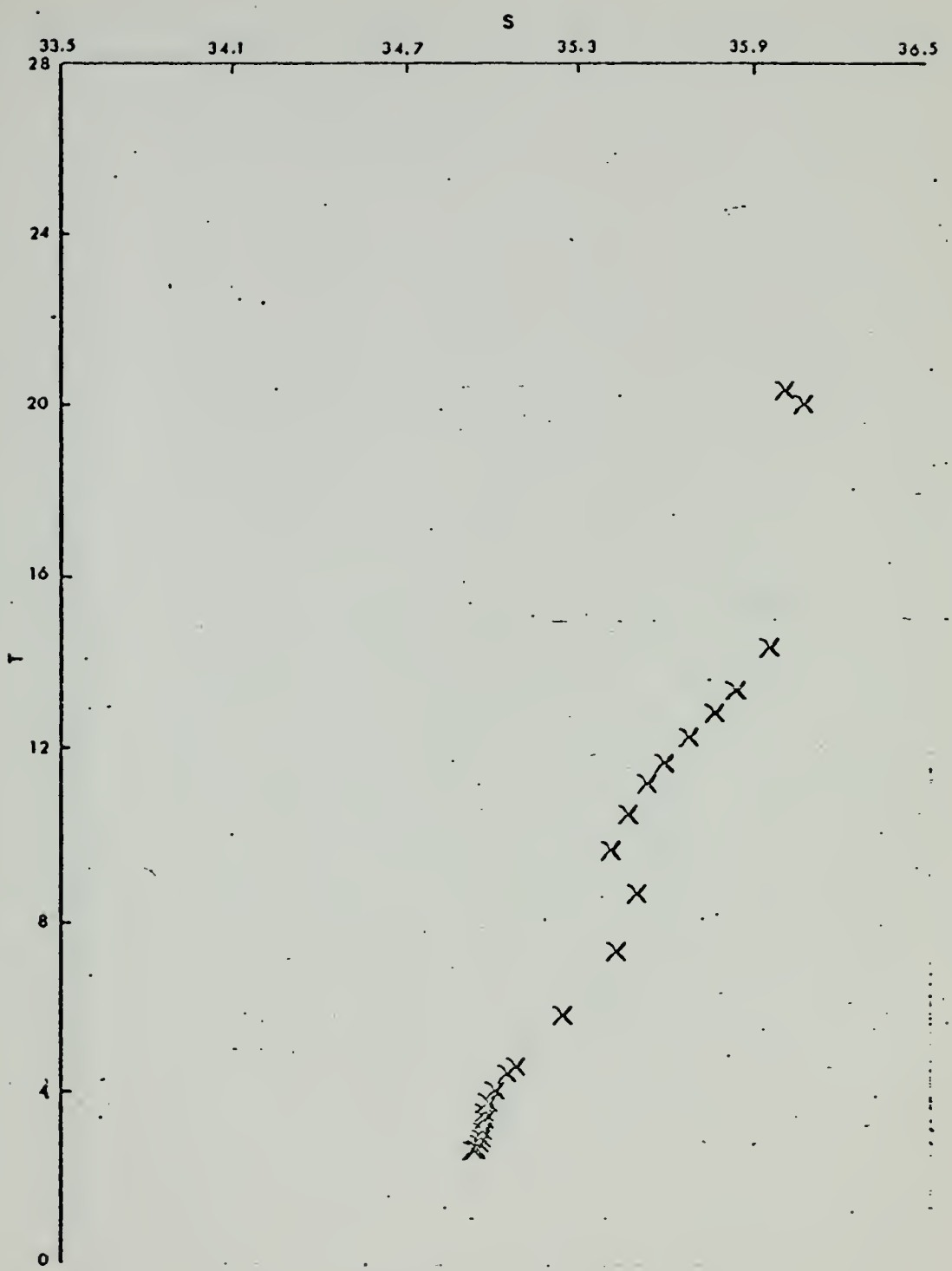

Crawford station 246

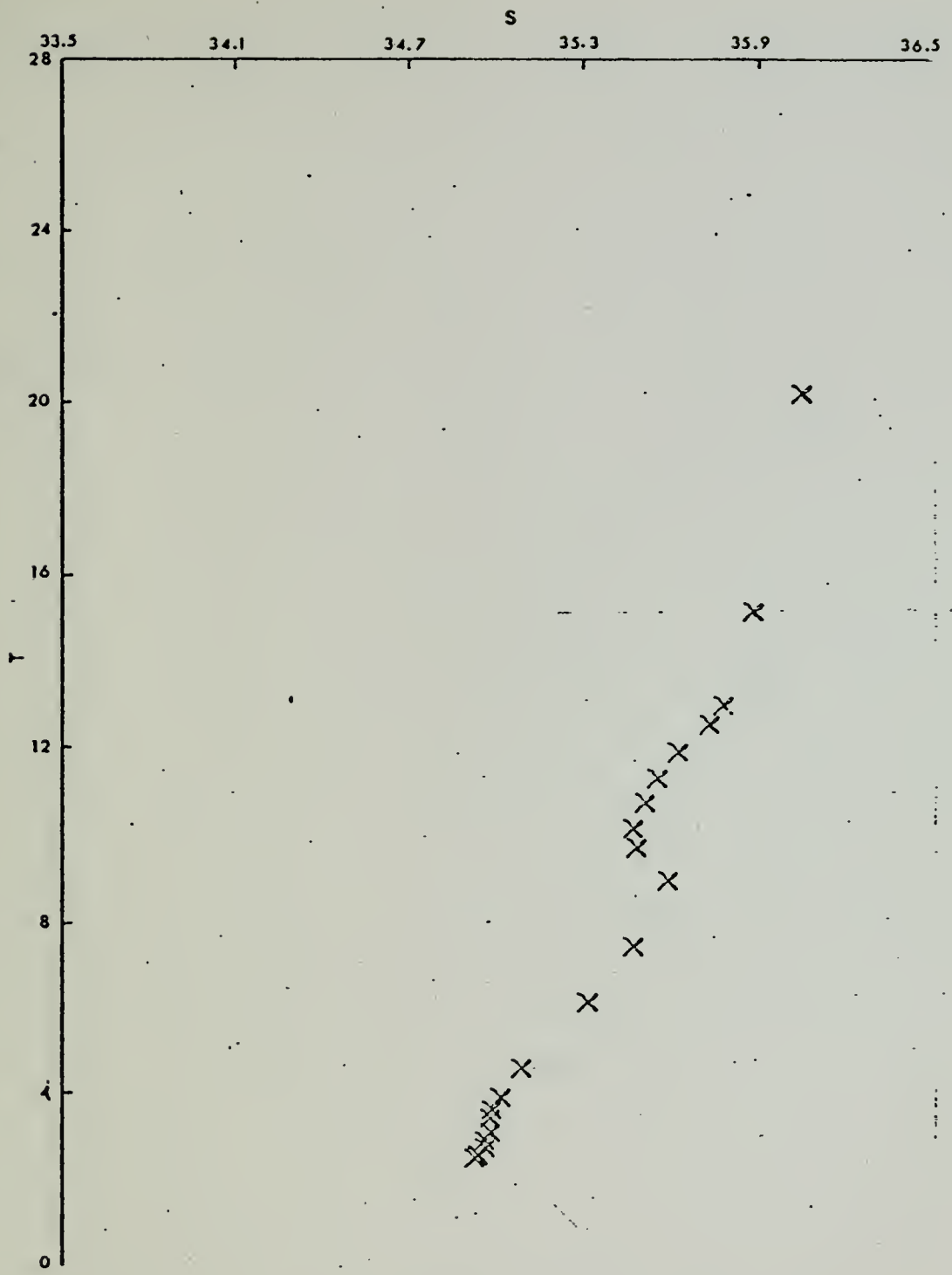

Crawford station 247

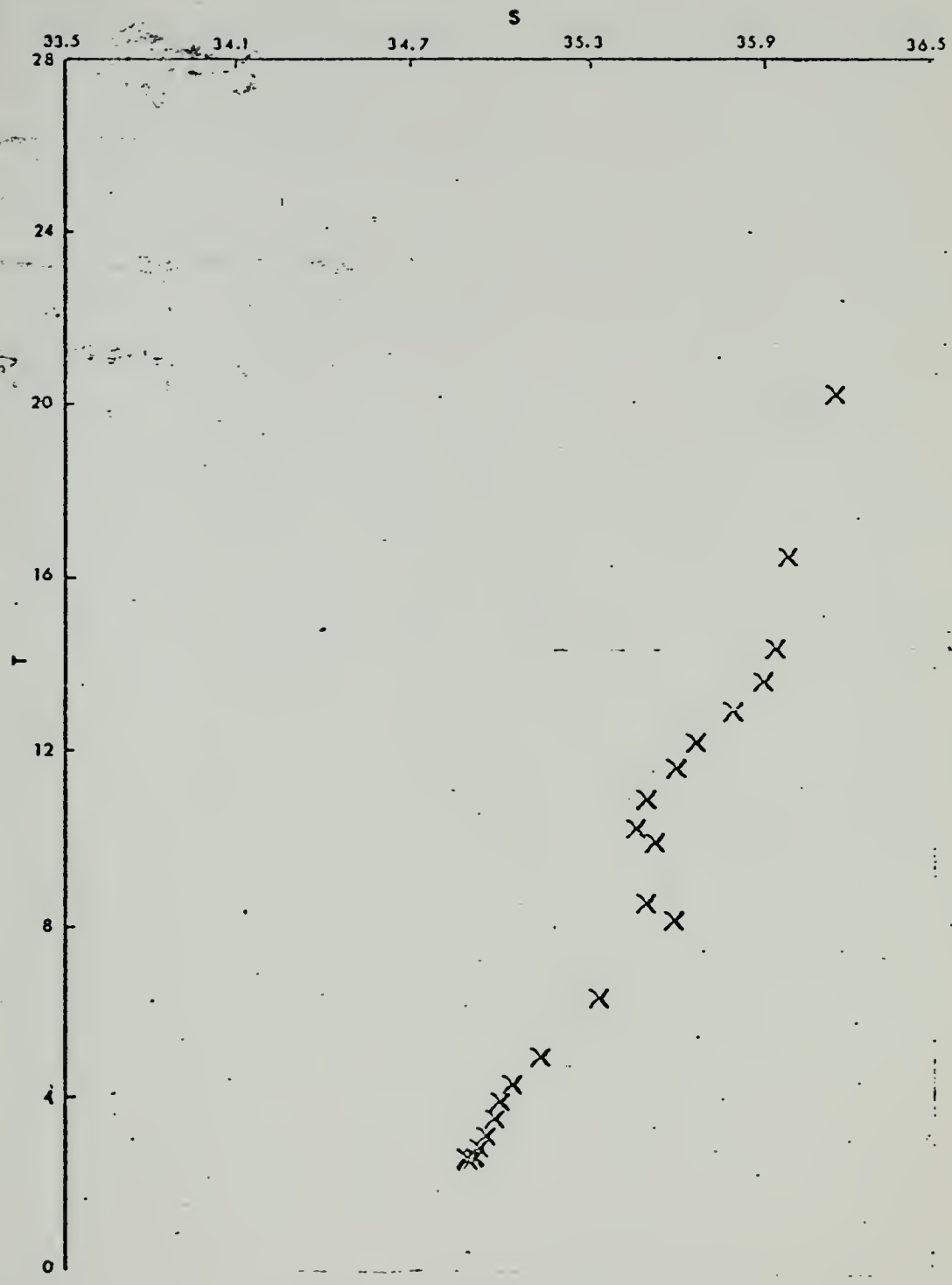

Crawford station 248

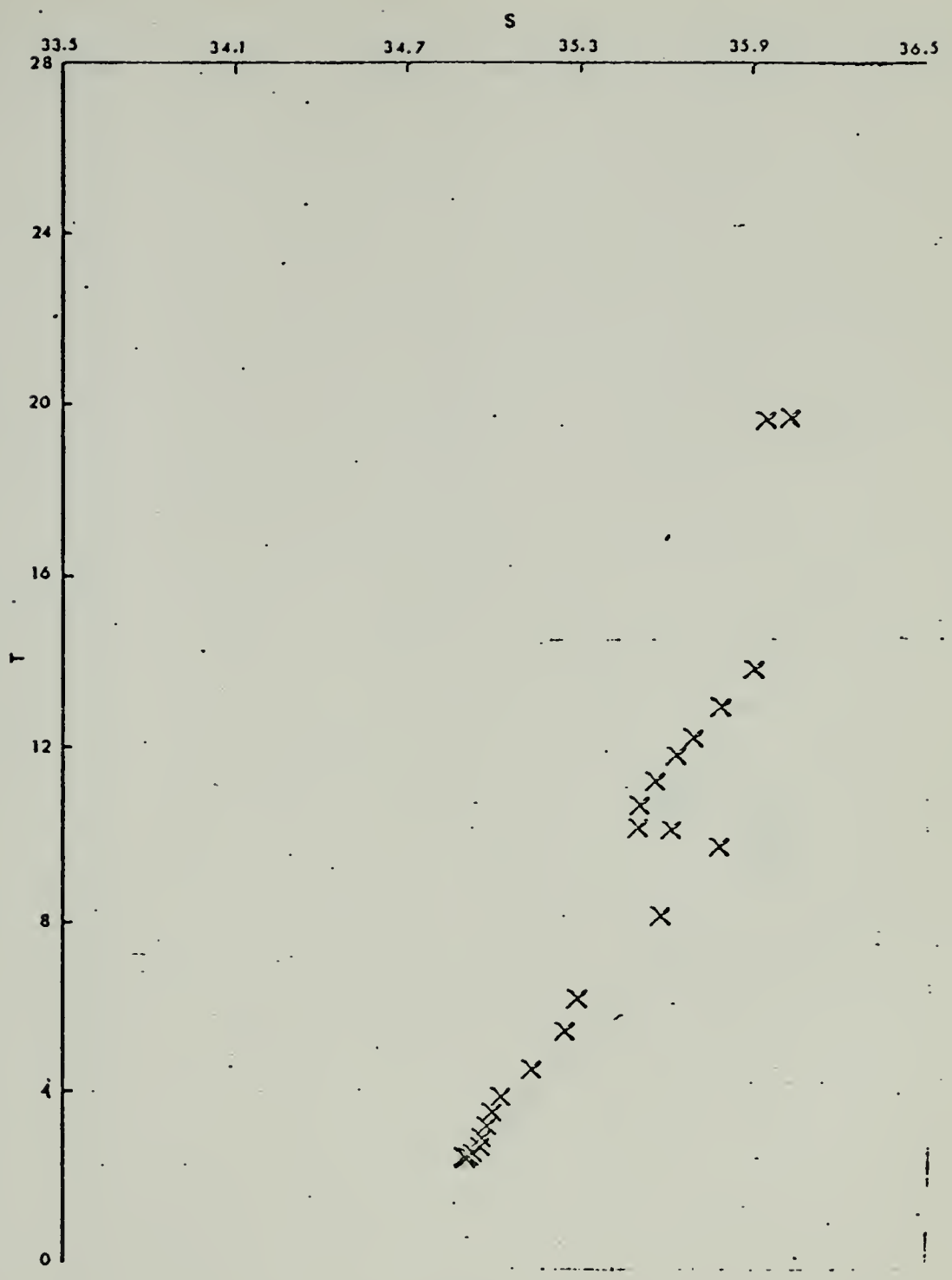

Crawford station 249

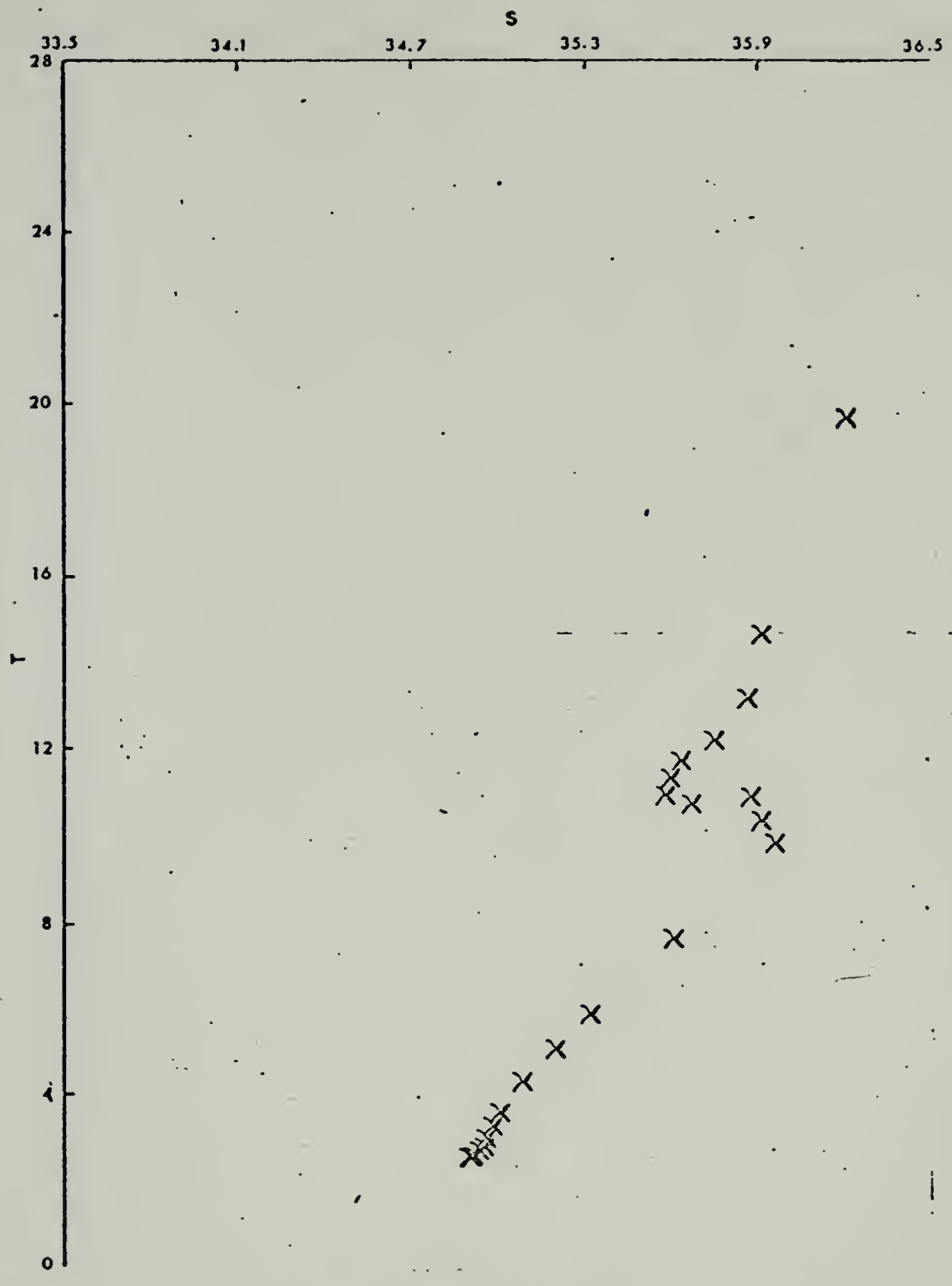

Crawford station 250

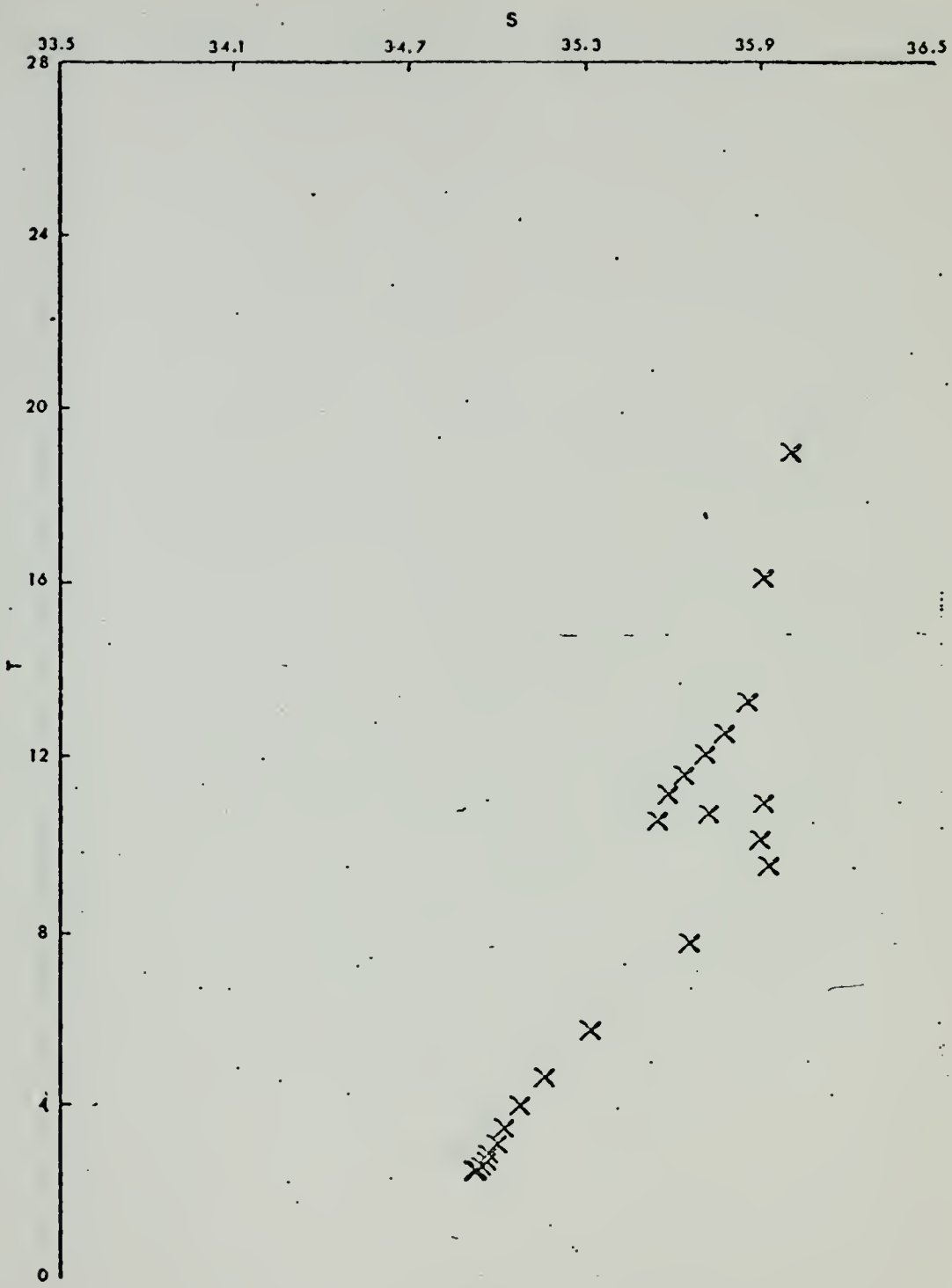

Crawford station 251

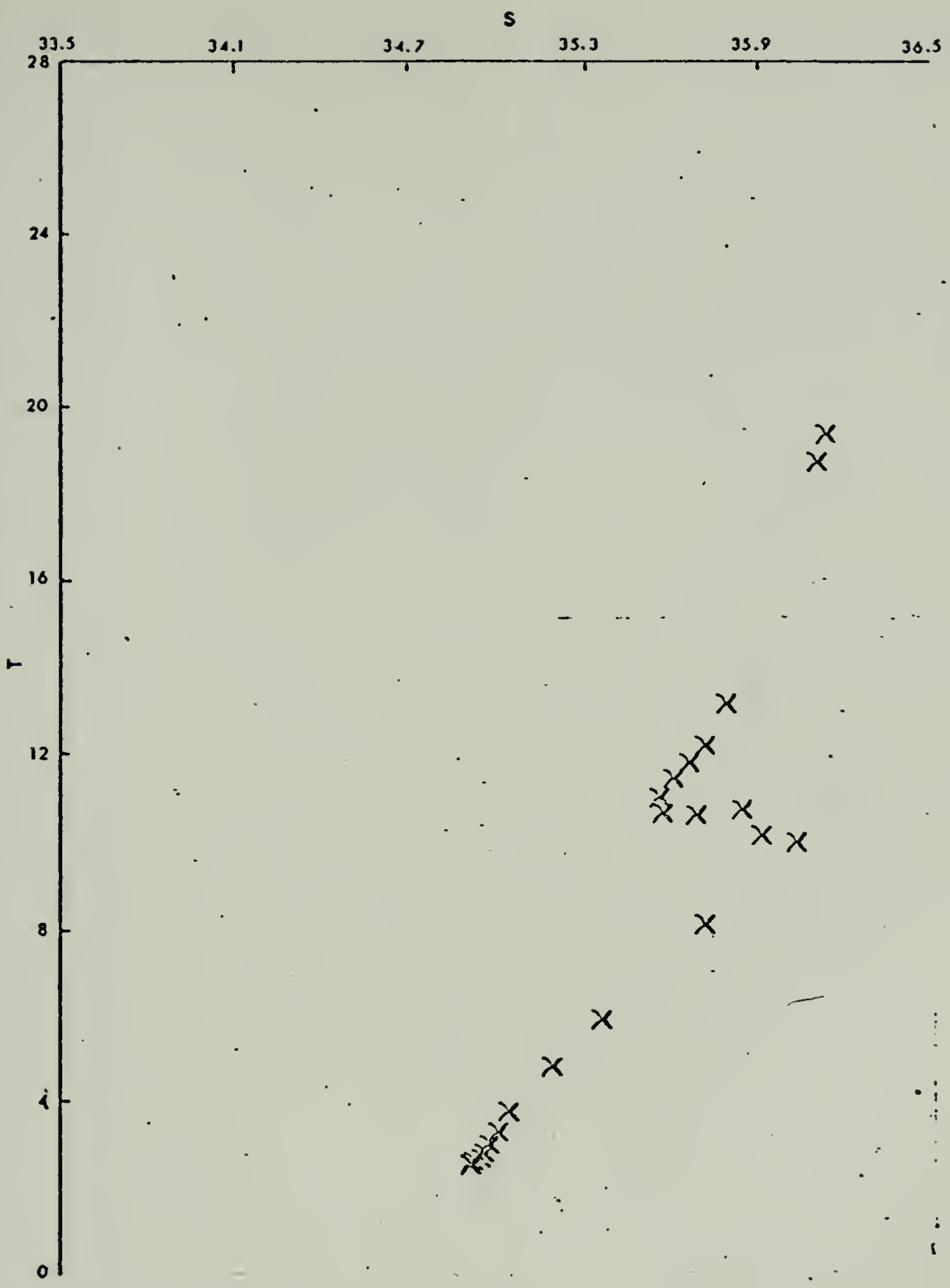

Crawford station 252

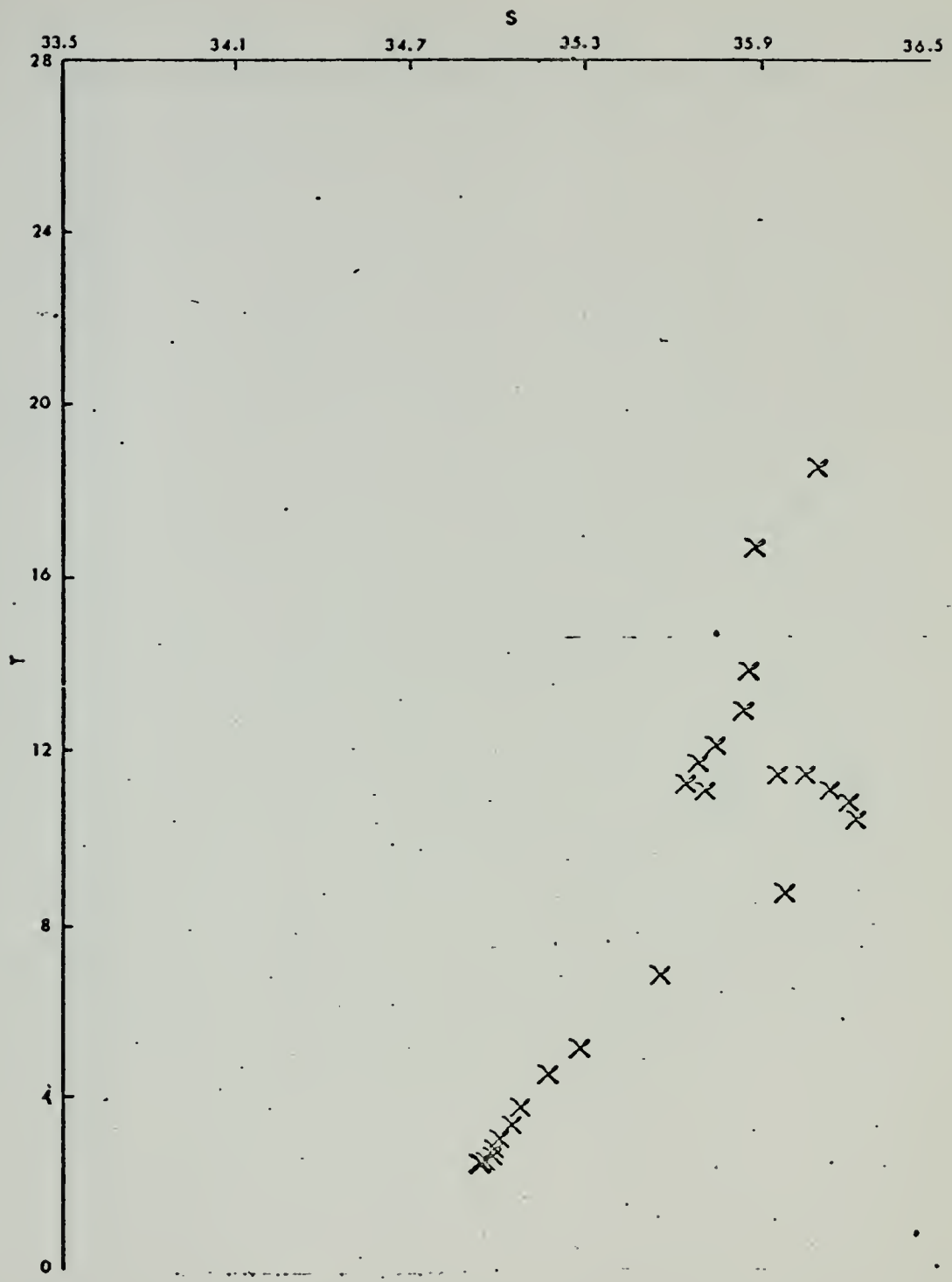

Crawford station 253

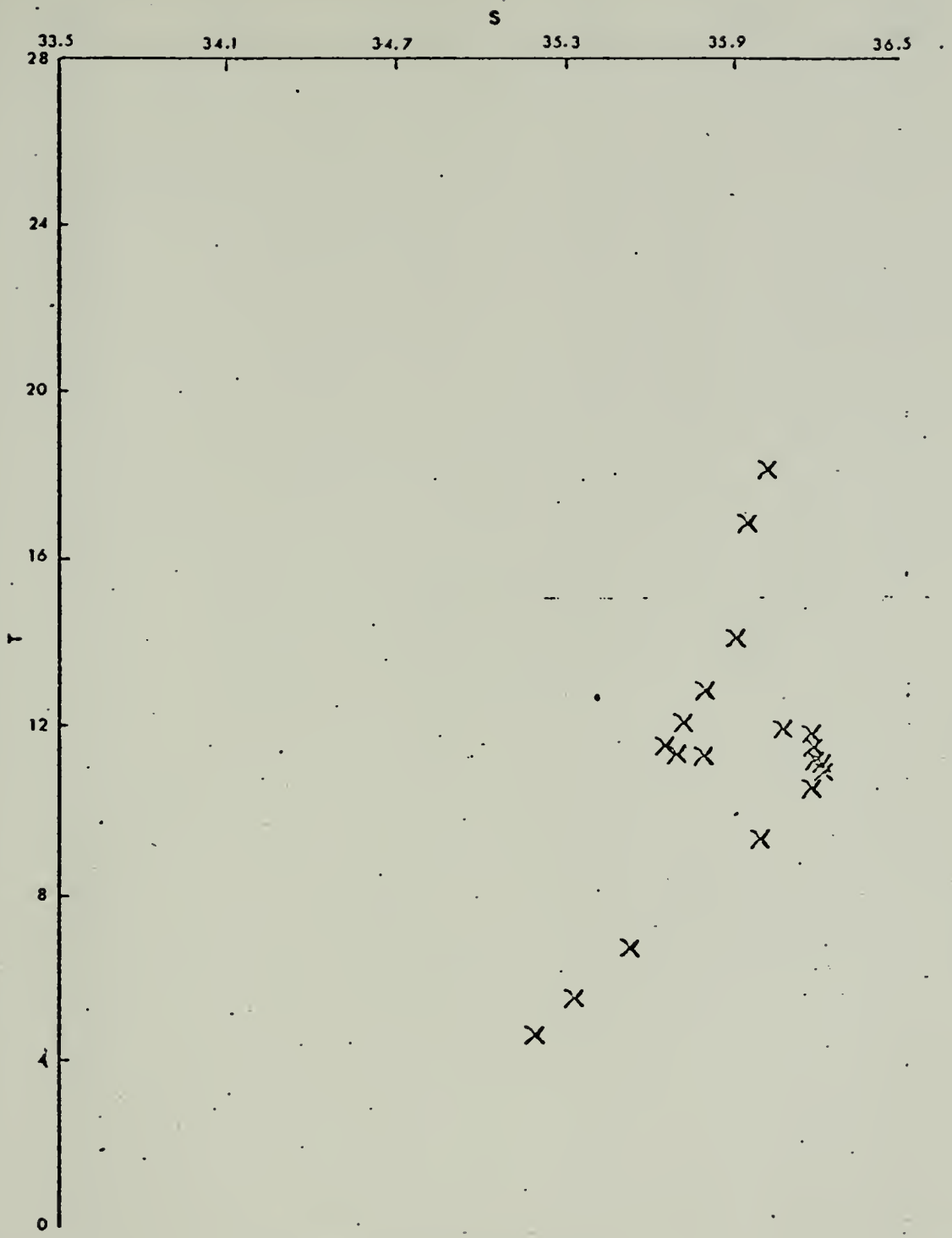

Crawford station 254

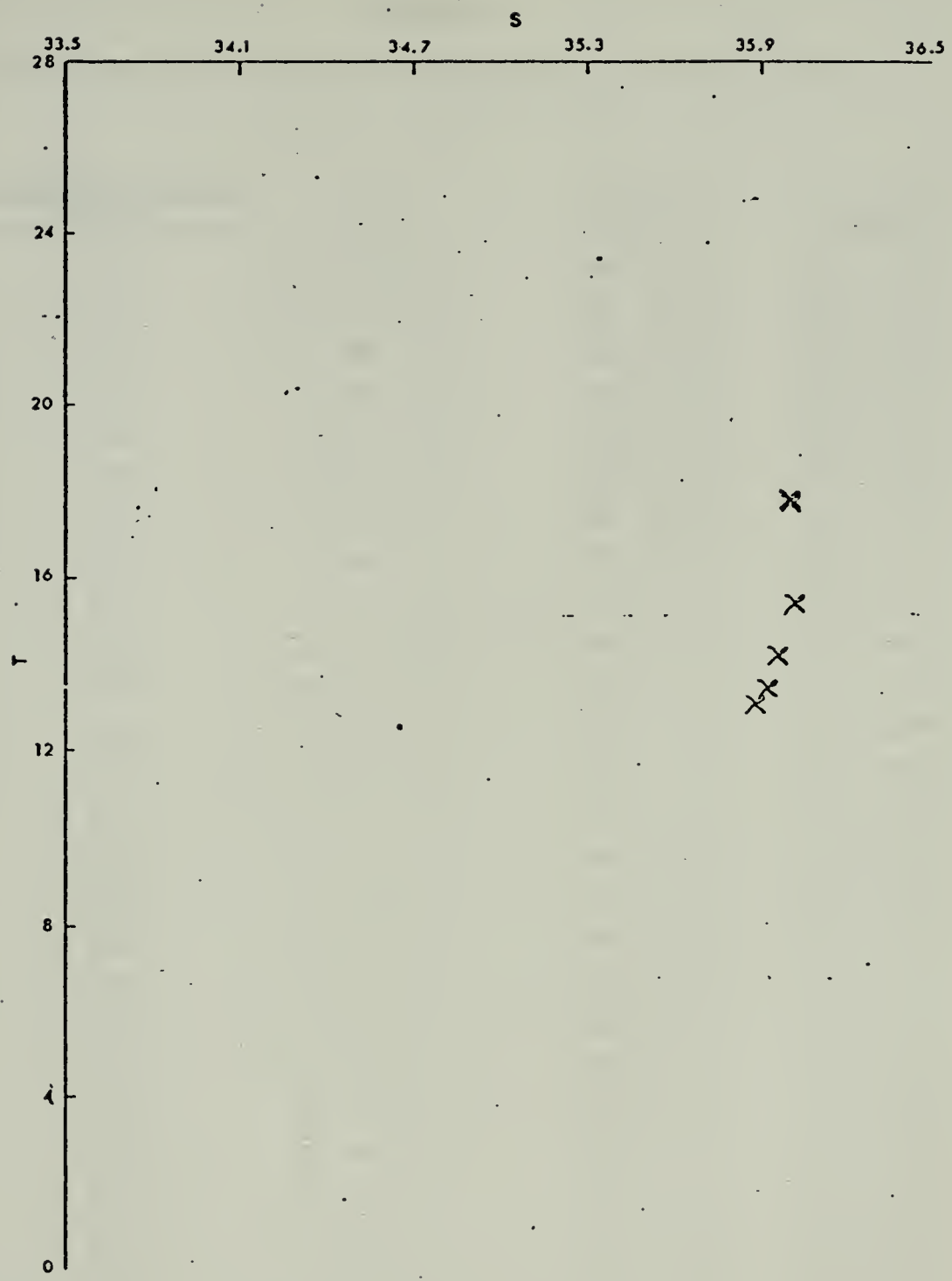

Crawford station 255

APPENDIX C

LATITUDE AND LONGITUDE FOR CRAWFORD STATIONS 218-255

Crawford Station Number	Date	Latitude	Longitude
218	2 Oct 57	40° 15'N	68° 25'W
219	2 Oct 57	40° 15'N	67° 58'W
220	7 Oct 57	40° 15'N	67° 20'W
221	7 Oct 57	40° 15'N	66° 28'W
222	8 Oct 57	40° 14'N	64° 40'W
223	8 Oct 57	40° 16'N	62° 56'W
224	8 Oct 57	40° 10'N	61° 07'W
225	9 Oct 57	40° 16'N	59° 35'W
226	9 Oct 57	40° 12'N	57° 39'W
227	10 Oct 57	40° 16'N	55° 59'W
228	10 Oct 57	40° 15'N	54° 12'W
229	11 Oct 57	40° 10'N	52° 18'W
230	11 Oct 57	40° 12'N	50° 42'W
231	12 Oct 57	40° 15'N	49° 00'W
232	12 Oct 57	40° 14'N	47° 12'W
233	13 Oct 57	40° 03'N	45° 39'W
234	13 Oct 57	40° 17'N	43° 40'W
235	14 Oct 57	40° 15'N	41° 56'W
236	14 Oct 57	40° 12'N	40° 18'W
237	15 Oct 57	40° 12'N	38° 34'W
238	15 Oct 57	40° 14'N	36° 44'W
239	16 Oct 57	40° 14'N	34° 58'W
240	16 Oct 57	40° 15'N	33° 13'W
241	16 Oct 57	40° 15'N	31° 29'W
242	17 Oct 57	40° 14'N	29° 48'W
243	17 Oct 57	40° 14'N	27° 58'W
244	18 Oct 57	40° 14'N	26° 13'W
245	18 Oct 57	40° 03'N	24° 27'W

Crawford Station Number	Date	Latitude	Longitude
246	18 Oct 57	40° 14'N	22° 41'W
247	19 Oct 57	40° 16'N	21° 00'W
248	19 Oct 57	40° 14'N	19° 12'W
249	20 Oct 57	40° 18'N	17° 26'W
250	20 Oct 57	40° 15'N	15° 46'W
251	21 Oct 57	40° 13'N	14° 00'W
252	21 Oct 57	40° 14'N	12° 09'W
253	22 Oct 57	40° 15'N	10° 50'W
254	22 Oct 57	40° 16'N	09° 53'W
255	22 Oct 57	40° 14'N	09° 33'W

BIBLIOGRAPHY

1. Bjerknes, V.F.K., J. Bjerknes, H.S. Solberg and T. Bergeron, Physicalische Hydrodynamik. Julius Springer, Berlin. 797 pp., 1933.

2. Borkowski, M.R. and Goulet, J.R., Comparison of methods for interpolating oceanographic data, Deep-Sea Research, 18, pp. 269-274, 1971.

3. Bryan, K., Measurements of Meridional Heat Transport by Ocean Currents, J. Geophys. Res., 67 (9), pp. 3403-3414, 1962.

4. Budyko, M.I., The Heat Balance of the Earth's Surface, translated by N.A. Stapanova, 1958, U.S. Department of Commerce, Washington, D.C., 259 pp., 1956.

5. Defant, A., 1941, Die absolute Topographic des physisikalischen Meeresniveaus und der Druckflachen, sowie die Wasserbewegungen im Atlantischen Ozean. Wiss. Ergebn. D. Deutschen Atlantischen Exped. auf d. Forschungs- u. Vermessungsschiff 'Meteor' – 1925-27, VI (2 Teil., 5 Leif.), Walter De Gruyter and Co., Berlin and Leipzig, pp. 191-260.

6. Dietrich, G., Aufbau and Bewegung von Golfstrom und Agulhasstrom. Naturwissenschaften no. 15., 1936.

7. Fomin, L.M., The Dynamic Method in Oceanography. Chap. IV, Methods for Computing the "Zero" Surface in the Sea, Elsevier Publishing Co., New York, pp. 117-148, 1964.

8. Fuglister, F.C., Gulf Stream '60, Ref. No. 64-4, Woods Hole Oceanographic Institution, Woods Hole, Mass., pp. 265-383, 1964.

9. Hidaka, K., Depth of motionless layer as inferred from the distribution of salinity in the ocean. Trans. Am. Geophys. Union, V. 30, No. 3., 1940

10. Howe, M.R., Some direct measurements of the non-tidal drift on the continental shelf between Cape Cod and Cape Hatteras, Deep-Sea Research, 9, 445-453, 1962.

11. Jacobsen, J.P., Contribution to the hydrography of the Atlantic. Medd. Komm. Havundersgelser, Ser. Hydrografi, V. 2., 1916.

12. Jung, G.H., Note on meridional transport of energy by the oceans. J. Marine Res., 11 (2), pp. 139-146, 1952.

13. Jung, G.H., Heat transport in the Atlantic Ocean, Ref. 53-34T, Dept. of Oceanography, A. and M. College of Texas, College Station, 1955.

14. Ketcham, B.H., and Keen, D.J., The accumulation of river water over the continental shelf between Cape Cod and Chesapeake Bay, Deep-Sea Research, Suppl. to vol. 3, pp. 346-357.

15. Metcalf, W.G., 1958: Oceanographic Data from Crawford Cruise 16, 1 Oct. - 11 Dec. 1957 for the International Geophysical Year of 1957-58, Ref. No. 58-31, Woods Hole Oceanographic Institution, Woods Hole, Mass., pp. 23-41, 1958. (unpublished manuscript)

16. Neumann, G. and Pierson, Jr., W.J., Principles of Physical Oceanography, pp. 244-247, Prentice-Hall, 1966.

17. Parr, A. 1938. Analysis of current profiles by a study of pycnomeric distortion and identifying properties. J. Marine., 4.

18. Seiwell, H.R., The minimum oxygen concentration in the western basin of the North Atlantic. Papers Phys. Oceanogr. Meteorol., v. 3, 1937.

19. Starr, V.P., Applications of energy principles to the general circulation. Compendium Meteor., Amer. meteor. Soc., Boston, pp. 568-574, 1951.

20. Stommel, H., On the determination of the depth of no meriodional motion. Deep-Sea Research, 3, pp. 273-278, 1956.

21. Sverdrup, H.V., M.W. Johnson and R.H. Fleming, The Oceans. Prentice-Hall, New York, 1087 pp., 1942.

22. Sverdrup, H.V., Oceanography, Handbuch der Physik. Springer Verlag, Berlin, 1957.

23. Walford, L.A., and Wicklund, R.I., Monthly Sea Temperature Structure from the Florida Keys to Cape Cod, Serial Atlas of the Marine Environment, U.S. Dept. of Sport Fisheries and Wildlife, 1968.

24. Wüst, G., Schichtung und Zirkulation des Atlantischen Ozeans. Die Stratosphäre. Wiss Ergeb. Deut. Atlant. Exped. "Meteor", V. 6, Part 2., 1925-1927, 1935.

INITIAL DISTRIBUTION LIST

		No. Copies
1.	Department of Oceanography, Code 58 Naval Postgraduate School Monterey, CA 93940	3
2.	Oceanographer of the Navy Hoffman Building No. 2 200 Stovall Street Alexandria, VA 22332	1
3.	Office of Naval Research Code 480 Arlington, VA 22217	1
4.	Dr. Robert E. Stevenson Scientific Liaison Office, ONR Scripps Institution of Oceanography La Jolla, CA 92037	1
5.	Library, Code 3330 Naval Oceanographic Office Washington, D.C. 20373	1
6.	SIO Library University of California, San Diego P.O. Box 2367 La Jolla, CA 92037	1
7.	Department of Oceanography Library University of Washington Seattle, WA 98105	1
8.	Department of Oceanography Library Oregon State University Corvallis, Oregon 97331	1
9.	Commanding Officer Fleet Numerical Weather Central Monterey, CA 93940	1
10.	Commanding Officer Environmental Prediction Research Facility Monterey, CA 93940	1
11.	Department of the Navy Commander Oceanographic System Pacific Box 1390 FPO San Francisco 96610	1

12.	Defense Documentation Center Cameron Station Alexandria, VA 22314	2
13.	Library, Code 0212 Naval Postgraduate School Monterey, CA 93940	2
14.	LCDR T.D. Greeson Box 2503 Harris Br. Greenwood, S.C. 29646	1
15.	Dr. Glenn H.Jung Department of Oceanography Naval Postgraduate School Monterey, CA 93940	1
16.	Dr. Robert Bourke Department of Oceanography Naval Postgraduate School Monterey, CA 93940	1

7 JUN 78 24186

Thesis 155686
G757 Greeson
c.1 Mass, salt, and heat transport across 40°N latitude in the Atlantic Ocean based on IGY data and dynamic height calculations.

7 JUN 78 24186

Thesis 155686
G757 Greeson
c.1 Mass, salt, and heat transport across 40°N latitude in the Atlantic Ocean based on IGY data and dynamic height calculations.

thesG757
Mass, salt, and heat transport across 40
3 2768 002 13900 8
DUDLEY KNOX LIBRARY